AD NUMBER

AD878216

NEW LIMITATION CHANGE

TO

Approved for public release, distribution unlimited

FROM

Distribution authorized to U.S. Gov't. agencies and their contractors; Administrative/Operational Use; 1 Oct 1970. Other requests shall be referred to Naval Ordnance Laboratory, White Oak, MD.

AUTHORITY

NOL ltr, 15 Nov 1971

NOLTR 70-211

SUPERSONIC MAGNUS MEASUREMENTS OF THE 10-CALIBER ARMY-NAVY SPINNER PROJECTILE WITH WRAP-AROUND FINS

By
Frank J. Regan
Virginia L. Schermerhorn

1 October 1970

NOL

UNITED STATES NAVAL ORDNANCE LABORATORY, WHITE OAK, MARYLAND 20910

SUPERSONIC MAGNUS MEASUREMENTS OF THE 10-CALIBER ARMY-NAVY SPINNER PROJECTILE WITH WRAP-AROUND FINS

Prepared by:
Frank J. Regan
Virginia L. Schermerhorn

ABSTRACT: A research configuration was formed by attaching wrap-around fins in a cruciform arrangement to a 10-caliber Army-Navy Spinner Projectile. This configuration was tested in the Naval Ordnance Laboratory's Supersonic Tunnel No. 2 to get the Magnus force and moment, as well as the normal force and pitching moment. Model spin rate was generated by means of fin cant.

U. S. NAVAL ORDNANCE LABORATORY
WHITE OAK, MARYLAND

NOLTR 70-211 1 October 1970

SUPERSONIC MAGNUS MEASUREMENTS OF THE 10-CALIBER ARMY-NAVY SPINNER PROJECTILE WITH WRAP-AROUND FINS

The purpose of this investigation was to obtain Magnus force and moment data on a research configuration employing wrap-around fins.

This project was performed at the request of the Naval Air Systems Command under Task No. A32 320/292/69F 20311202 WU-3.

The authors wish to acknowledge the assistance of Miss M. E. Falusi in data reduction.

GEORGE G. BALL
Captain, USN
Commander

Leon H. Schindel.
LEON H. SCHINDEL
By direction

CONTENTS

ILLUSTRATIONS

BLANK PAGE

INTRODUCTION

The wrap-around-fin stabilizer has become increasingly attractive to designers of unguided aerobalistic ordnance. The reason is, of course, that the wrap-around-fin concept nearly obviates the space requirements of the more conventional rigid planar stabilizers. By causing the stabilizer to conform to the circular contour of a weapon, it is possible to minimize space requirements and to increase weapon packing density. The wrap-around stabilizer also makes it feasible to launch a fin-stabilized weapon from a tube whose inside diameter is only slightly greater than the weapon's maximum body diameter. The tube may be anything from a disposable storage container to a rifled gun barrel, 40 or more body diameters in length.

To gain the above mentioned advantages, the wrap-around fin also presents the weapons designer with certain problems not encountered by the rigid planar fin. For purposes of discussion, these problems may be separated into two distinct areas - mechanical and aerodynamic. The mechanical complications center around providing a hinge at the body-fin junction for fin rotation during deployment. Once deployment is completed, the hinge must become rigid to prevent further rotation of the curved fin panel relative to the body. Wrap-around-fin configurations in operation on weapons prove that a successful deployment mechanism is feasible.

The aerodynamic effects introduced by the curved surface of the wrap-around stabilizer are more difficult to define than are the mechanical complications. The main obstacle appears to be a lack of understanding of the effect of stabilizer curvature on pressure distribution, especially for a fairly general class of fin geometries. One example of the complications introduced by the wrap-around-fin curvature is the rolling moment generated by a nominally uncanted fin. In the course of an early wind-tunnel investigation of this phenomenon it was discovered that this rolling moment reversed sign with Mach number (see Ref. (1)). This spurious rolling moment was found to be in the opposite direction for subsonic flows. Of course the weapon designer becomes quite interested in how the Mach number, at which the fin-curvature-induced rolling moment changes sign, might be controlled. In Reference (1), and unpublished investigations, it was found that the Mach number of rolling-moment sign reversal is strongly dependent upon fin geometry. For example, in one investigation a rectangular fin encountered a rolling-moment sign reversal at about a Mach number of 1.0. If the leading edge of the fins was swept (45 degrees in this investigation), the rolling moment would not reverse until a Mach number of 1.75 had been reached.

Attempts were made to compare the wind-tunnel measurements of normal force and pitching moment with theoretical estimates. Although the estimates are based upon flat fins (of the same chord and span as the wrap-around fin), the good agreement obtained indicates that fin curvature has little influence on the normal-force

and pitching-moment coefficients. Since no suitable theory exists for estimating the Magnus moment on finned bodies, Magnus data must be presented without theoretical corroboration.

SYMBOLS

c.p.	center of pressure
C_ℓ	rolling-moment coefficient, M_x/QSd
C_{ℓ_p}	roll-damping derivative, $\partial C_\ell/\partial(pd/2V_\infty)$
C_{ℓ_δ}	rolling-moment derivative due to fin cant, $\frac{\partial C_\ell}{\partial \delta}$
C_m	pitching-moment coefficient, M_y/QSd
C_n	yawing-moment coefficient, M_z/QSd
C_{n_p}	Magnus-moment coefficient, $\partial C_n/\partial(pd/2V_\infty)$
C_N	normal-force coefficient, $-F_z/QS$
C_y	side-force coefficient, F_y/QS
C_{y_p}	Magnus-force coefficient, $\partial C_y/\partial(pd/2V_\infty)$
d	reference length, body diameter
F_y	component of aerodynamic force along y axis
F_z	component of aerodynamic force along z axis
M	Mach number
M_x	rolling moment, moment about x axis
M_y	pitching moment, moment about y axis
M_z	yawing moment, moment about z axis
p	spin rate
$\hat{p}$	reduced spin rate, $pd/2V_\infty$
P_o	stagnation pressure

Q	dynamic pressure, $1/2\rho V_\infty^2$
S	reference area, $\pi d^2/4$
V_∞	free-stream airspeed
x	body axis through center of gravity to vertex along longitudinal axis of symmetry
y	body axis orthogonal to x axis and normal to angle-of-attack plane
z	body axis orthogonal to x and y axes
α	angle of attack
ρ	density of free stream
δ	fin-cant angle

DESCRIPTION OF CONFIGURATION

The primary purpose of this investigation was to obtain Magnus and static loads on a configuration with a wrap-around-fin stabilizer. Since the shape of the body to which these fins are attached will influence the measured loads, a shape without contour irregularities was chosen to minimize forebody contributions. It was decided that the Army-Navy Spinner Projectile would be used as the basic body for the following reasons: first, the Army-Navy Spinner Projectile is relatively free from configurational irregularities; secondly, supersonic static and Magnus measurements were made earlier on this configuration at the Naval Ordnance Laboratory (NOL). These data are available in Reference (2). The availability of body-alone data is important if one wishes to make use of the analytic methods of References (3) and (4).

Figure 1 shows the wrap-around-fin model used in these tests. As mentioned above, the body is a 10-caliber-long version of the Army-Navy Spinner Projectile. This configuration has a two-caliber-long secant ogival nose of radius 8.5 body calibers.

Stabilizer details are illustrated in Figure 2. The upper left-hand photograph presents an axial view of a typical wrap-around fin. It is clearly evident that the fin curvature closely matches that of the body contour. Since spin was provided by means of fin cant, three sets of fins were constructed with fin-cant angles of 2.00, 3.25 and 4.50 degrees, respectively. These are illustrated in the remaining photographs of Figure 2. For all sets of fins, fin chord is 1.75 calibers; the thickness is constant (0.046 calibers), and each fin has a 45-degree bevel at both the leading and trailing edges.

TEST TECHNIQUE

The wind-tunnel tests described in this report were carried out in the NOL Supersonic Tunnel No. 2; an open-jet, fixed nozzle blowdown facility with a 16- by 16-inch test section. Even though this tunnel can be operated in an intermittant fashion, it is intended to be used mainly as a continuous recirculating facility. For a rough description of the operational capabilities of this wind tunnel the following range of variables might be listed: Mach numbers range between 1.2 and 5.0; Reynolds number between 0.9 and 12 million per foot; total pressure between 0.5 and 15 atmospheres, and total temperature from ambient to 600° Rankine. The above variables are interrelated, which means that some of the extremes are not possible under certain conditions. Of primary interest to the aerodynamicist is the Reynolds number-Mach number operational profile. This profile is given in Figure 3.

All data presented in this report were made at a total pressure of one atmosphere, as indicated in Figure 3. Measurements were made at Mach numbers of 1.76, 2.0, 2.5, 3.0 and 3.5.

The most important single instrument used in making successful Magnus measurements is the Magnus wind-tunnel balance. The balance used in making the reported measurements is described in detail in Reference (5). While the details of balance construction will not be included here, it might be of value to consider the nature of the Magnus effect and how the size and direction of the Magnus force influence balance design.

The Magnus force acts normal to the angle-of-attack plane, which is the plane defined by the free-stream velocity vector and the body's longitudinal axis. The Magnus force, therefore, must be measured in the presence of an orthogonal force (normal force) which is at least ten times greater in magnitude. In addition, the Magnus measurements must be made on a body which is spinning. The model is, therefore, mounted on essentially a four-component static balance with the added complications of providing and measuring spin.

Model spin can be provided in a variety of ways; however, the most common procedures are to use an internal motor (electrical or pneumatic) or to cant the model's fins. For the present tests of the wrap-around-fin configuration, spin is provided by differential fin cant, and is varied by using different cant angles.

The wind-tunnel technique used in making these Magnus measurements will be outlined now. After tunnel flow has been established, the model is swept through the angle-of-attack range. The sweep rate is slow enough to assure that the model is at all times spinning at the steady-state spin rate corresponding to the instantaneous angle of attack. Checks were made of this spin rate-angle of attack assumption by measuring spin rates and loads at discrete angles of attack. As the model is being swept through the prescribed angle-of-attack range,

the strain gages are sampled 80 times per second. The result is a nearly continous record of the four coefficients, C_m, C_N, C_n and C_y, with angle of attack.

DATA REDUCTION

The sampled strain-gage signals are recorded in digital form on magnetic tape. This tape, together with an additional tape record of the balance calibration, is input into a digital computer data-reduction program. The output from this program is a plotting tape and a printed record of coefficients and pertinent test information. In these Magnus tests this information consists of spin rate, reduced spin rate, Mach number, total pressure and total temperature. The plotting tape is then used as an input into an automatic plotter to provide the graphical data records which make up this report.

DISCUSSION OF RESULTS

The normal-force and pitching-moment coefficients are presented in Figures 4 through 31. The normal force is defined as that component of the total aerodynamic force which acts normal to the body's axis of symmetry and lies in the plane defined by the axis of symmetry and the free-stream velocity vector (angle-of-attack plane). The pitching moment is the component of the total aerodynamic moment normal to the angle-of-attack plane.

A quick perusal of these static measurements reveals two rather interesting results. First, the normal-force and pitching-moment coefficients are linear up to six-degrees angle of attack and only deviate significantly from linearity after 10-degrees angle of attack. To within the range of angle-of-attack measurements shown here, the pitching-moment coefficient slope shows a tendency to increase in magnitude with angle of attack above 10 degrees. This trend is consistent with measurements made on flat fins (see, for example, Ref. (6)). Secondly, the pitching-moment and normal-force coefficients indicate no dependency on spin rate. As would be expected, the largest fin cant of 4.50 degrees gives a spin rate at least twice that of the lowest fin cant of 2.00 degrees. This spin-rate variation is not detectable in the normal-force and pitching-moment coefficients.

As mentioned earlier, no adequate theory exists for calculating the effect of fin curvature on the normal-force and pitching-moment data. Nevertheless, in obtaining an estimate of these effects, the obvious simplification is to ignore fin curvature and to "replace" the curved fin by a rectangular fin of the same chord and span. When this is done, the aerodynamicist has at his disposal the low-aspect ratio theories of Pitts, Nielsen and Kaattari, as presented in Reference (3). This analysis has been put in a form more amenable to quick analysis by DeJonge in which fin-body interference effects have been included (see Ref. (4)). DeJong's analysis requires a knowledge of body-alone normal-force and pitching-moment

characteristics. Fortunately, this information is available since body-alone measurements had been made earlier on the 10-caliber Army-Navy Spinner Projectile (see Ref. (2)).

Calculations were made of the normal-force and pitching-moment derivatives using DeJong's methods. In the table below comparisons are made between the theoretical and measured values of these derivatives:

	Theoretical		Measured	
Mach No.	C_{N_α}	C_{m_α}	C_{N_α}	C_{m_α}
2.0	0.192	-1.33	0.182	-1.12
2.5	0.171	-1.045	0.168	-0.970
3.0	0.137	-0.878	0.156	-0.880

The above theoretical estimates are sketched on Figures 4 through 31, where appropriate. Pitching-moment coefficient comparisons are shown on Figures 8, 11 and 14 and those for the normal force on Figures 22, 25 and 28.

It will be noted in the graphical and tabular comparisons that agreement between theory and measurement is quite satisfactory. Some disagreement should be expected since the theoretical calculations are based upon zero roll angle (two opposing fins normal to the angle-of-attack plane; the other two opposing fins are located in the angle-of-attack plane). The measurements, on the other hand, were made on spinning models where spinning will "average out" the variations in static loads which are a consequence of roll angle.

In the case of Magnus measurements, no theoretical estimates of any value exist. For this reason, Magnus data will be presented without attempts at theoretical corroboration.

It was mentioned earlier that the model sweep rate in angle of attack was sufficiently slow that the measured values of spin rate were essentially steady-state values. This steady-state spin is assumed to be defined by the following relat onship

$$p_{ss} = \frac{C_{\ell_\delta}{}^{\delta}}{C_{\ell_p}} \frac{2V_\infty}{d} \qquad (1)$$

where C_{ℓ_δ} is the rolling-moment coefficient due to fin cant, and C_{ℓ_p} is the damping-in-roll derivative. Since C_{ℓ_δ} and C_{ℓ_p} are solely functions of angle of attack (for fixed Mach number and Reynolds number), the steady-state spin, p_{ss}, may be thought of as a unique function of angle of attack.

Figures 32 through 36 present the reduced spin rate versus angle of attack. It will be noted that in all cases the reduced spin rate is nearly a constant for angles of attack up to three degrees; above this angle, however, there is a rather sudden increase in the spin rate. Variation of spin rate with fin cant is indicated in Figure 37.

Magnus measurements are presented in Figures 38 through 51 in terms of the yaw-moment coefficient versus angle of attack; and, in Figures 52 through 65 in terms of the side-force coefficient versus angle of attack. In analytically describing the Magnus moment, the following functional relationship will be assumed:

$$C_n = f\ (\tilde{p},\ \alpha,\ M,\ Re) \qquad , \qquad (2)$$

where $\tilde{p}$, α, M and Re are the reduced frequency, angle of attack, Mach number and Reynolds number, respectively. A similar relationship presumably could be written for the side-force coefficient. The reason for the inclusion of, and restriction to, these variables is based upon various experiments conducted over the past 100 years, as well as conjecture into the essential fluid mechanics of the Magnus phenomenon (see Ref. (7)). Classically, the Magnus force is the component of the total aerodynamic load acting on a spinning body which acts normal to the angle-of-attack plane (defined earlier). Of course, this force results in a moment (moment vector lying in the angle-of-attack plane) about some suitable reference point.

Supposedly, there should be no load normal to the angle-of-attack plane on a body which is symmetric with respect to this plane. On a finned body there is a "roll-induced" force and moment which varies cyclically with roll angle. As the body roll violates the symmetry, with respect to the angle-of-attack plane, one should expect a load normal to this plane. Nevertheless, this induced load is not associated with the Magnus effect, since induced effects depend upon roll angle and Magnus effects on roll rate.

The use of the reduced spin rate (rather than the spin rate alone) may be supported by the simplified flow model illustrated below:

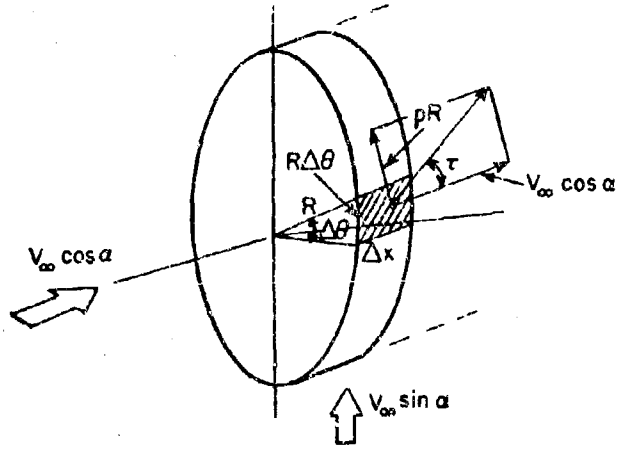

The area element $R\Delta\theta\Delta X$ "sees" a local fluid velocity which has a spin component of magnitude pR and a longitudinal component of $V_\infty \cos\alpha$. A measure of the relative magnitude of these two components is the angle, τ, whose tangent may be written and then approximated as,

$$\tan\tau = \frac{pR}{V_\infty \cos\alpha} \approx \frac{pR}{V_\infty} \approx \frac{pd}{2V_\infty} \qquad (3)$$

where the local body radius, R, has been replaced by the reference length, d, (maximum body diameter) and the small angle assumption has been made on the angle of attack, α. Since $pd/2 << V_\infty$, a further small angle assumption can be made in Equation (3) by equating τ to $pd/2V_\infty$ which gives a sort of physical identity to the reduced spin rate, $\tilde{p} = pd/2V_\infty$.

The sign of the forebody Magnus force might be anticipated on the basis of the following oversimplified fluid dynamics argument. This argument is adequate only because the Magnus effect is being looked at qualitatively - merely to indicate force direction.

Consider the element $R\Delta\theta\Delta X$, designated by (1), and the corresponding diametrically opposite element, designated by (2):

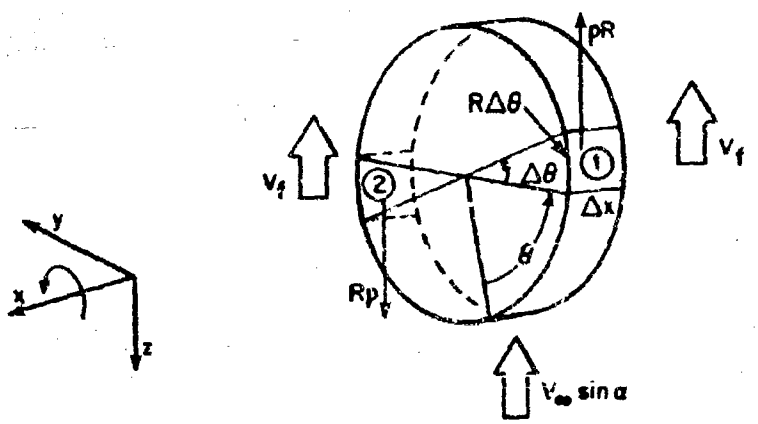

here

$$V_f = V_\infty \sin\alpha \, (2 + 2\cos 2\theta)^{1/2} \qquad (4)^*$$

Assuming two-dimensional flow about a cylinder, it can be seen that the spin and crossflow velocities, pR, and V_f, respectively, add at element (1) and subtract at element (2). From Bernoulli's equation

---

* See any text on elementary incompressible fluid mechanics, e.g., page 388, Karamchetti, "Principles of Ideal-Fluid Aerodynamics," John Wiley and Sons, 1966

it can be shown that the pressure is greater at element (2) than at element (1). The resulting pressure difference produces a net force in the negative direction of the y axis. Integrated around the volume element, this force per unit length, dF_y/dx, should be

$$-2 \pi d \rho V_\infty^2 \sin \alpha = dF_y/dx \qquad (5)$$

with the negative sign indicating a force direction along the negative y axis. Thus, Equations (3) and (5) indicate that the reduced spin rate, $\tilde{p}$, and angle of attack, α, are necessary independent variables. Of course, Equation (5), being based upon inviscid incompressible flow, is not satisfactory for load estimates.

Aerodynamic coefficients are used to describe loads and, since coefficients are loads normalized by the dynamic pressure, it would be expected that the coefficients will be functions of flow similarity parameters (Mach number, Reynolds number) only*.

Since the functional form of Equation (1) is not known, an attempt might be made to expand it in a Taylor series for the reduced spin rate, $\tilde{p}$. The first term of such a series might be written as,

$$C_n = \frac{\partial C_n}{\partial \tilde{p}} \tilde{p} \qquad (6)$$

where $\partial C_n/\partial \tilde{p}$ is a function of the angle of attack, Mach number and Reynolds number. While Equation (5) is adequate for nonfinned bodies, the presence of fins causes the Magnus effect to vary nonlinearly with $\tilde{p}$.

If one wishes to persist in a Taylor expansion of Equation (1), by retaining more terms, it must be emphasized that to do so requires that only one variable be changed, at a time, in any experiment to measure the additional terms. In conducting this test, however, loads were measured while continually rotating the model through angle of attack. However, while the angle of attack is changing, the spin rate is also changing (see Figs. 32 through 36). Of course, cross plots can be made to show variations in the coefficients with a single variable. However, it will be pointed out now that this is neither necessary nor desirable.

Through some simple arguments it has been indicated that the Magnus effect is a function of reduced spin rate. This reduced spin-rate parameter can be related to fin-cant angle, θ, through the

---

*Actually, hydrodynamicists consider the reduced spin rate to be a similarity parameter also. In this context it is often referred to as the Strouhal number.

following simple relationship,

$$\tilde{p} = \left(\frac{C_{\ell_\delta}}{C_{\ell_p}}\right)\delta \qquad (6)$$

where C_{ℓ_δ} and C_{ℓ_p} are the rolling-moment derivative due to fin cant and the roll-damping derivative, respectively. Since each of these derivatives depends on angle of attack and the Reynolds and Mach numbers, it seems logical that if fin cant is fixed the reduced spin rate, $\tilde{p}$, will depend only on angle of attack, Reynolds number and Mach number. In other words, if Re, M and δ are fixed, then the reduced spin rate, $\tilde{p}$, is a unique function of angle of attack, α. It is, therefore, not appropriate to consider variations in reduced spin rate independent of angle of attack. Thus, once a fin-cant angle has been selected aerodynamic coefficients, as measured in the wind tunnel, should be applicable to any other flight regime in which Mach number, Reynolds number and angle of attack are matched. Once the quantities M, Re, δ and α are selected, the reduced spin rate is automatically fixed through Equation (6).

Now it is also of some interest to examine the Mach number and Reynolds number effects. The effect of Mach number on the Magnus moment may be appreciated by examining Figures 38 through 51. As the Mach number increases it is seen that the Magnus moment becomes less negative, and then becomes increasingly positive. For example, in Figure 39 the yaw-moment coefficient is approximately 0.4 at an angle of attack of 8 degrees and Mach number of 1.76. In Figure 40, where the Mach number is now 2.0, the yaw moment is strongly dependent upon fin cant, being about 0.0$ at 8 degrees angle of attack and at a fin cant of 2.0 degrees. As the Mach number is increased to 2.5, the Magnus moment becomes slightly positive at Mach 2.5 and then increasingly positive as the Mach number is increased to 3.5.

The Magnus force is represented by the side-force coefficient, C_y, and is presented in Figures 52 through 65. According to Equation (5), the Magnus force should be directed along the negative y axis. At Mach numbers of 1.76 and 2.0 the side force is negative, but at the higher Mach numbers of 2.5, 3.0 and 3.5 the side force is positive. Also, it should be noted that the Magnus force and moment are nonzero at zero angle of attack. If the fluid dynamic argument presented earlier is recalled it will be remembered that there should be no side force at zero angle of attack. The fact that a sizable force and moment do exist at zero angle of attack seems to indicate, strongly, that the fins make an important contribution to the total Magnus effect.

The final variable in Equation (1) is the Reynolds number. It is difficult to assess the influence of Reynolds number because this parameter was not varied independent of the Mach number. An important effect that occurs when the Reynolds number is varied is the change in the location of boundary-layer transition on the body. Thus, it was decided to determine the position of the transition point for the various conditions of Mach number and angle of attack. In order to do this, a comprehensive schlieren photographic coverage was made of the entire test program. The negatives of these photographs were greatly enlarged on a film reader. Thus, it was possible to examine the boundary layer in detail and to determine, within one-quarter caliber, where, on the leeward side of the body, transition takes place. Figure 66 is a summary of this effort. This figure shows that the transition point on the leeward side is at about seven calibers aft of the body vertex at zero-degree angle of attack; and, from this point, moves forward toward the vertex as the angle of attack increases. The uncertainties in the determination of the transition point have clearly masked all Mach number effects. Since the larger Reynolds numbers occur at the low Mach numbers, it would be expected that the transition point would be closer to the vertex for the lower Mach numbers.

Figures 67, 68 and 69 present a sample of the above mentioned schlieren photographs taken at Mach numbers of 2.0, 3.0 and 3.5, respectively. The photographs in these figures are much too small to show boundary-layer details, but separation can be seen, clearly (on Fig. 67b for example).

CONCLUSION

The static measurements clearly indicate that adequate load predictions can be made using a planar-fin assumption. The Magnus force and moment may be described in terms of angle of attack, Mach number and Reynolds number. Spin rate need not be varied independently, since it is a function of angle of attack, Mach number and Reynolds number once a fin-cant angle is chosen. The Magnus force is small compared to the normal force which is acting under the same flow conditions. As an example, the normal force is about 30 times as great as the Magnus force. In comparison to a nonfinned projectile, the Magnus force varies in a complex fashion with Mach number, Reynolds number and angle of attack. Also, unlike a nonfinned body, the Magnus force and moment is nonzero at zero-degree angle of attack.

As a result of these tests, certain recommendations can be made for future work. First, a systematic investigation should be made to ascertain the effect of Reynolds number variation at several fixed values of Mach number. Secondly, trajectory studies should be made to determine the significance of the Magnus effect on vehicles configurationally similar to the test vehicle. Finally, new wind-tunnel balances should be constructed in order to improve the accuracy with which these side loads can be measured.

REFERENCES

(1) Featherstone, H. A., "Aerodynamic Characteristics of Curved Tail Fins," Engineering Research Report ERR-po-019 Convair/Pomona General Dynamics, Sep 1960

(2) Holmes, J. E., Regan, F. J. and Falusi, M. E., "Supersonic Wind-Tunnel Magnus Measurements of the 7-, 8-, 9-, and 10-Caliber Army-Navy Spinner Projectile," NOLTR 68-172, Oct 1968

(3) Pitts, W. C., Nielsen, J. N. and Kaattari, G. E., "Lift and Center of Pressure of Wing-Body-Tail Combinations at Subsonic, Transonic and Supersonic Speeds," NACA Report 1307, 1959

(4) DeJong, Clark, "The Effect of Low Aspect Ratio Rectangular and Delta Cruciform Fins on the Stability of Bodies of Revolution with Tangent Ogives at Small Angles of Attack through a Mach Number Range of 0 to 3.5," Report No. RF-TR-62-1, Redstone Arsenal, Jul 1962

(5) Regan, F. J. and Iandolo, J. A., "Instrumentation, Techniques, and Analysis Used at the Naval Ordnance Laboratory for the Determination of Dynamic Derivatives in the Wind Tunnel," NOLTR 66-23, Aug 1966

(6) Regan, F. J., et al, "Static Wind Tunnel Tests of the M823 Research Store with Fixed and Free-Spinning Tails," NOLTR 65-14, Apr 1967

(7) Regan, F. J., "Survey-Magnus Effects," AGARD Conference Proceedings No. 10, Fluid Dynamics Aspects of Ballistics, Sep 1966

FIG. 1 WRAP AROUND FIN MAGNUS MODEL

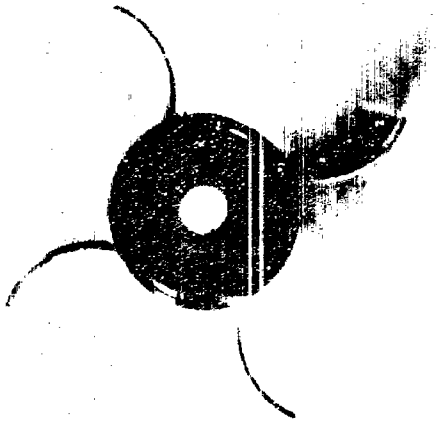

END VIEW

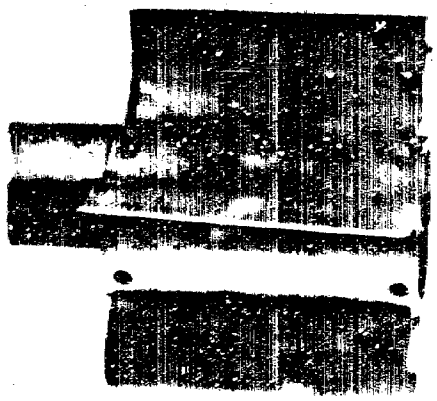

2.00 DEG FIN CANT

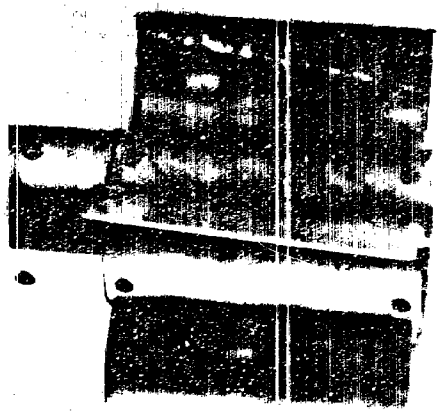

3.25 DEG FIN CANT

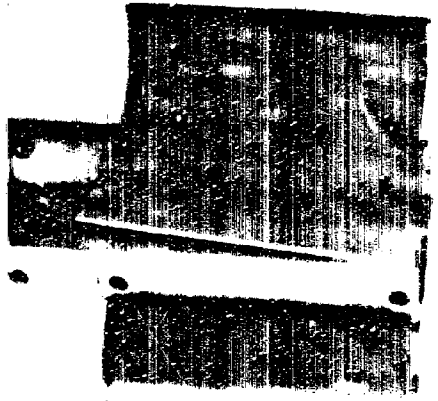

4.50 DEG FIN CANT

FIG. 2 FIN DETAILS OF WRAP AROUND FIN MAGNUS MODEL

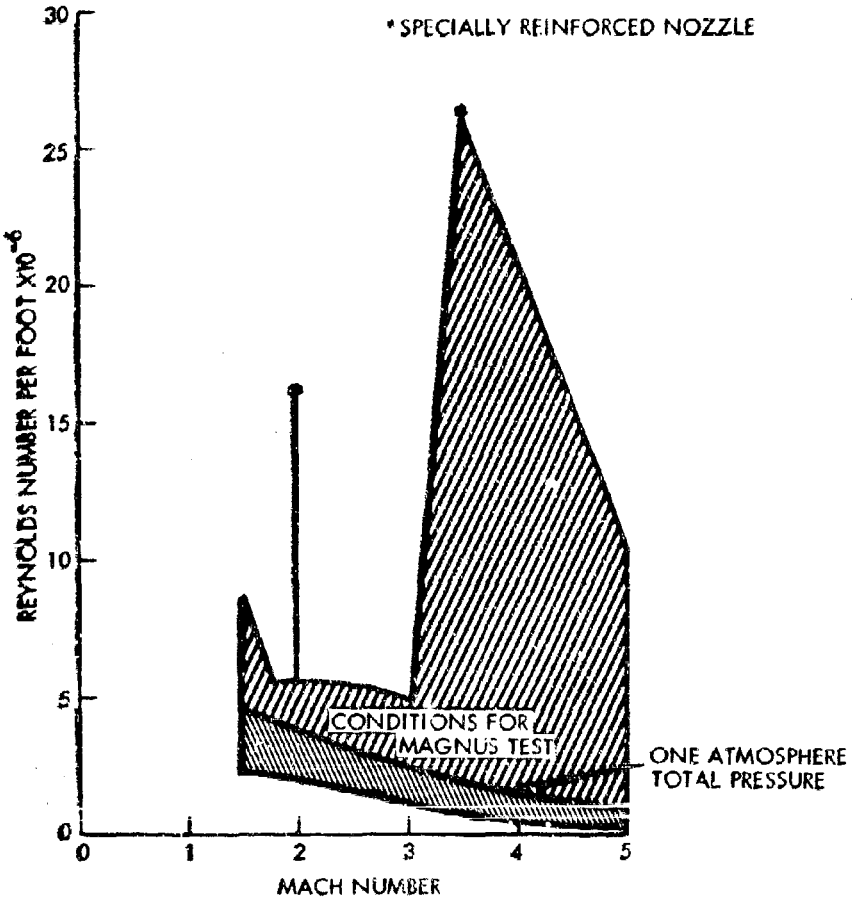

FIG. 3 REYNOLDS NUMBER PER FOOT VERSUS MACH NUMBER FOR NOL SUPERSONIC TUNNEL NO. 2

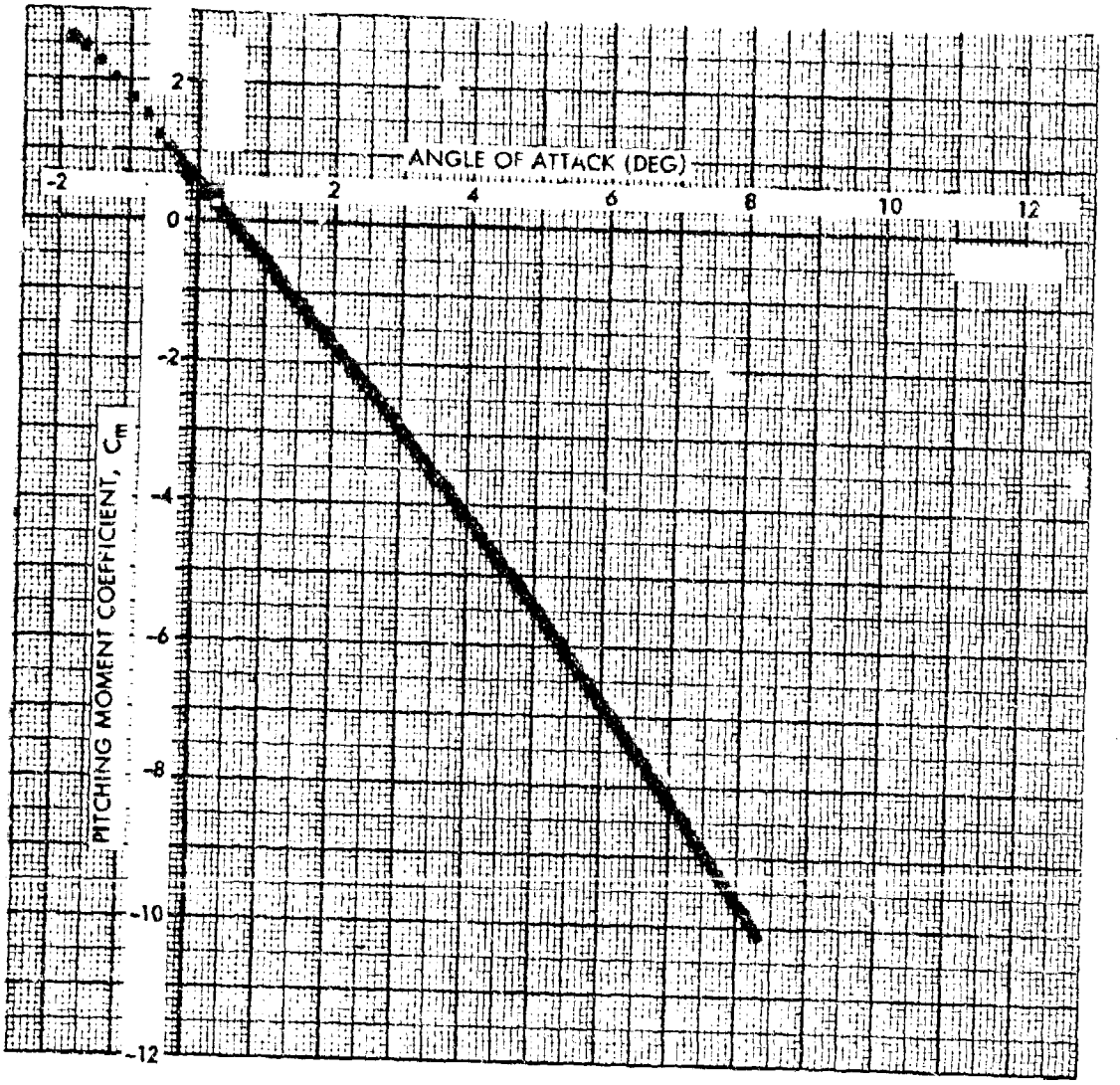

FIG. 4 PITCHING MOMENT COEFFICIENT VERSUS ANGLE OF ATTACK AT A MACH NUMBER OF 1.76 AND A FIN CANT ANGLE OF 2.0 DEGREES

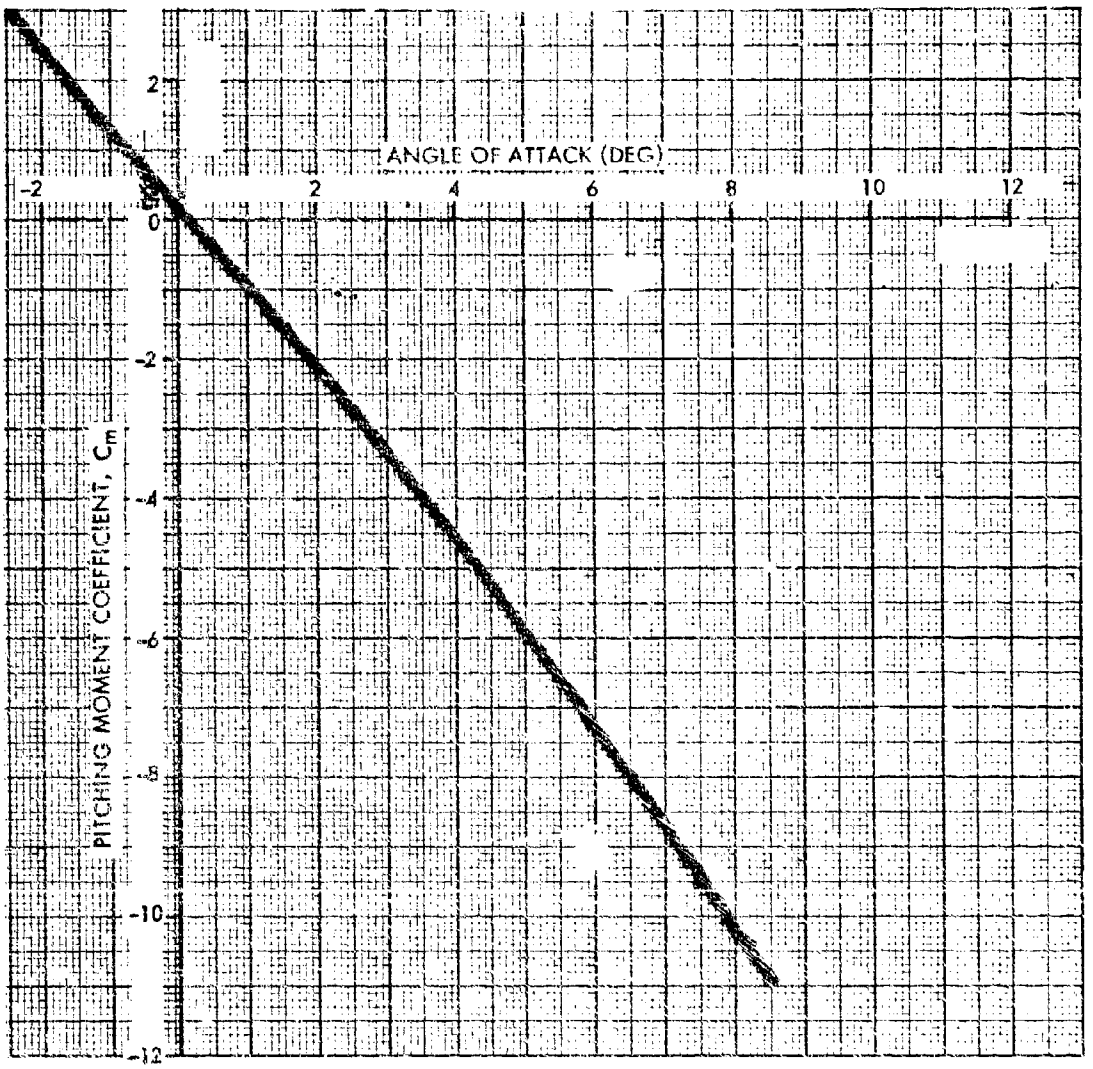

FIG. 5 PITCHING MOMENT COEFFICIENT VERSUS ANGLE OF ATTACK AT A MACH NUMBER OF 1.76 AND A FIN CANT ANGLE OF 3.25 DEGREES

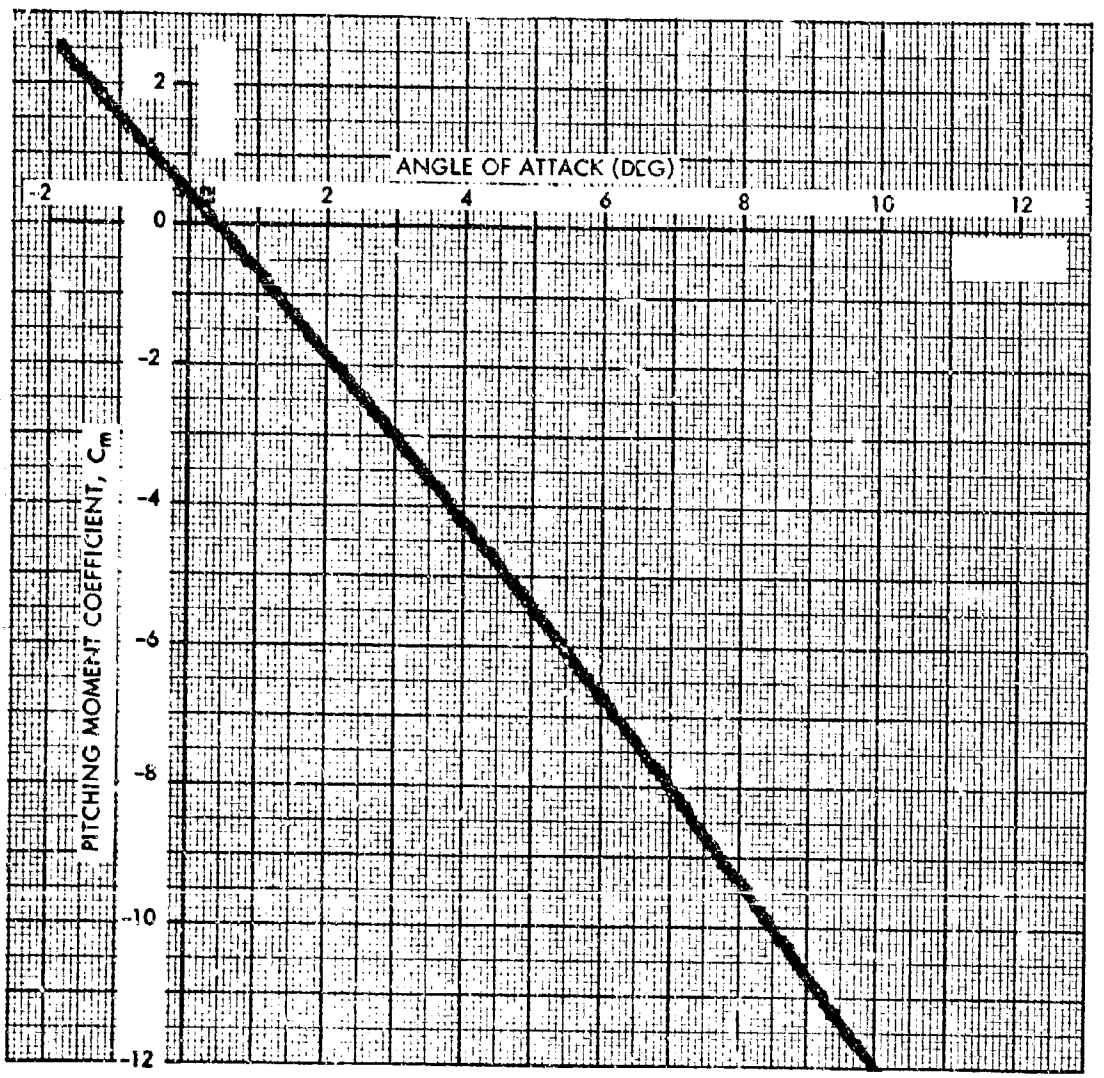

FIG. 6 PITCHING MOMENT COEFFICIENT VERSUS ANGLE OF ATTACK AT A MACH NUMBER OF 2.0 AND A FIN CANT ANGLE OF 2.0 DEGREES

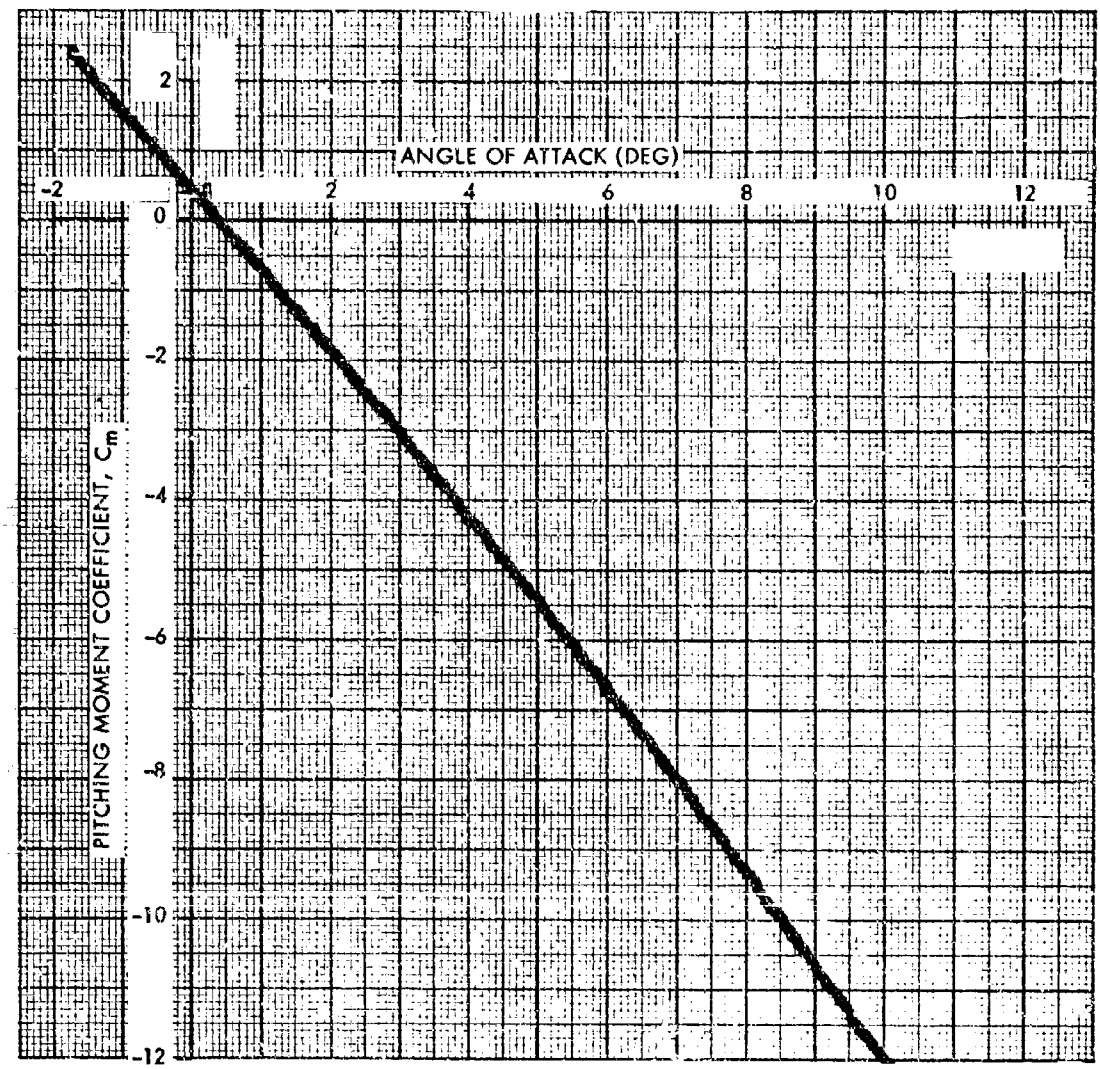

FIG. 7 PITCHING MOMENT COEFFICIENT VERSUS ANGLE OF ATTACK AT A MACH NUMBER OF 2.0 AND A FIN CANT ANGLE OF 3.25 DEGREES

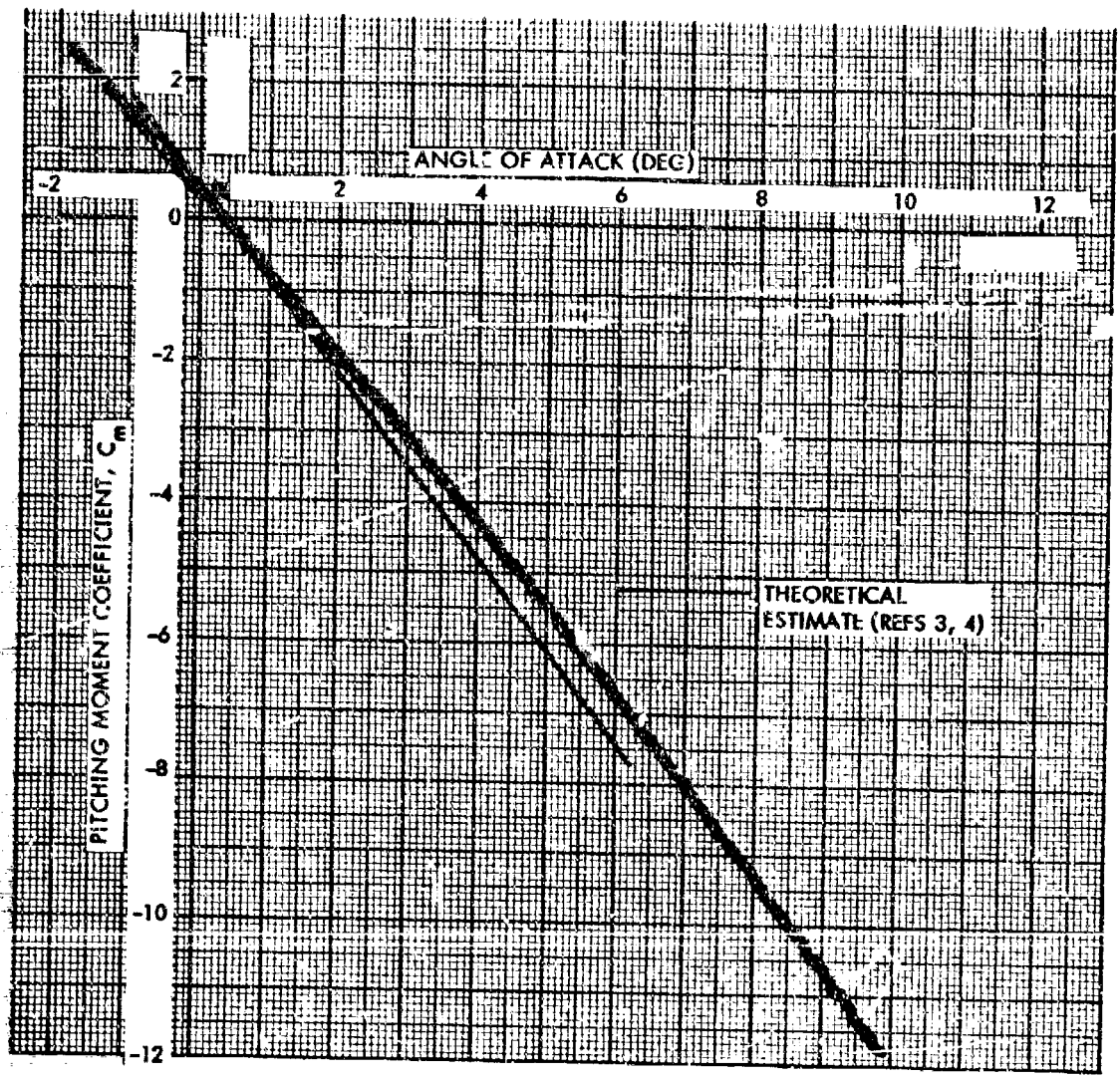

FIG. 8 PITCHING MOMENT COEFFICIENT VERSUS ANGLE OF ATTACK AT A MACH NUMBER OF 2.0 AND A FIN CANT ANGLE OF 4.50 DEGREES

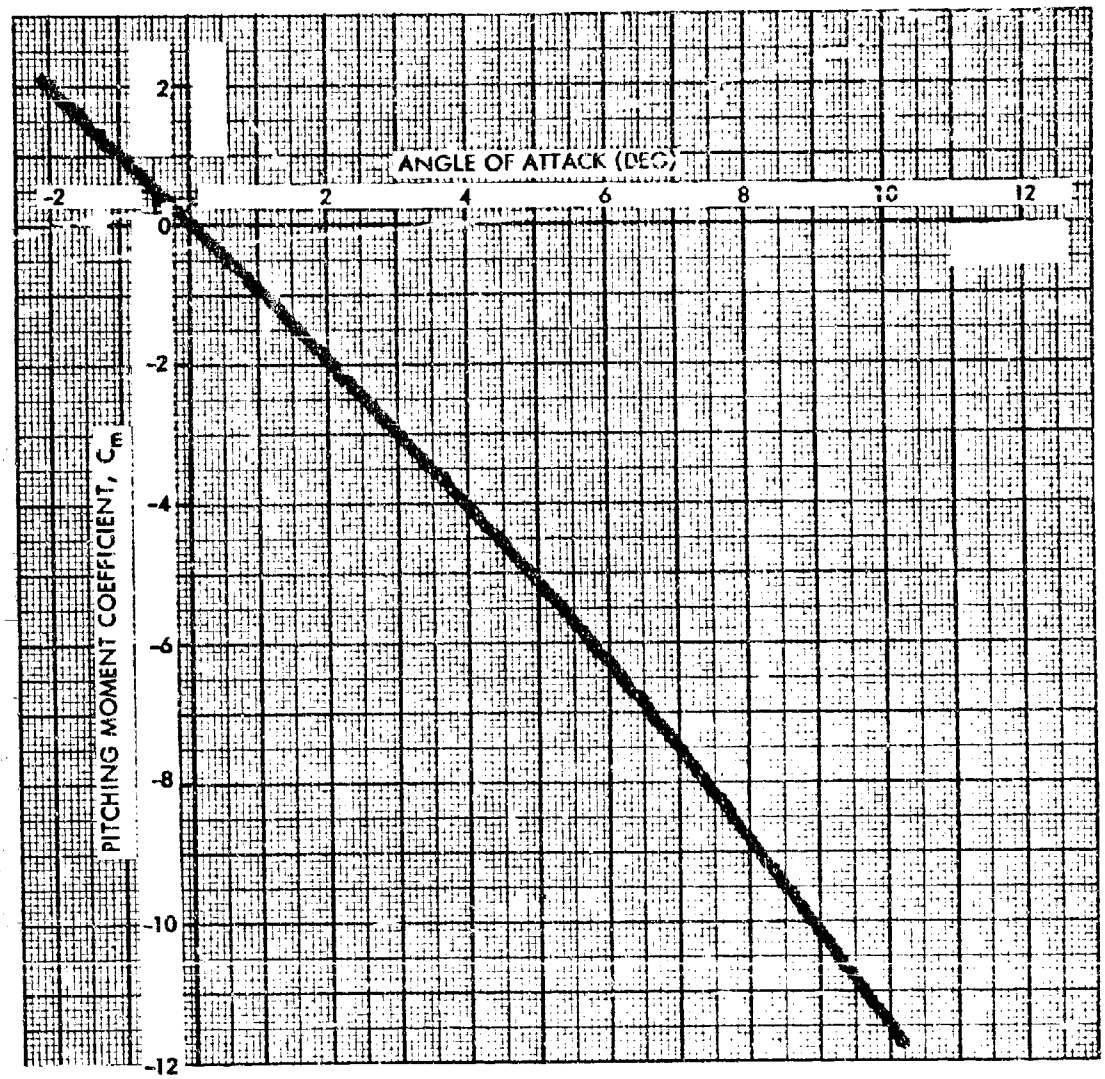

FIG. 9 PITCHING MOMENT COEFFICIENT VERSUS ANGLE OF ATTACK AT A MACH NUMBER OF 2.5 AND A FIN CANT ANGLE OF 2.0 DEGREES

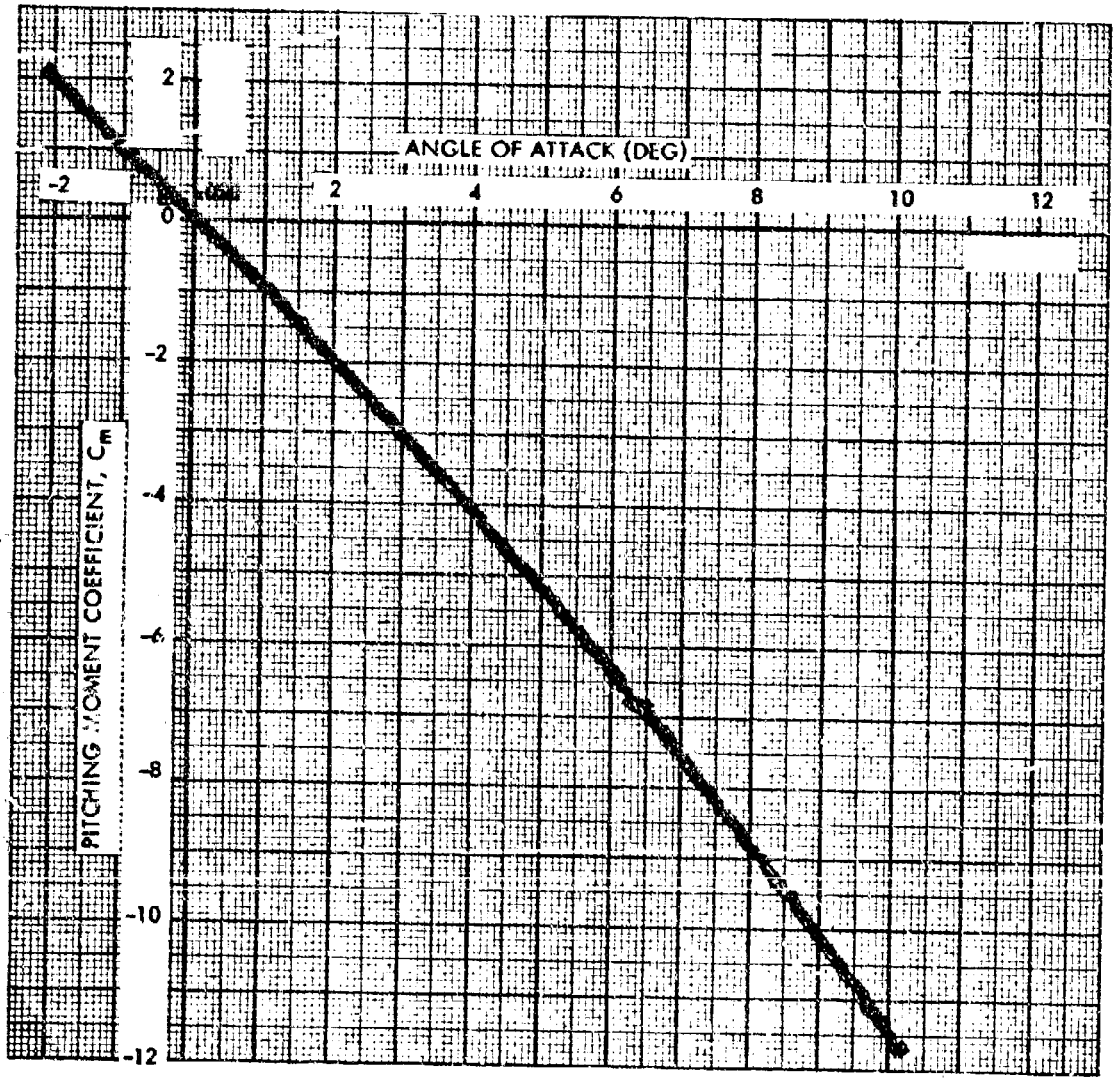

FIG. 10 PITCHING MOMENT COEFFICIENT VERSUS ANGLE OF ATTACK AT A MACH NUMBER OF 2.5 AND A FIN CANT ANGLE OF 3.25 DEGREES

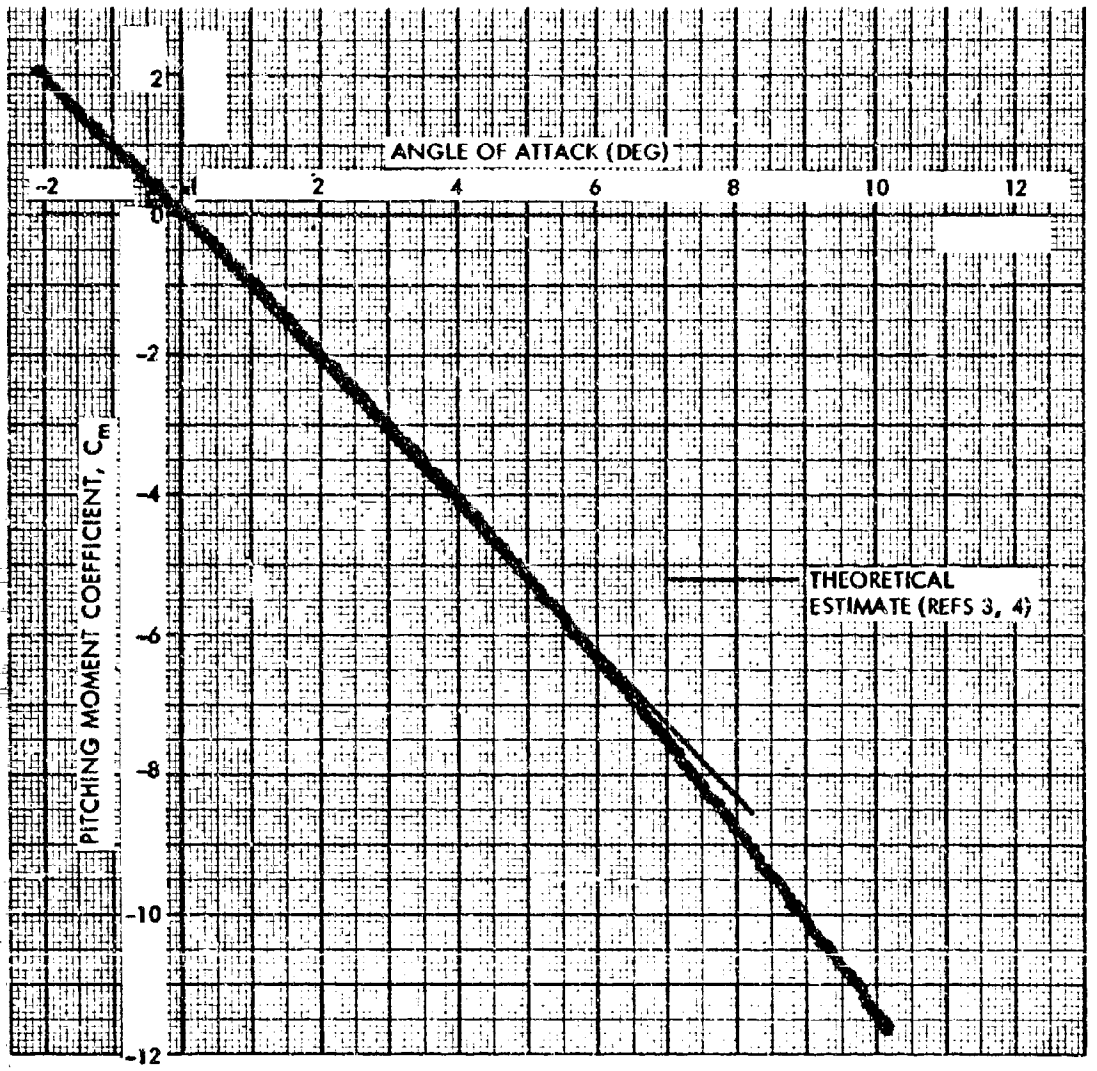

FIG. 11 PITCHING MOMENT COEFFICIENT VERSUS ANGLE OF ATTACK AT A MACH NUMBER OF 2.5 AND A FIN CANT ANGLE OF 4.50 DEGREES

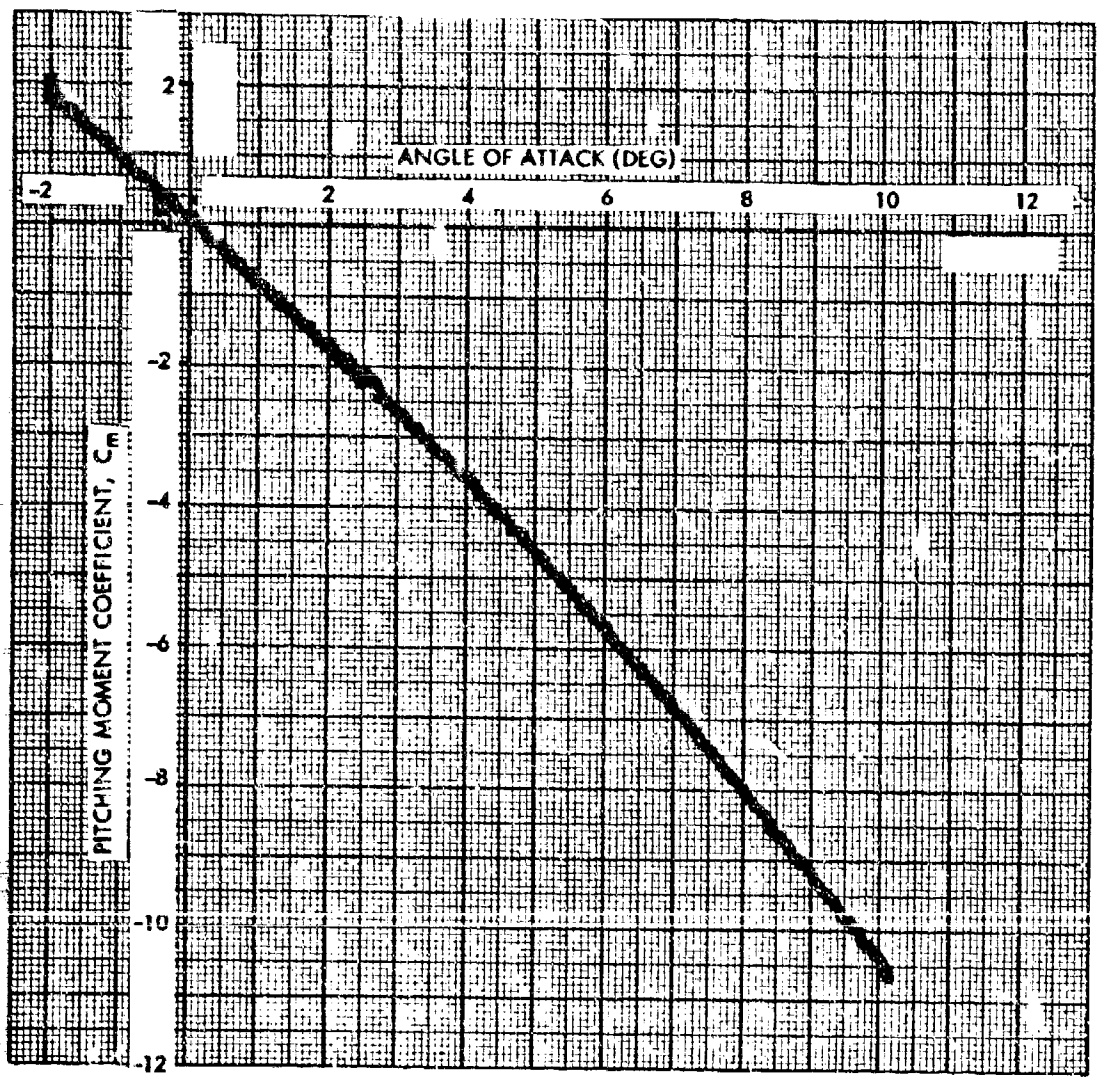

FIG. 12 PITCHING MOMENT COEFFICIENT VERSUS ANGLE OF ATTACK AT A MACH NUMBER OF 3.0 AND A FIN CANT ANGLE OF 2.0 DEGREES

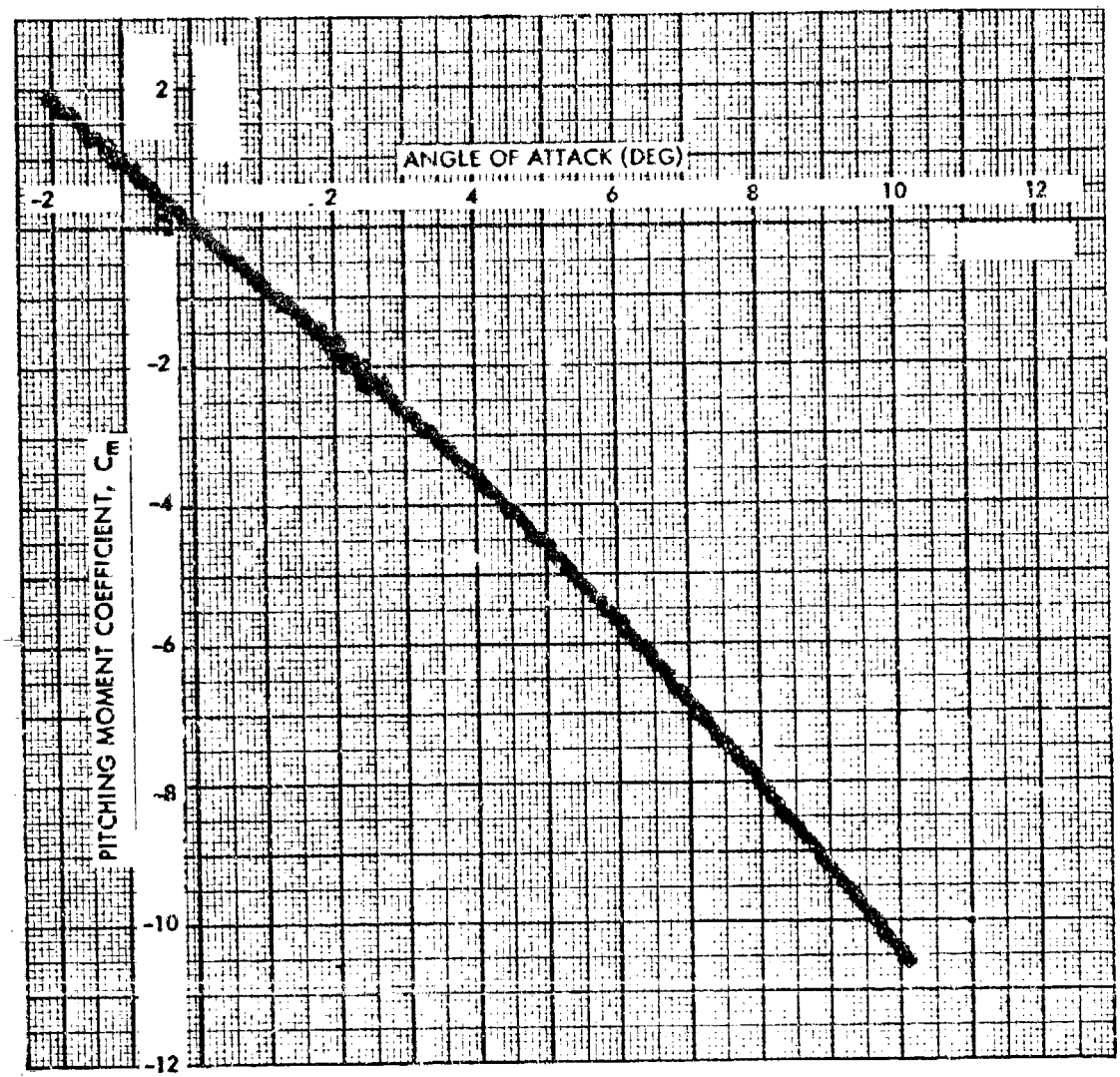

FIG. 13 PITCHING MOMENT COEFFICIENT VERSUS ANGLE OF ATTACK AT A MACH NUMBER OF 3.0 AND A FIN CANT ANGLE OF 3.25 DEGREES

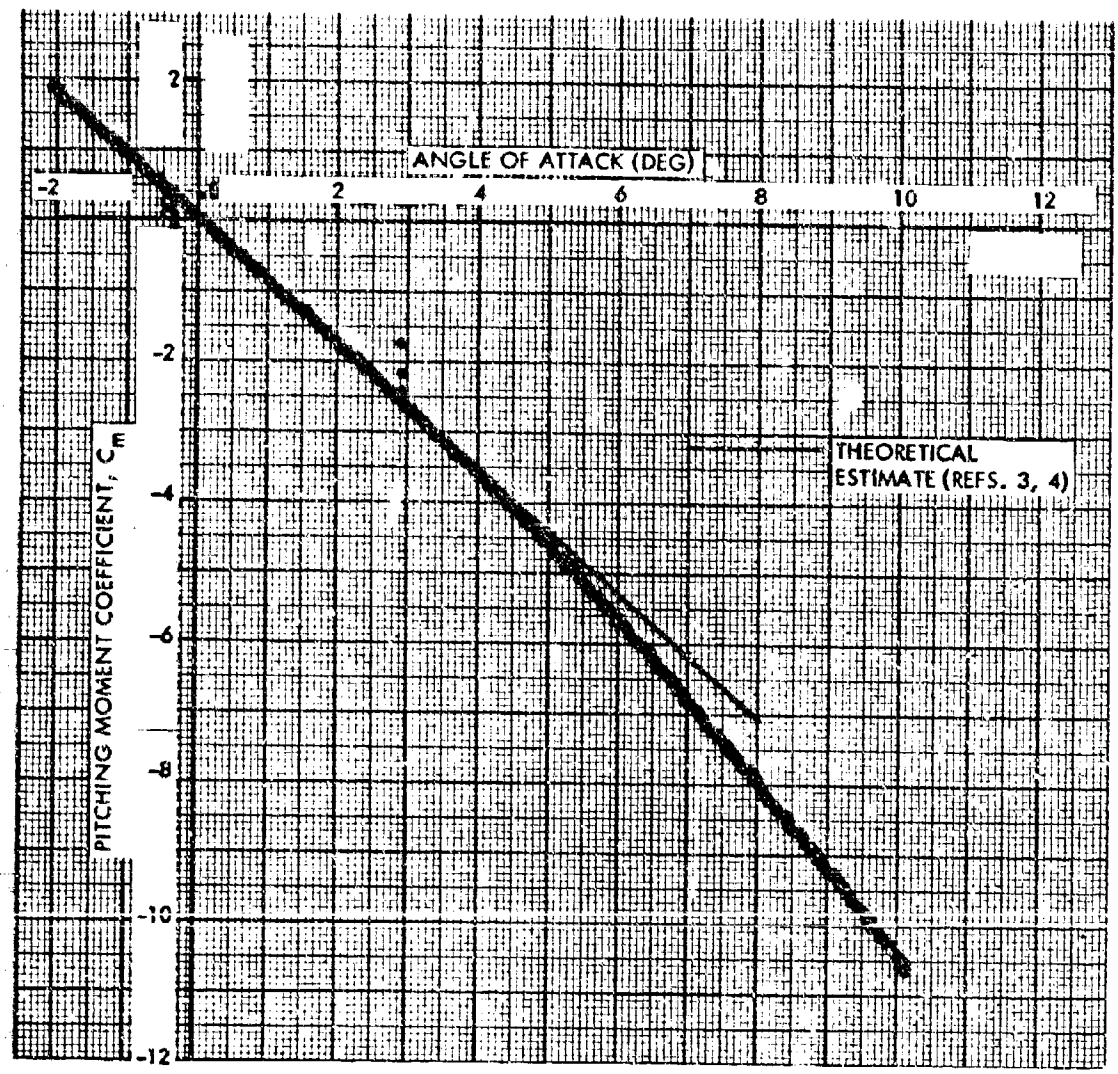

FIG. 14 PITCHING MOMENT COEFFICIENT VERSUS ANGLE OF ATTACK AT A MACH NUMBER OF 3.0 AND A FIN CANT ANGLE OF 4.50 DEGREES

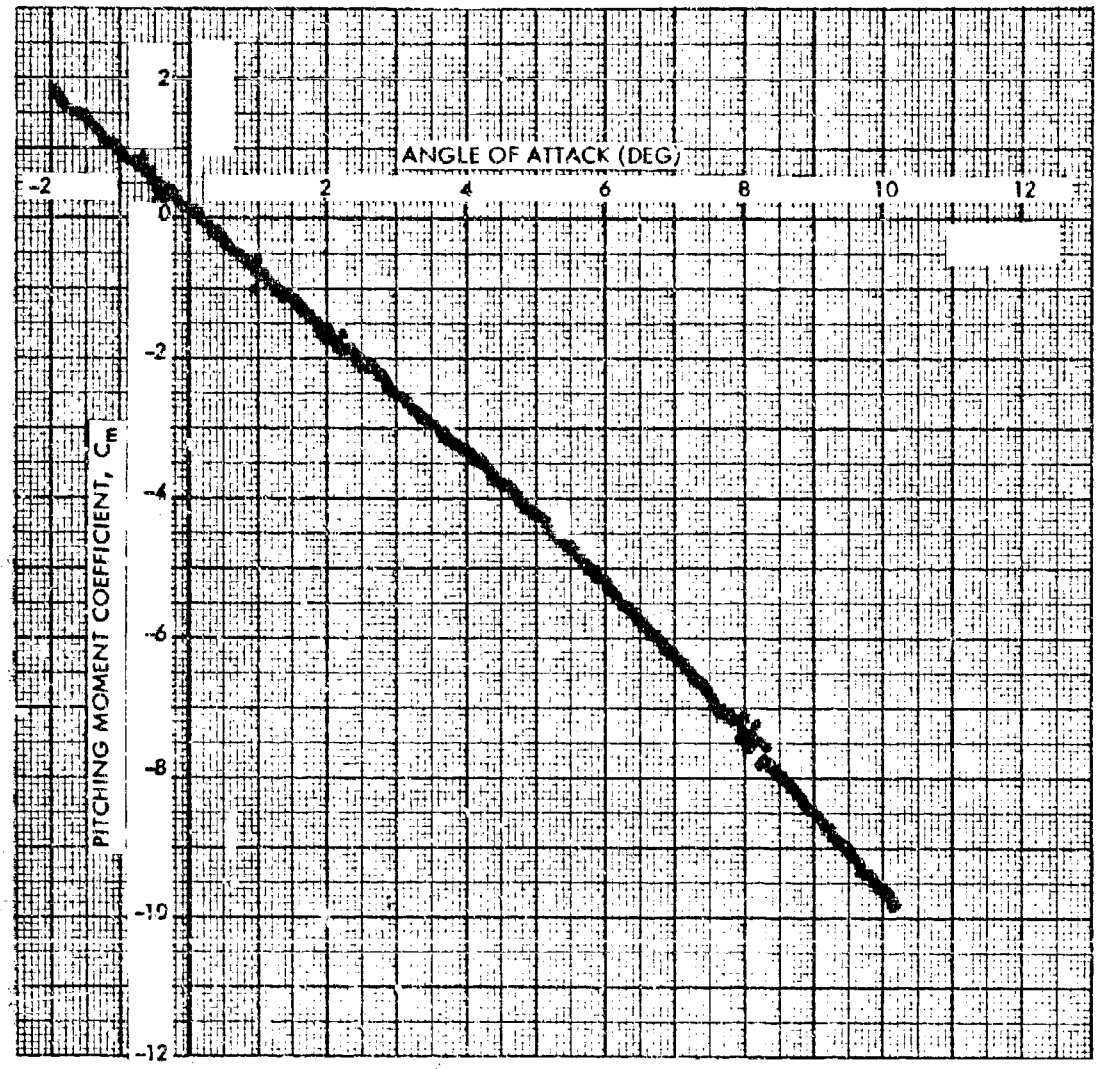

FIG. 15 PITCHING MOMENT COEFFICIENT VERSUS ANGLE OF ATTACK AT A MACH NUMBER OF 3.5 AND A FIN CANT ANGLE OF 2.0 DEGREES

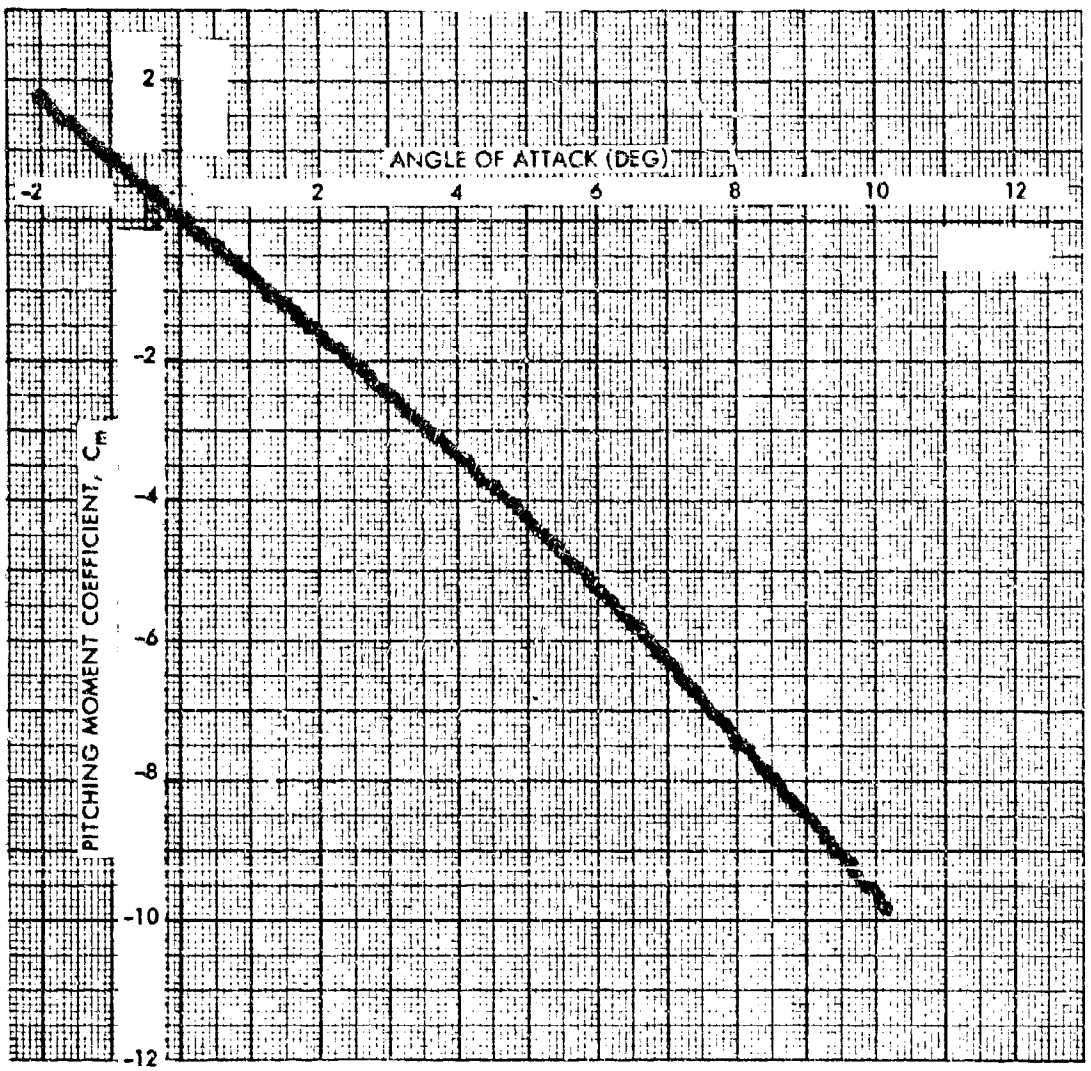

FIG. 16 PITCHING MOMENT COEFFICIENT VERSUS ANGLE OF ATTACK AT A MACH NUMBER OF 3.5 AND A FIN CANT ANGLE OF 3.25 DEGREES

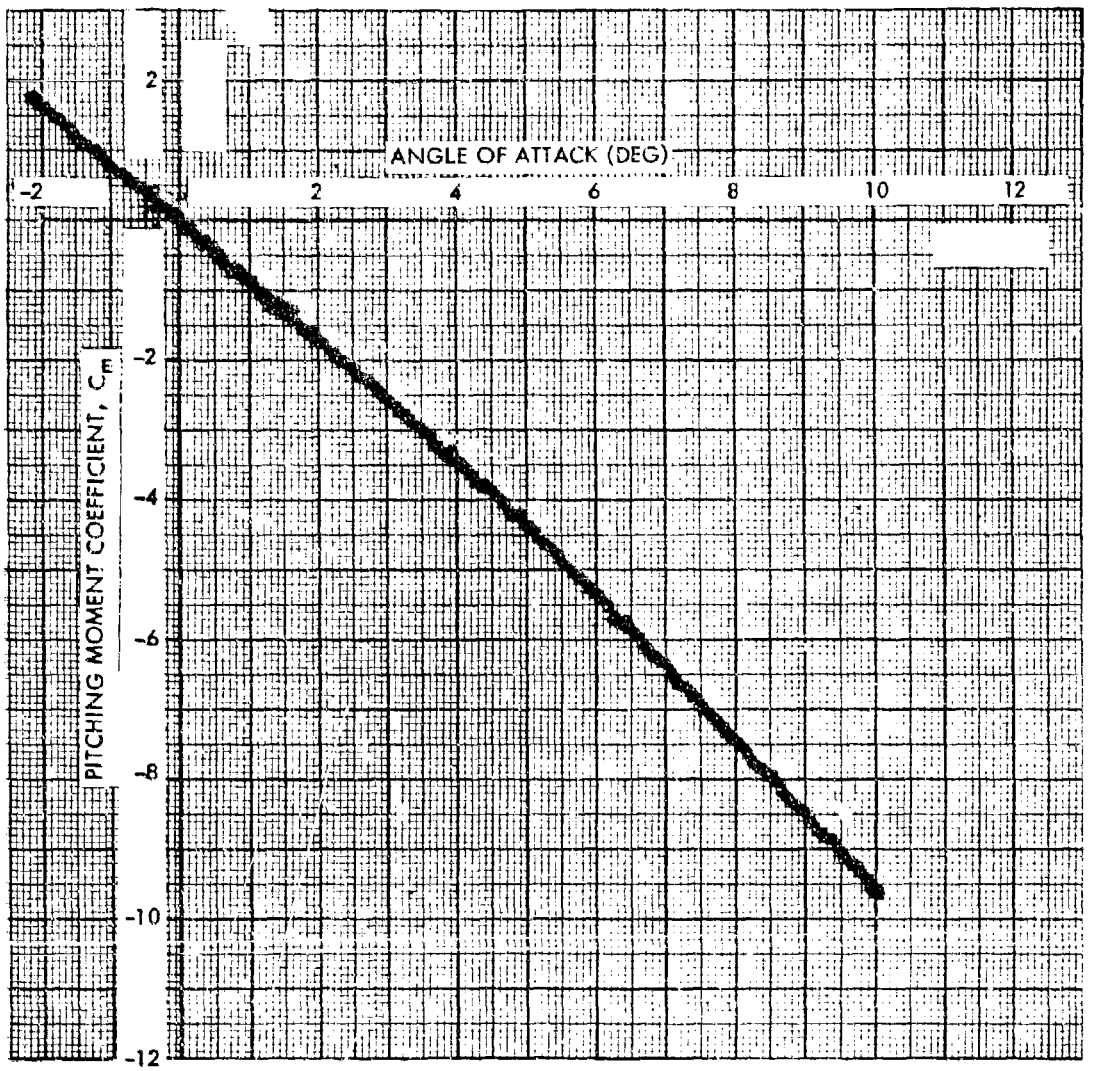

FIG. 17 PITCHING MOMENT COEFFICIENT VERSUS ANGLE OF ATTACK AT A MACH NUMBER OF 3.5 AND A FIN CANT ANGLE OF 4.50 DEGREES

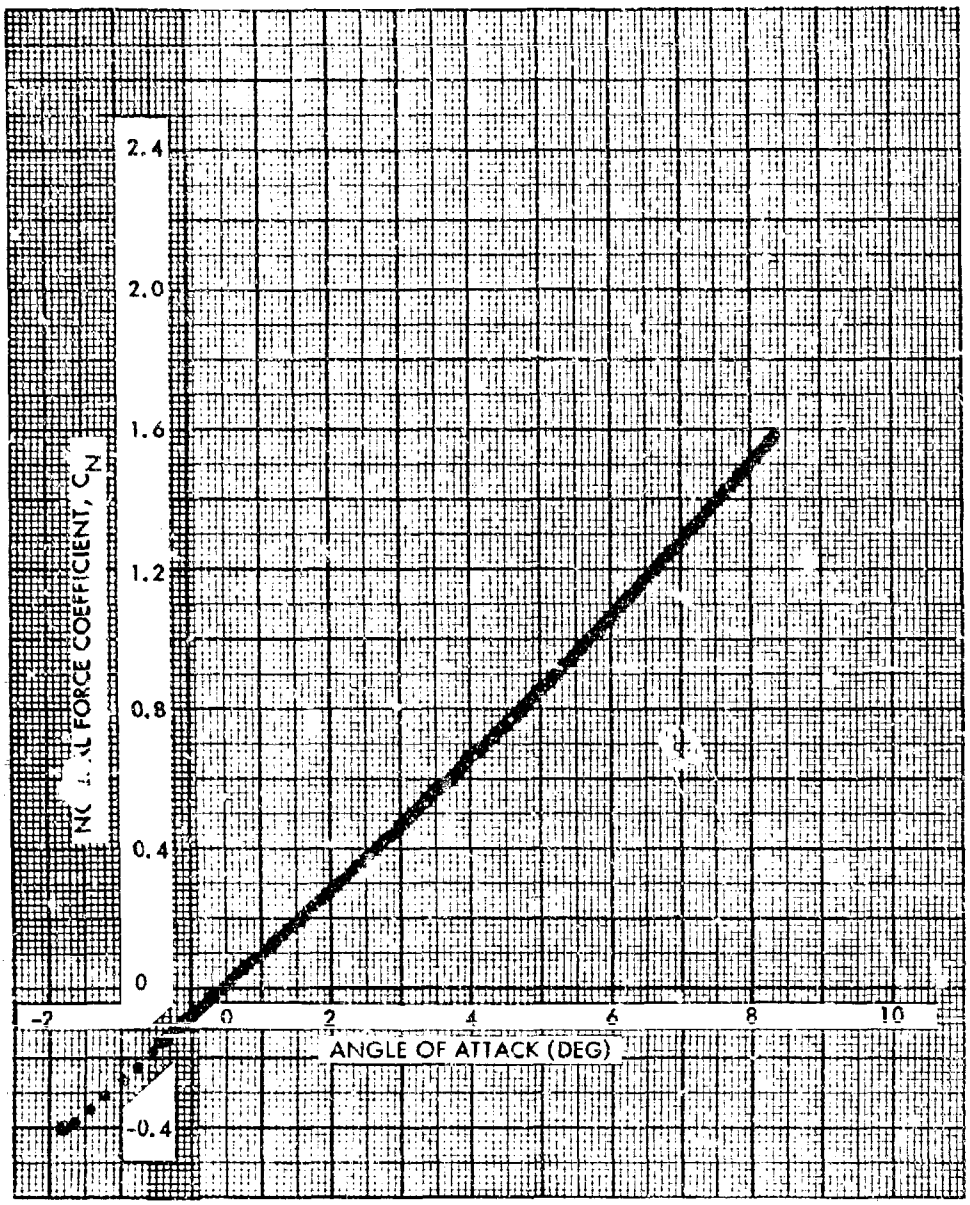

FIG. 18 NORMAL FORCE COEFFICIENT VERSUS ANGLE OF ATTACK AT A MACH NUMBER OF 1.76 AND A FIN CANT ANGLE OF 2.0 DEGREES

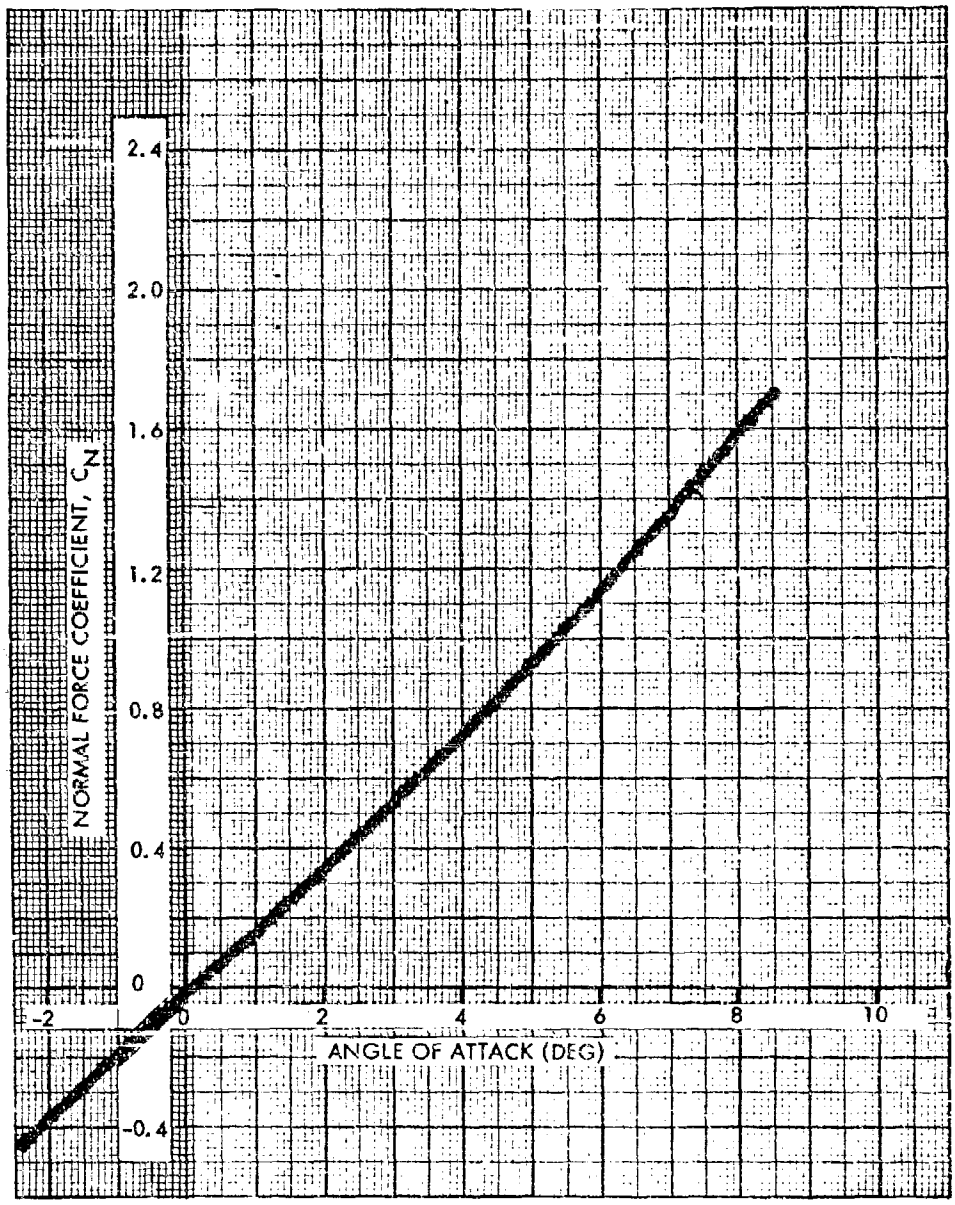

FIG. 19 NORMAL FORCE COEFFICIENT VERSUS ANGLE OF ATTACK AT A MACH NUMBER OF 1.76 AND A FIN CANT ANGLE OF 3.25 DEGREES

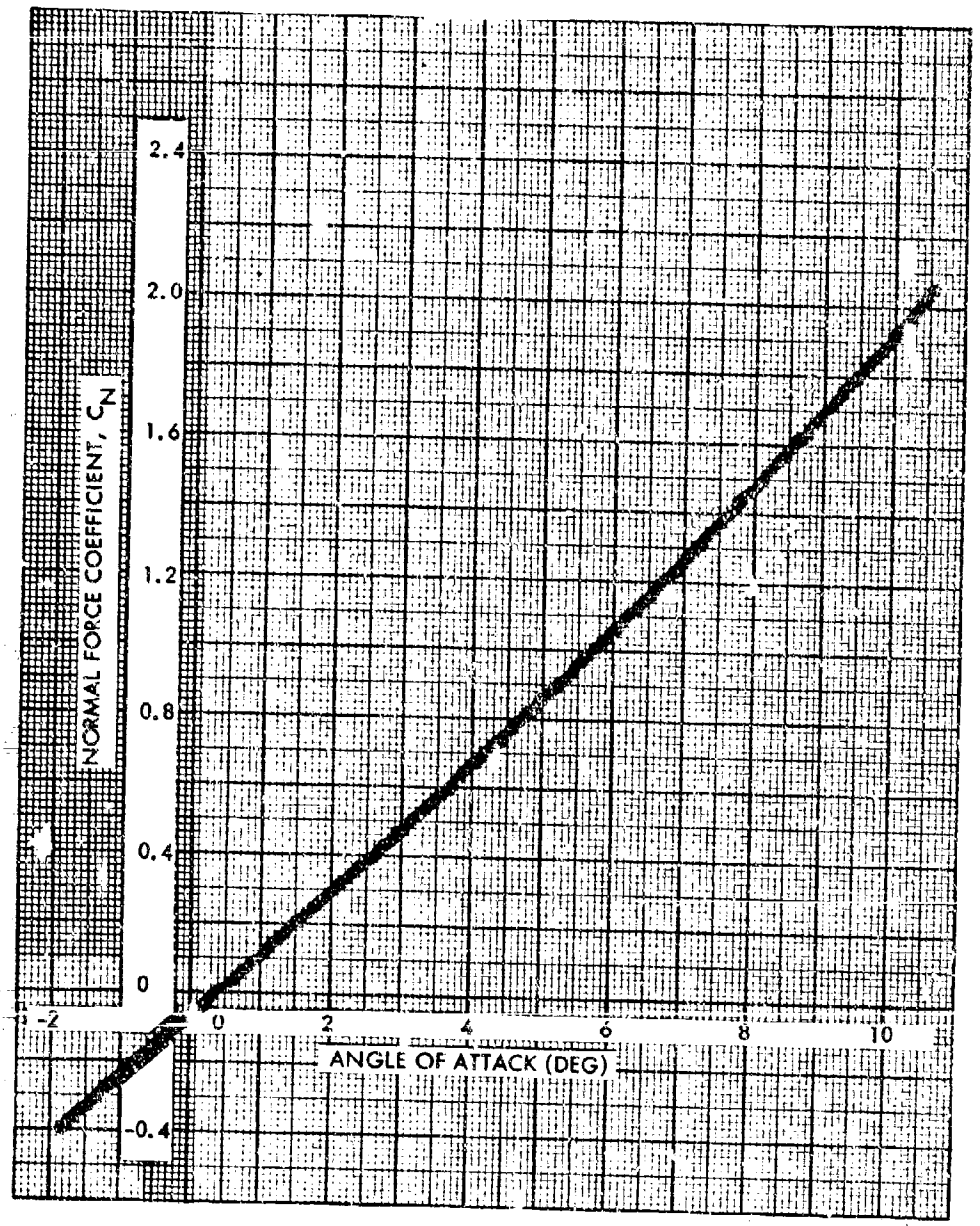

FIG. 20 NORMAL FORCE COEFFICIENT VERSUS ANGLE OF ATTACK AT A MACH NUMBER OF 2.0 AND A FIN CANT ANGLE OF 2.0 DEGREES

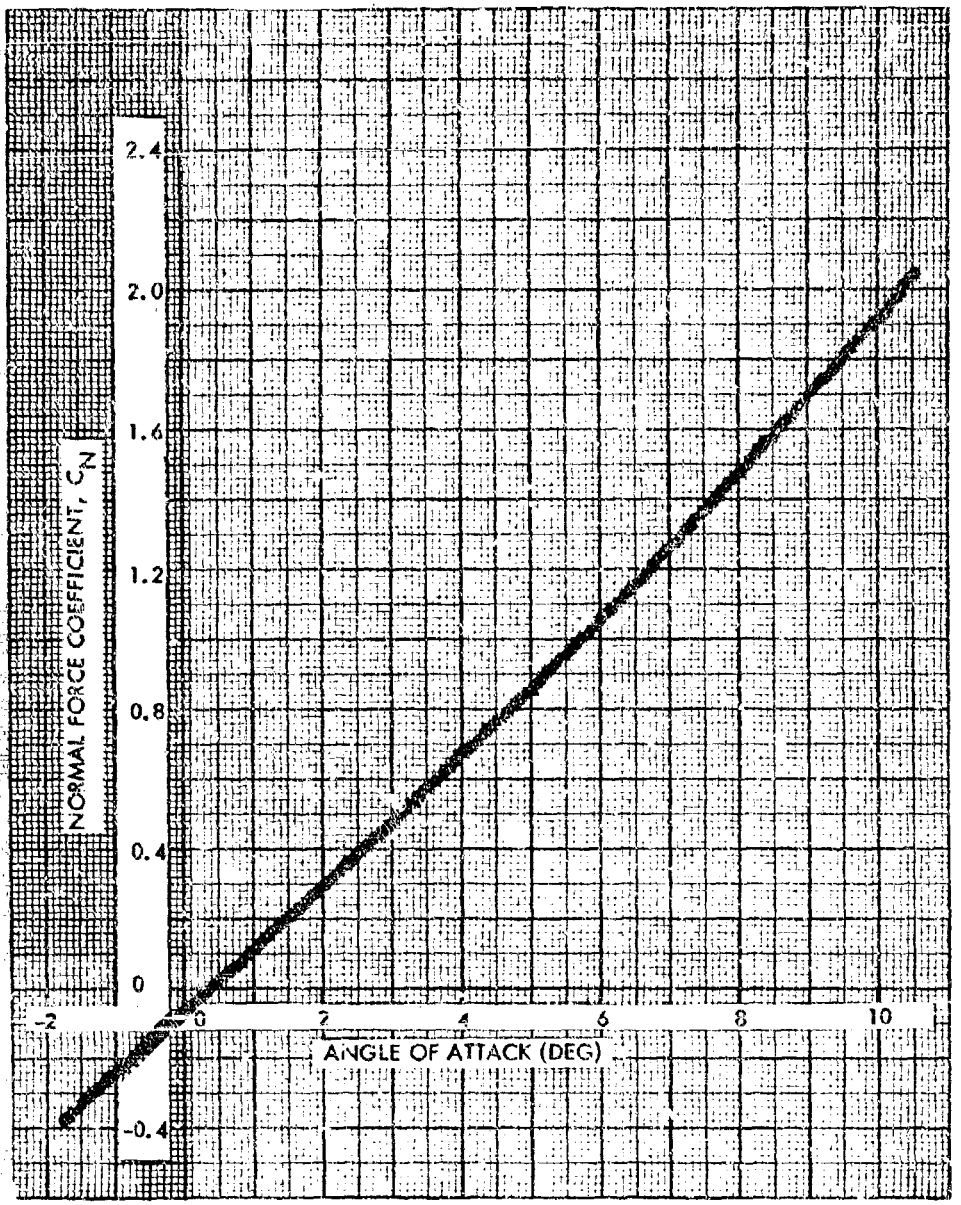

FIG. 21 NORMAL FORCE COEFFICIENT VERSUS ANGLE OF ATTACK AT A MACH NUMBER OF 2.0 AND A FIN CANT ANGLE OF 3.25 DEGREES

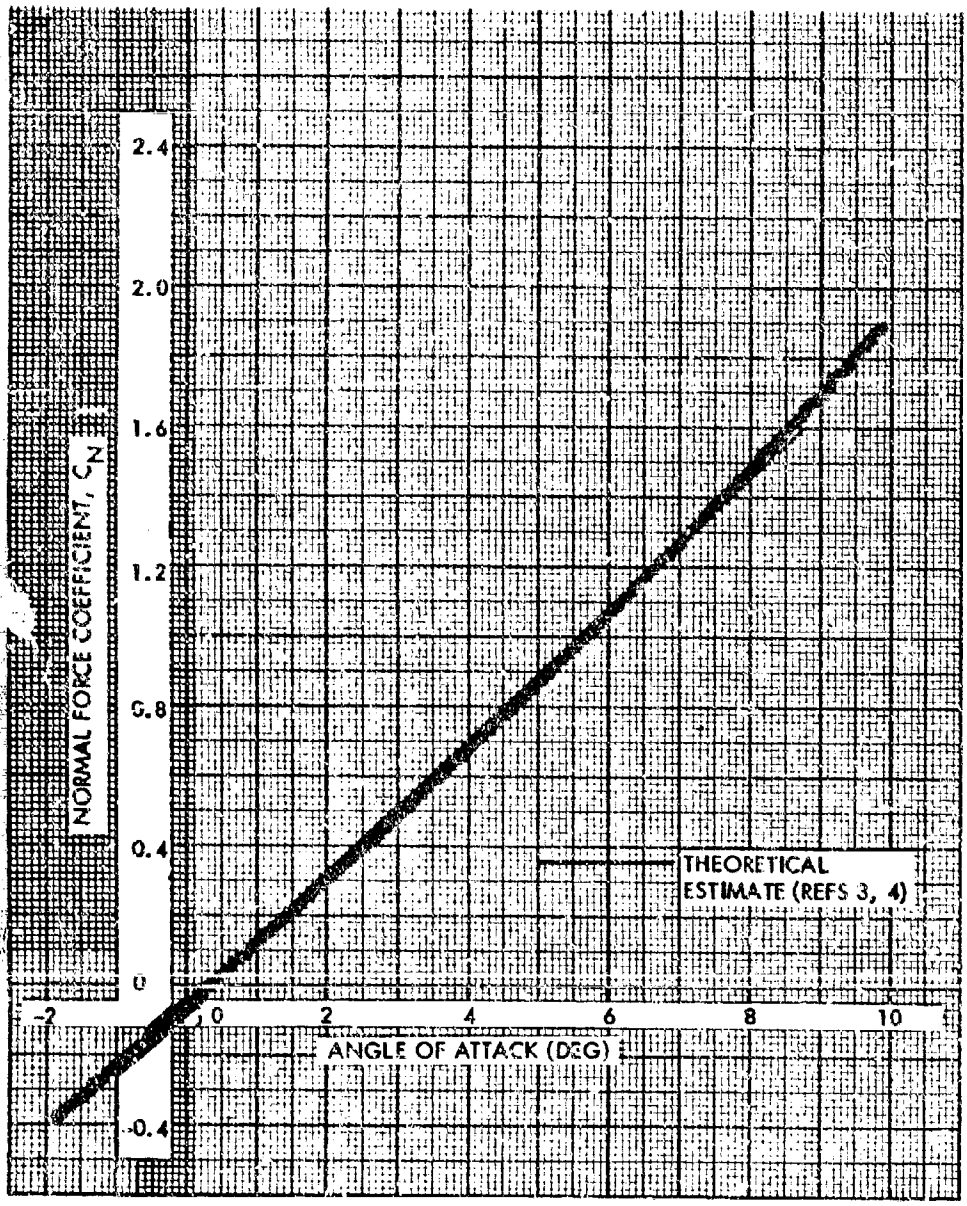

FIG. 22 NORMAL FORCE COEFFICIENT VERSUS ANGLE OF ATTACK AT A MACH NUMBER OF 2.0 AND A FIN CANT ANGLE OF 4.50 DEGREES

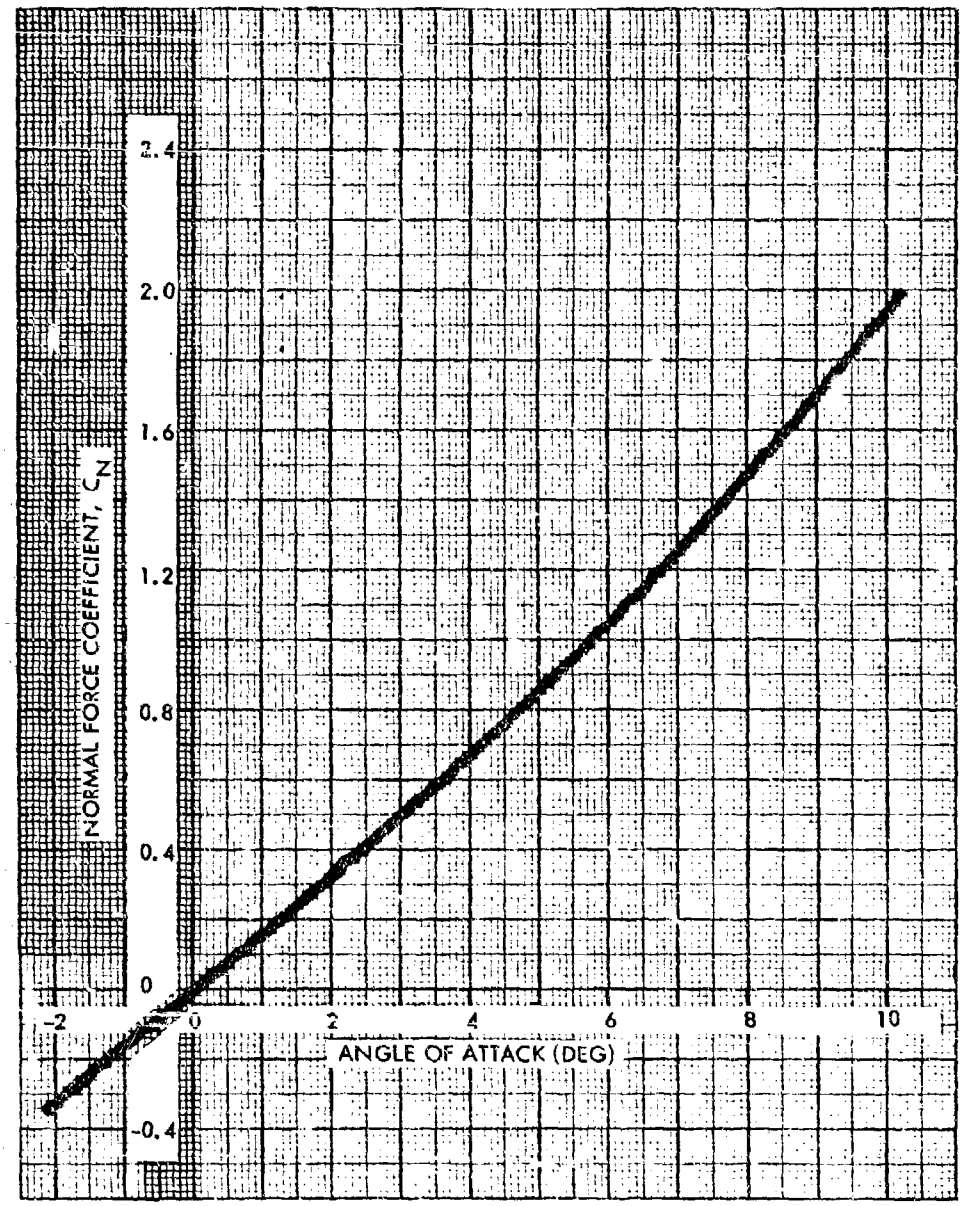

FIG. 23 NORMAL FORCE COEFFICIENT VERSUS ANGLE OF ATTACK AT A MACH NUMBER OF 2.5 AND A FIN CANT ANGLE OF 2.0 DEGREES

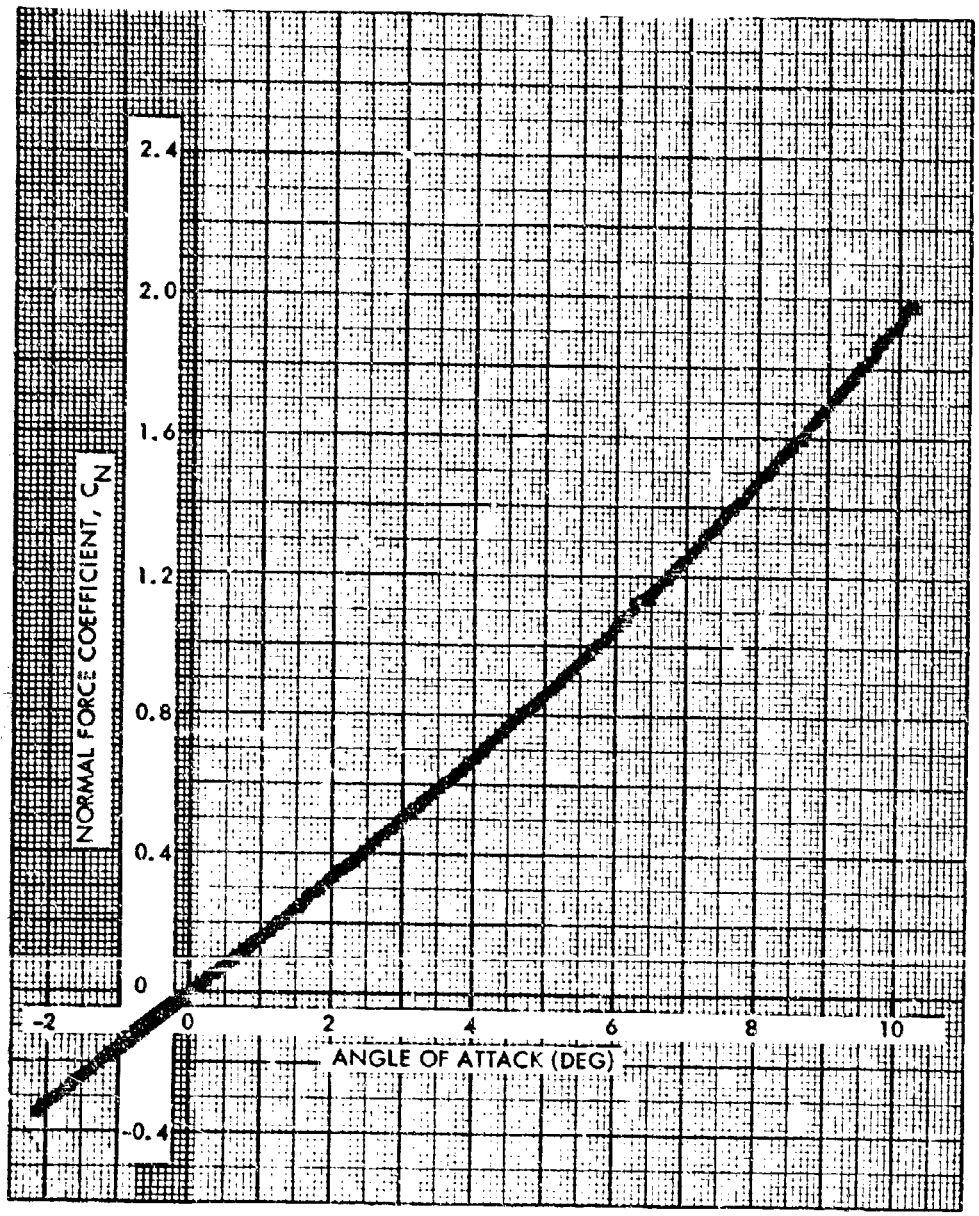

FIG. 24 NORMAL FORCE COEFFICIENT VERSUS ANGLE OF ATTACK AT A MACH NUMBER OF 2.5 AND A FIN CANT ANGLE OF 3.25 DEGREES

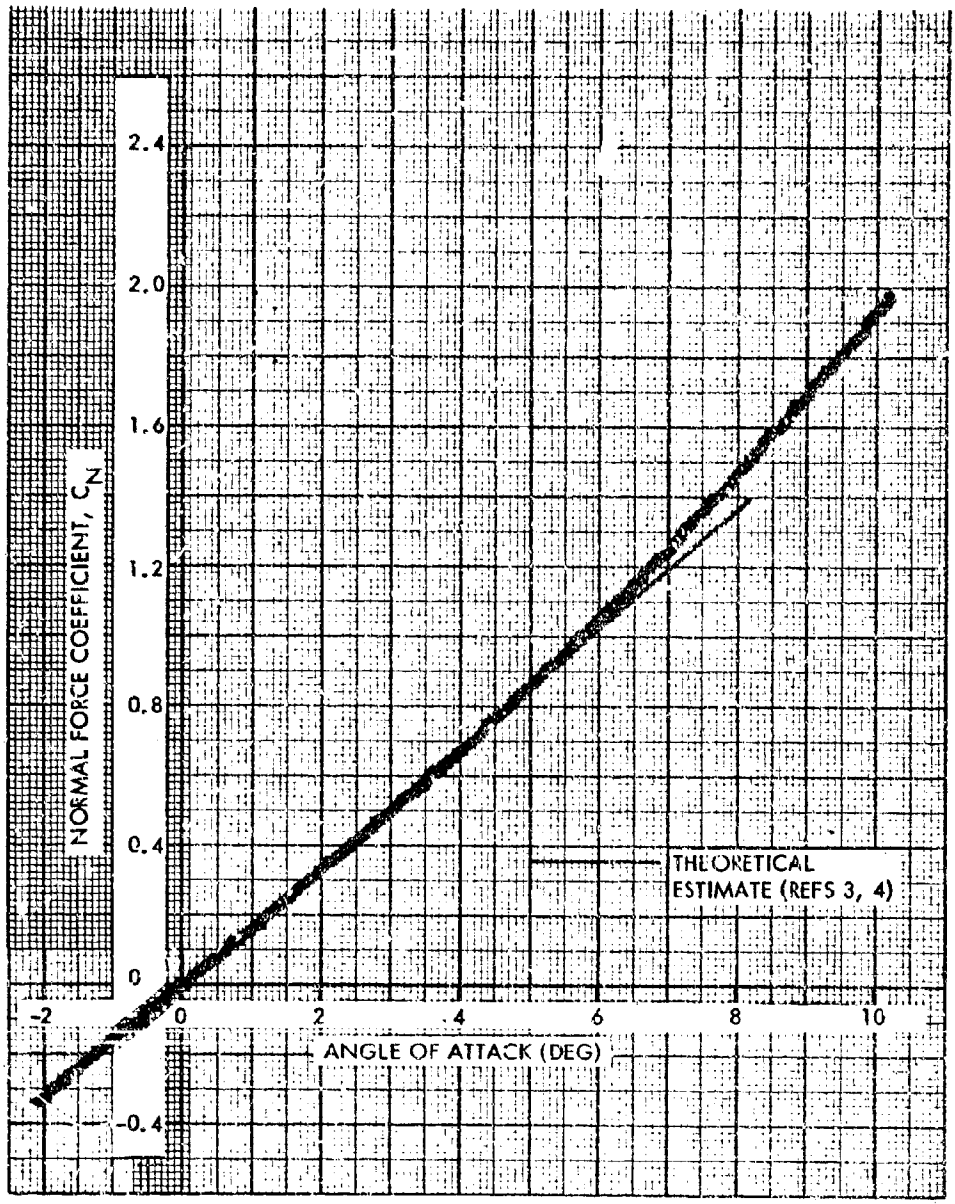

FIG. 25 NORMAL FORCE COEFFICIENT VERSUS ANGLE OF ATTACK AT A MACH NUMBER OF 2.5 AND A FIN CANT ANGLE OF 4.50 DEGREES

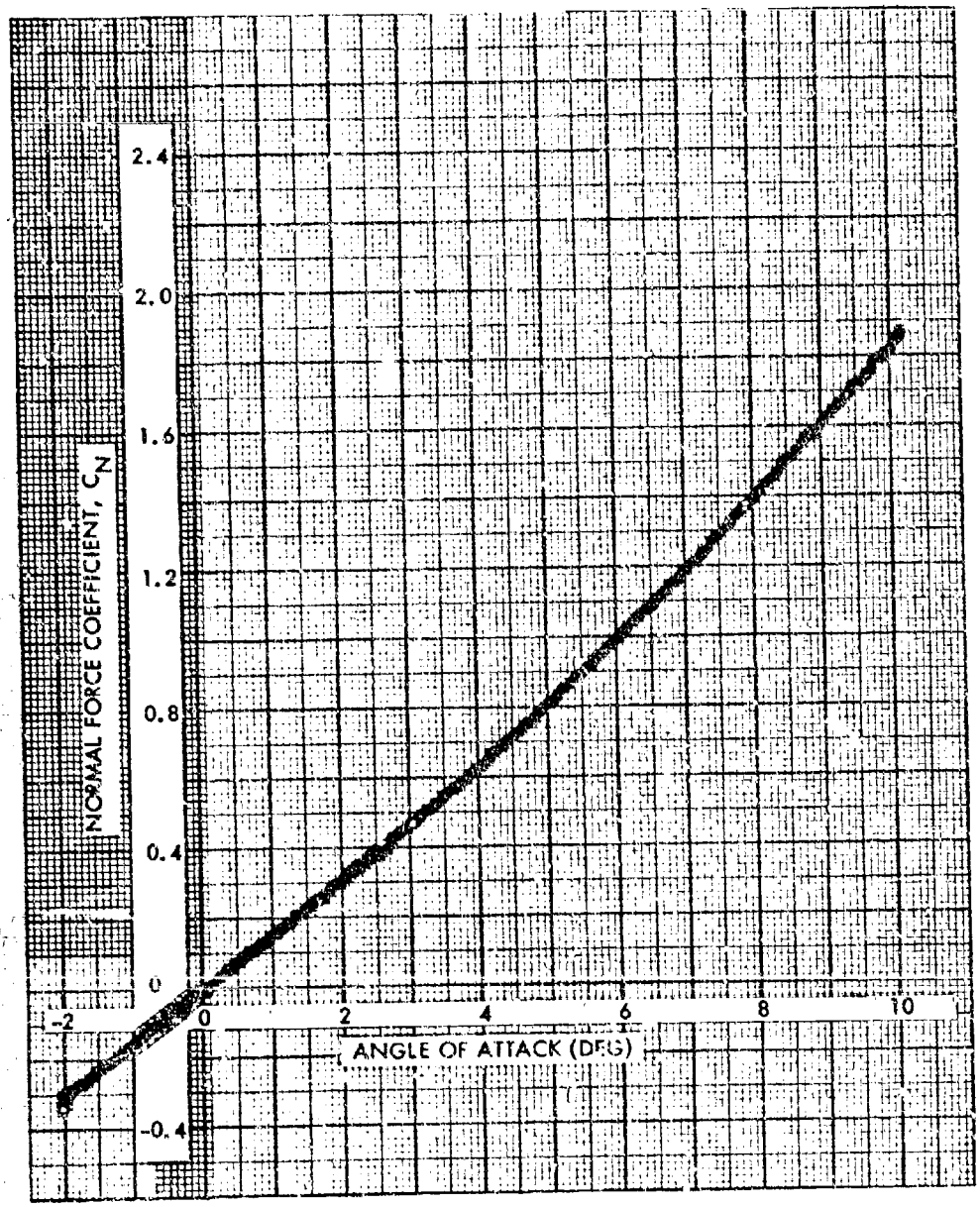

FIG. 26 NORMAL FORCE COEFFICIENT VERSUS ANGLE OF ATTACK AT A MACH NUMBER OF 3.0 AND A FIN CANT ANGLE OF 2.0 DEGREES

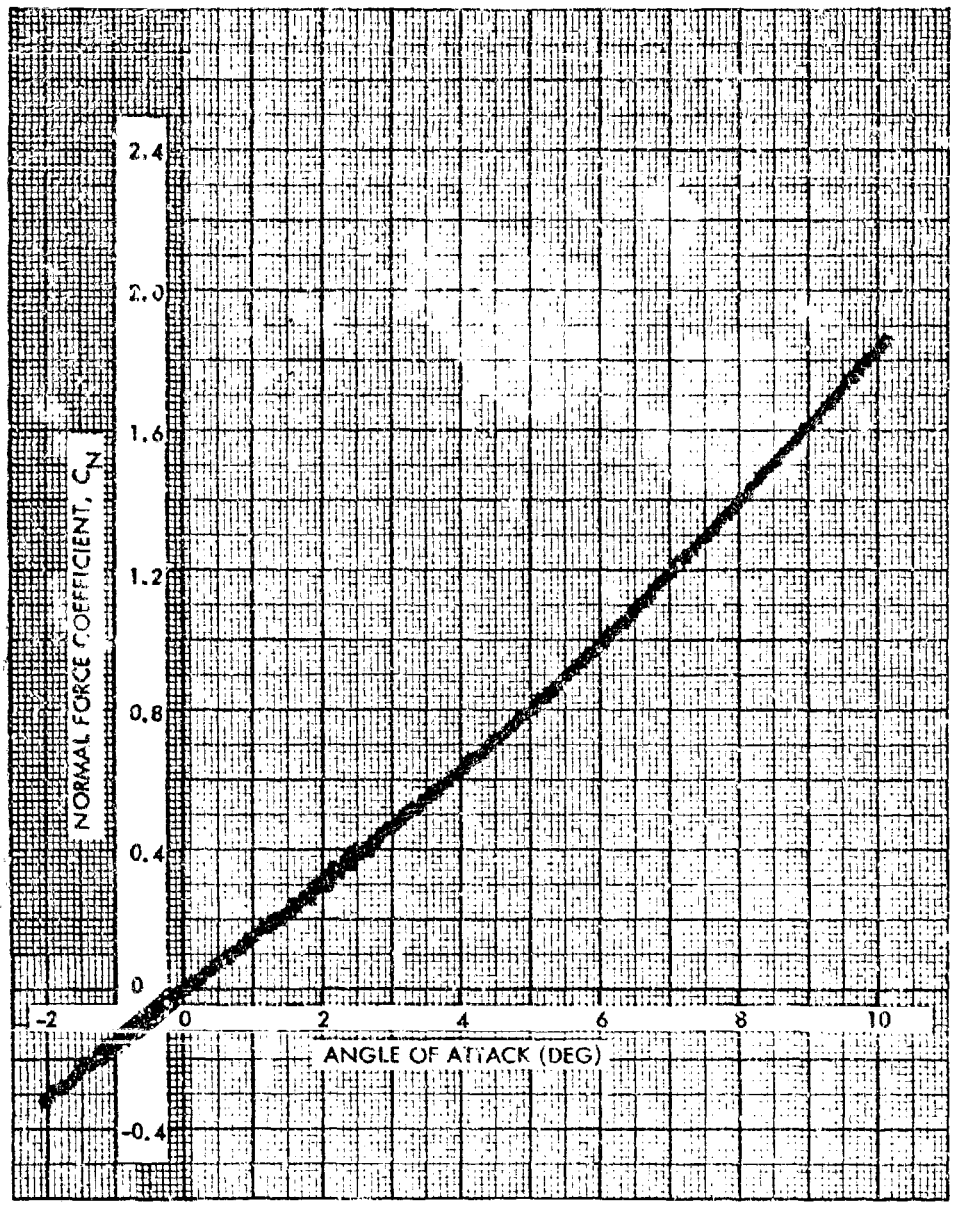

FIG. 27 NORMAL FORCE COEFFICIENT VERSUS ANGLE OF ATTACK AT A MACH NUMBER OF 3.0 AND A FIN CANT ANGLE OF 3.25 DEGREES

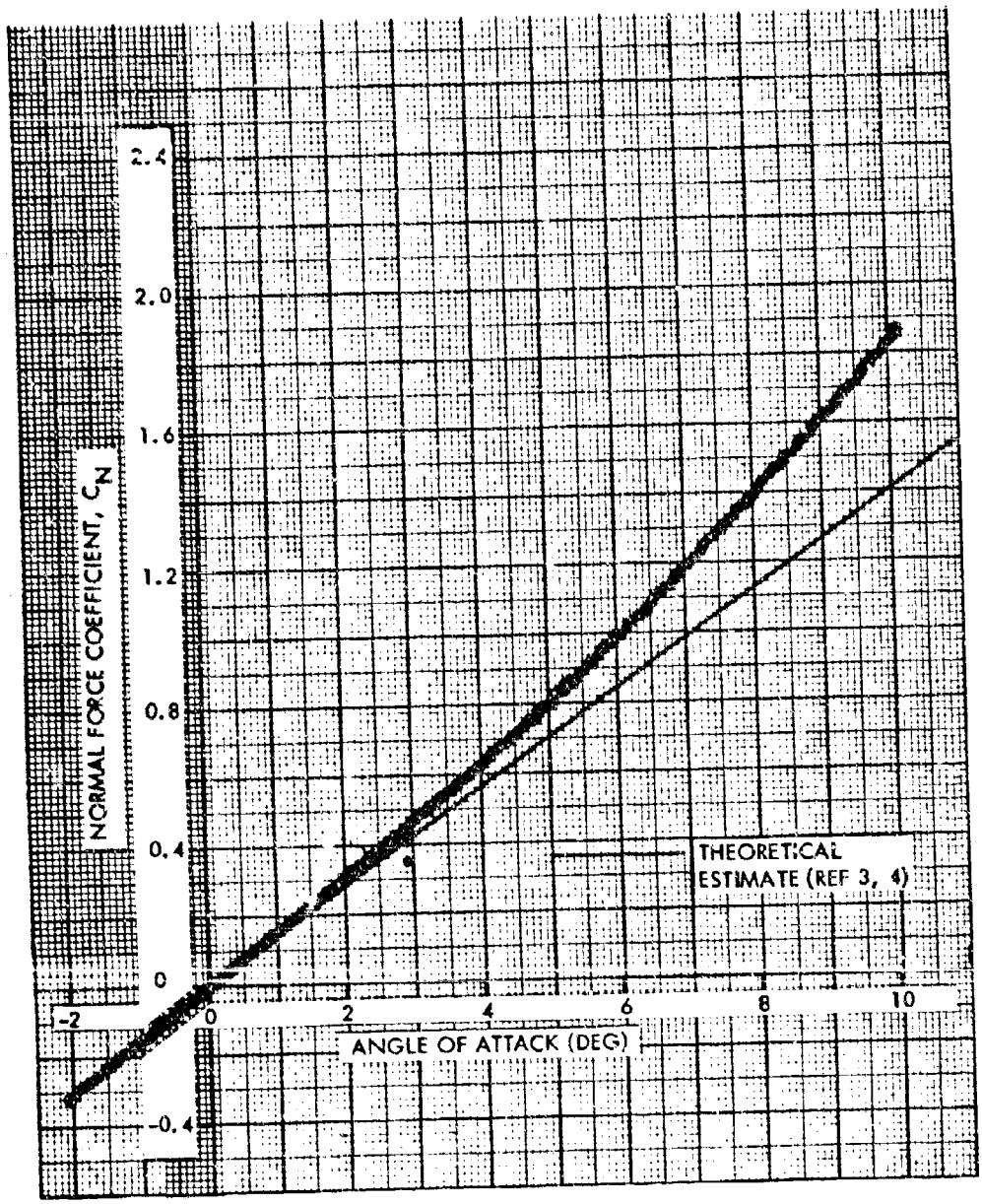

FIG. 28 NORMAL FORCE COEFFICIENT VERSUS ANGLE OF ATTACK AT A MACH NUMBER OF 3.0 AND A FIN CANT ANGLE OF 4.50 DEGREES

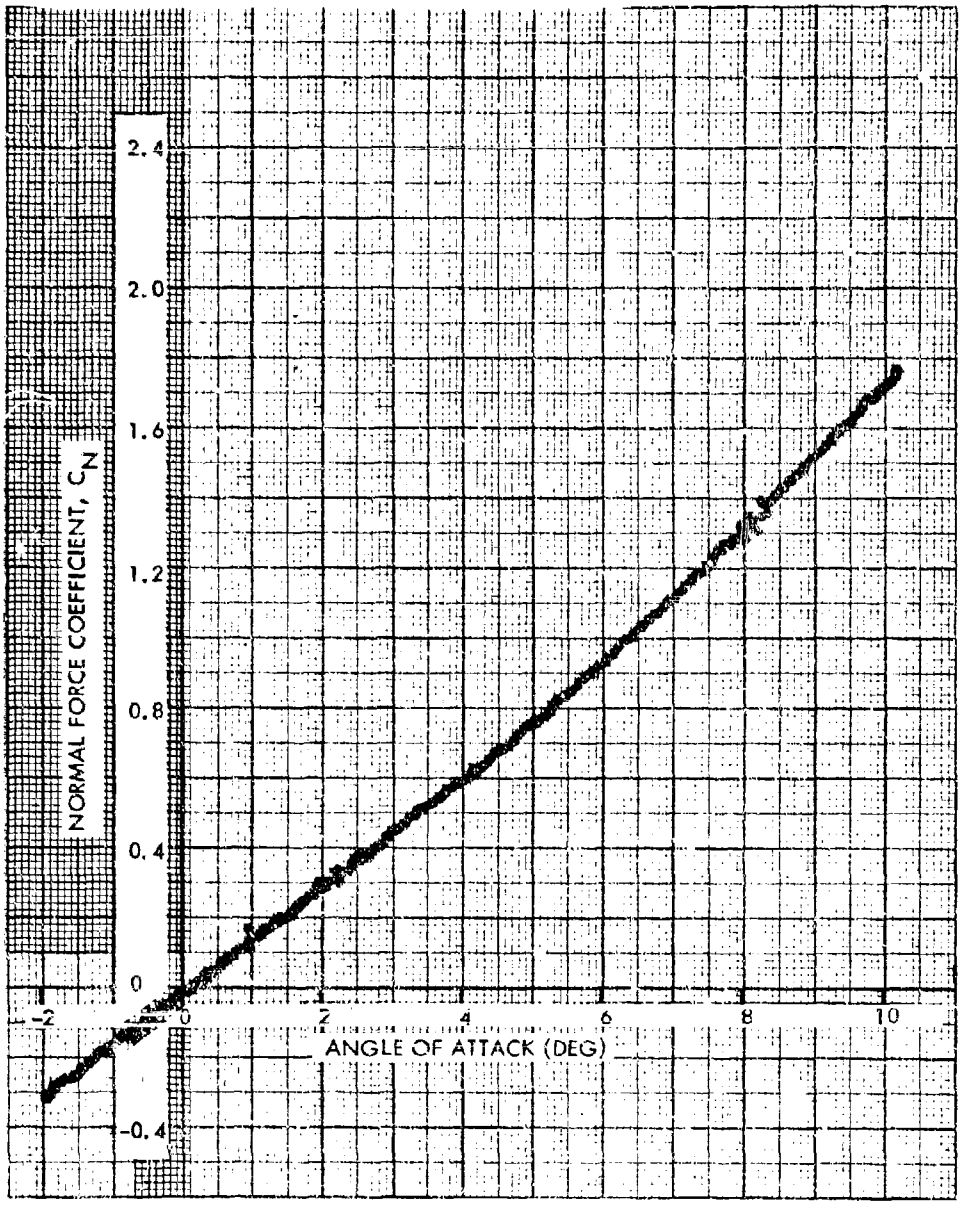

FIG. 29 NORMAL FORCE COEFFICIENT VERSUS ANGLE OF ATTACK AT A MACH NUMBER OF 3.5 AND A FIN CANT ANGLE OF 2.0 DEGREES

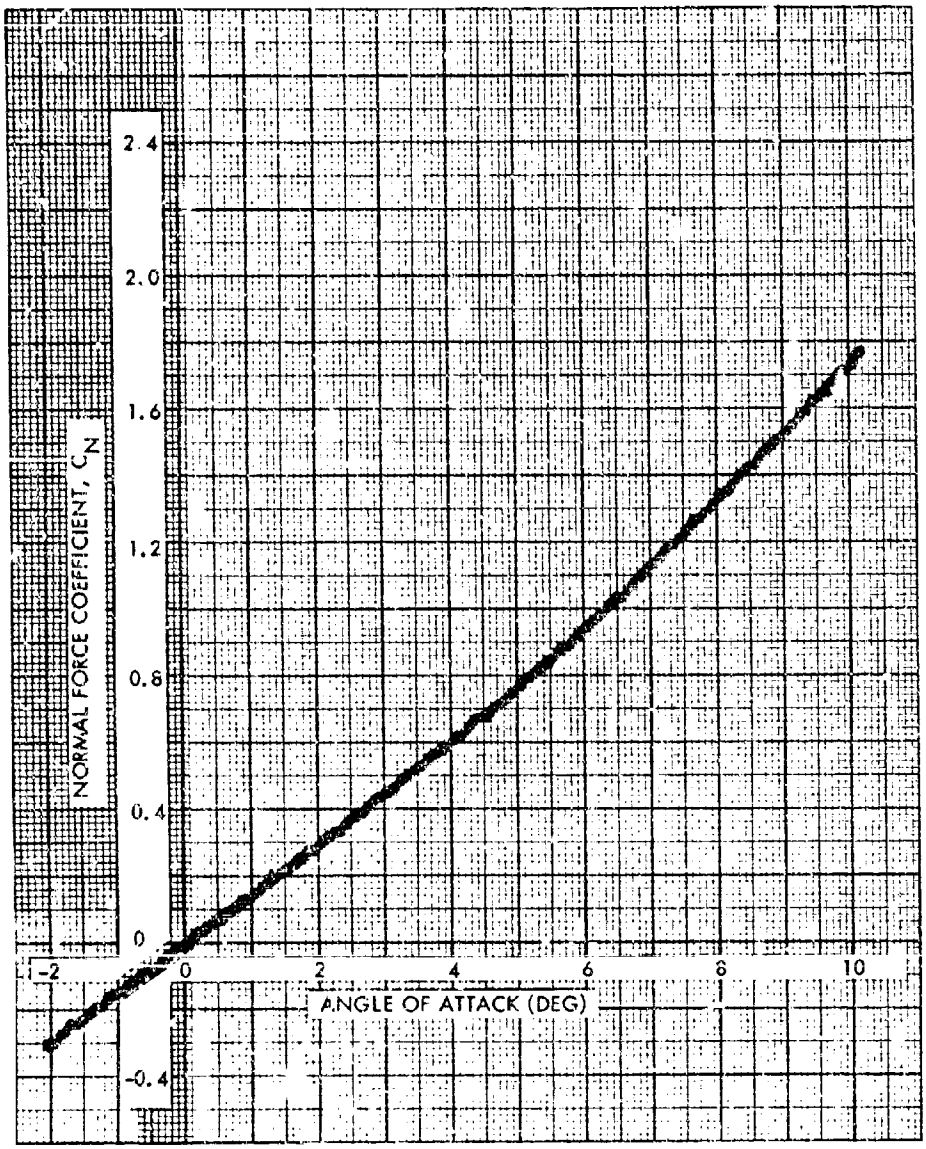

FIG. 30 NORMAL FORCE COEFFICIENT VERSUS ANGLE OF ATTACK AT A MACH NUMBER OF 3.5 AND A FIN CANT ANGLE OF 3.25 DEGREES

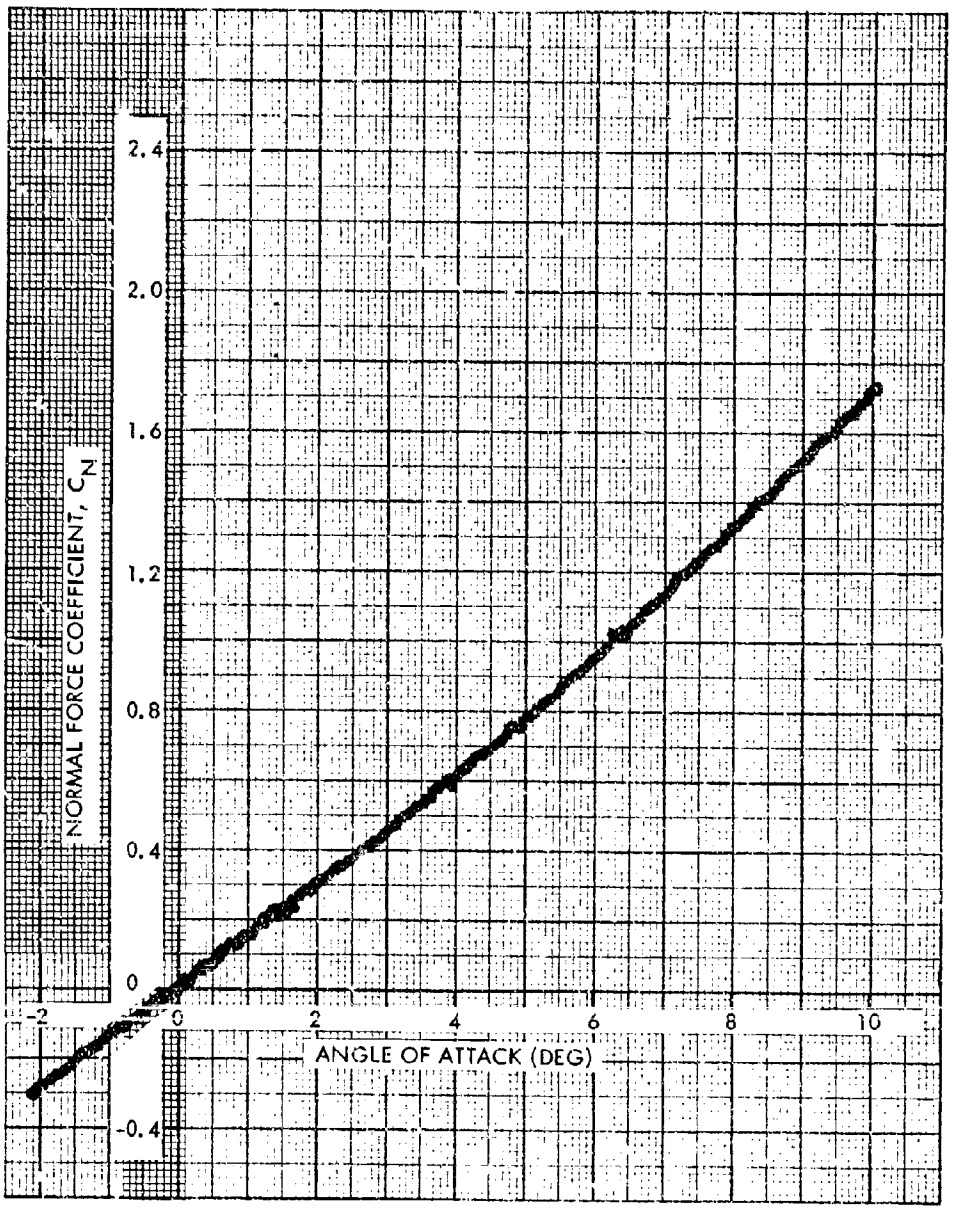

FIG. 31 NORMAL FORCE COEFFICIENT VERSUS ANGLE OF ATTACK AT A MACH NUMBER OF 3.5 AND A FIN CANT ANGLE OF 4.50 DEGREES

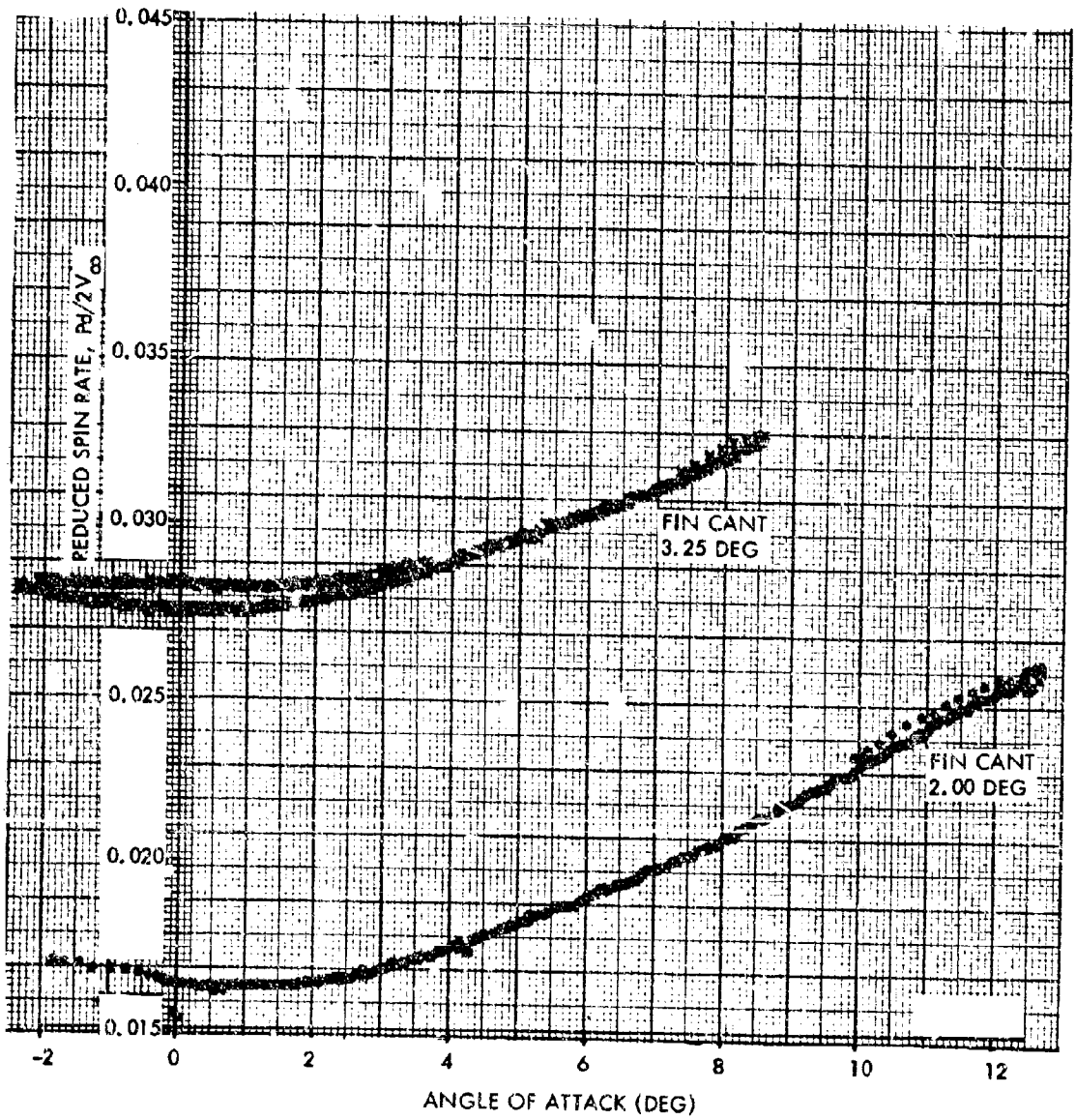

FIG. 32 REDUCED SPIN RATE VERSUS ANGLE OF ATTACK FOR INDICATED ANGLES OF FIN CANT AT A MACH NUMBER 1.76

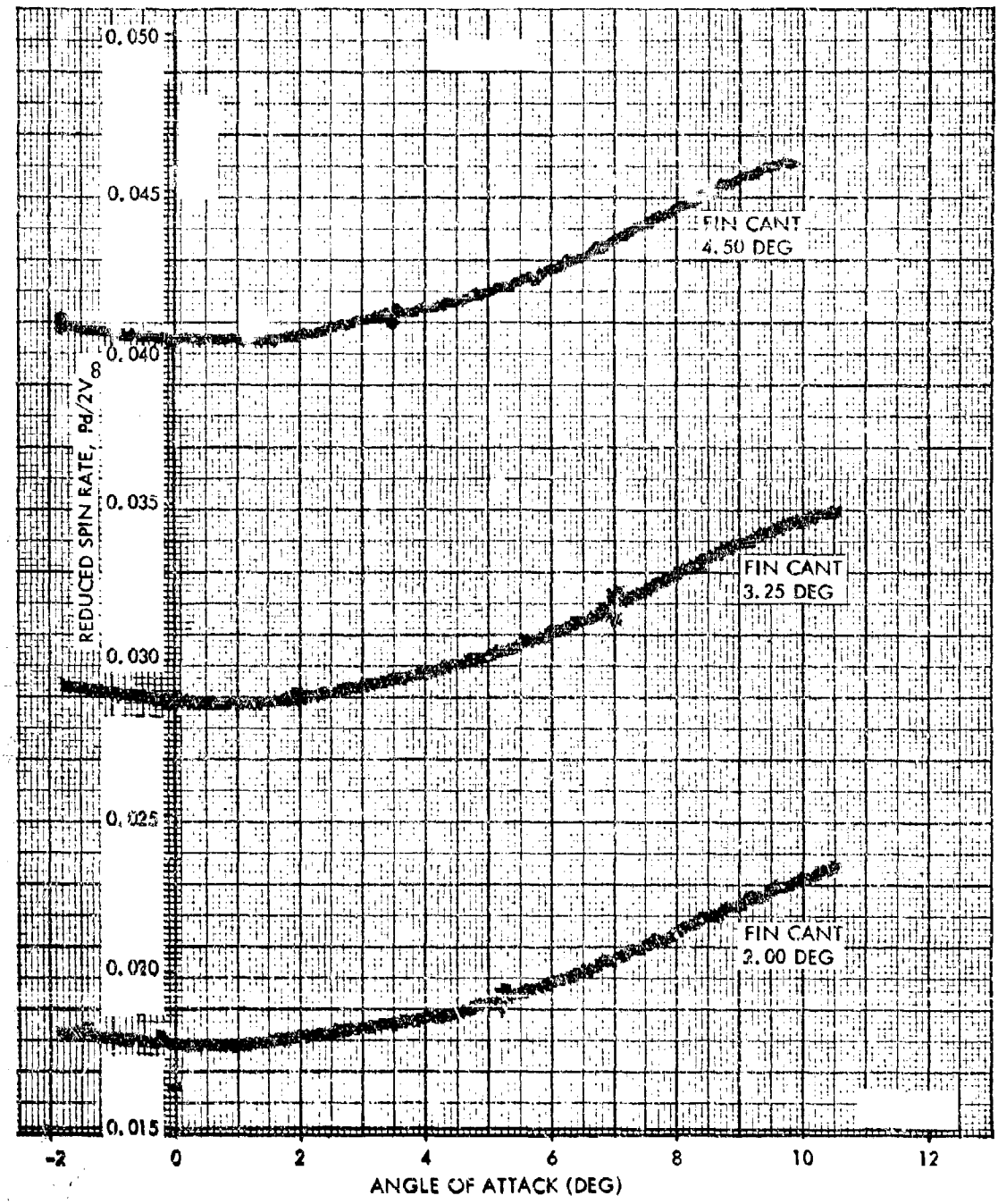

FIG. 33 REDUCED SPIN RATE VERSUS ANGLE OF ATTACK FOR INDICATED ANGLES OF FIN CANT AT A MACH NUMBER OF 2.0

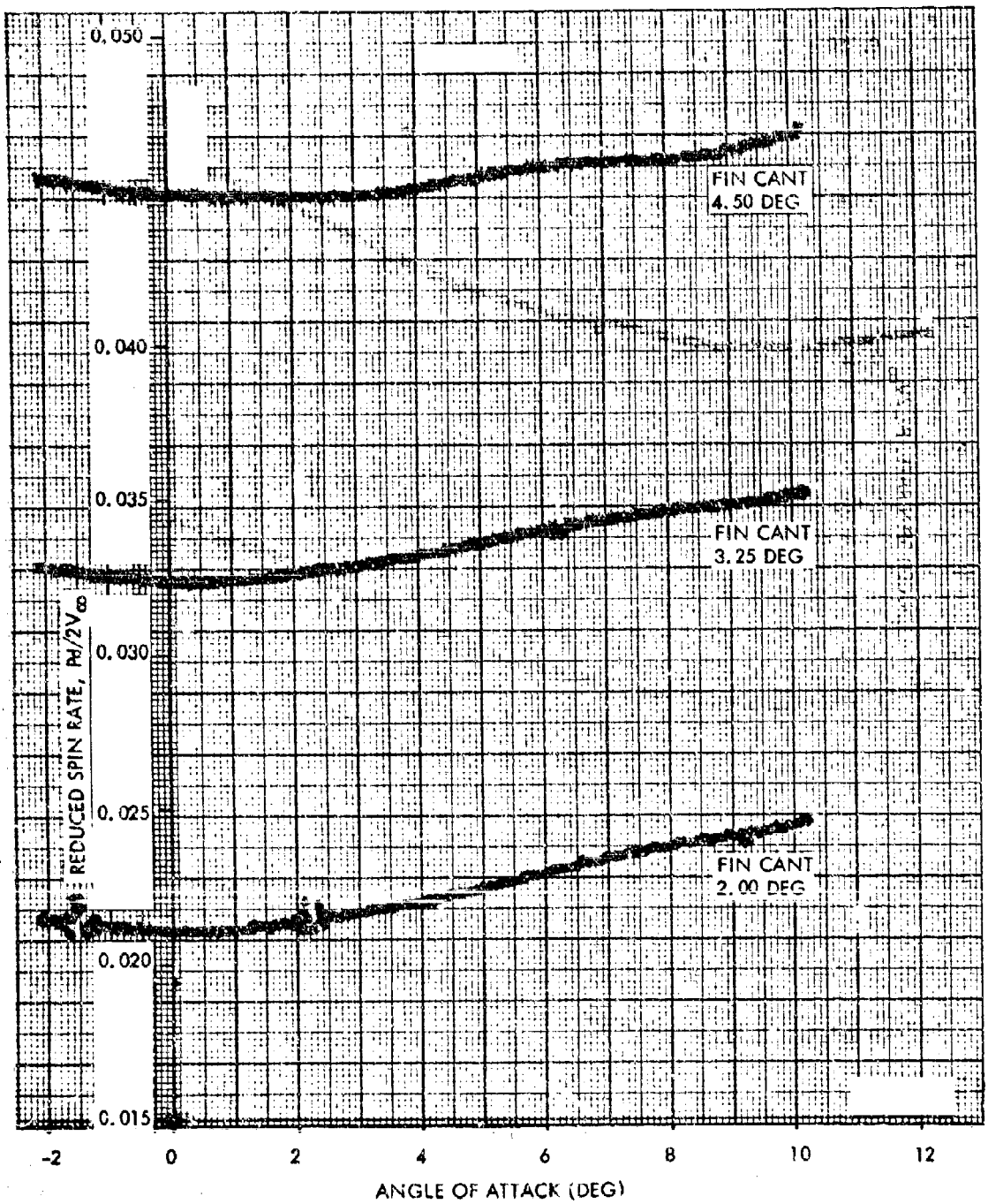

FIG. 34 REDUCED SPIN RATE VERSUS ANGLE OF ATTACK FOR INDICATED ANGLES OF FIN CANT AT A MACH NUMBER OF 2.5

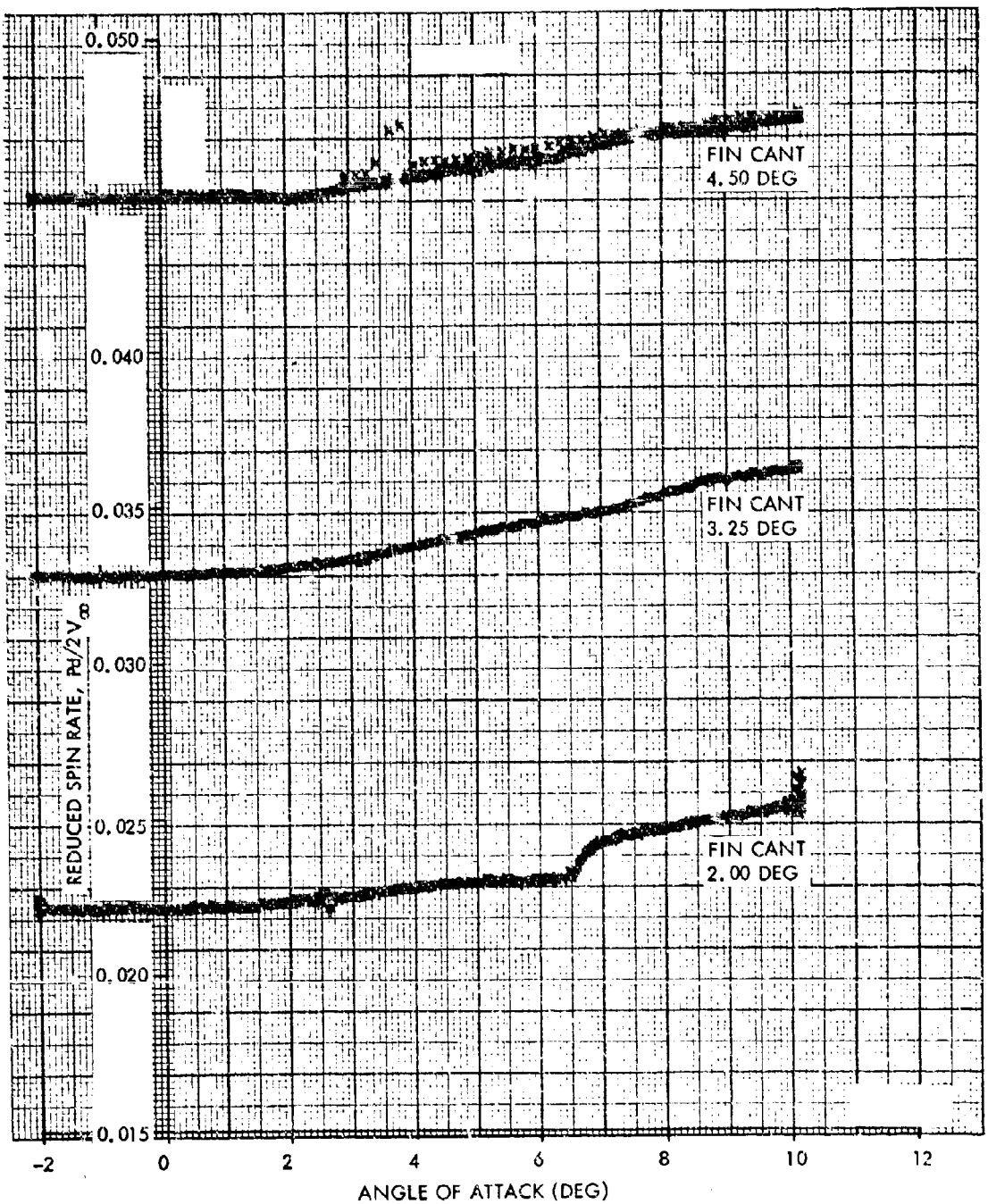

FIG. 35 REDUCED SPIN RATE VERSUS ANGLE OF ATTACK FOR INDICATED ANGLES OF FIN CANT AT A MACH NUMBER OF 3.0

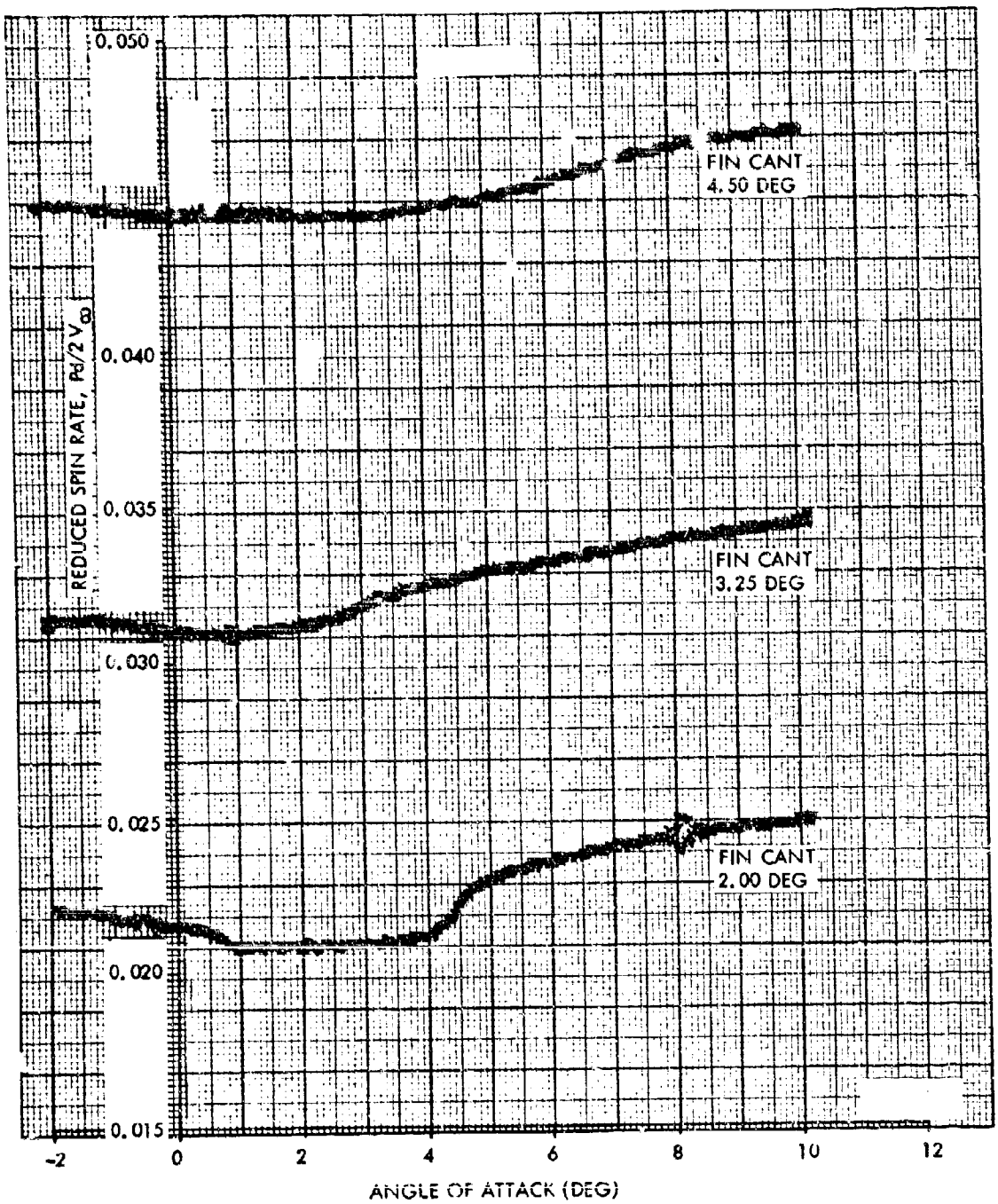

FIG. 36 REDUCED SPIN RATE VERSUS ANGLE OF ATTACK FOR INDICATED ANGLES OF FIN CANT AT A MACH NUMBER OF 3.5

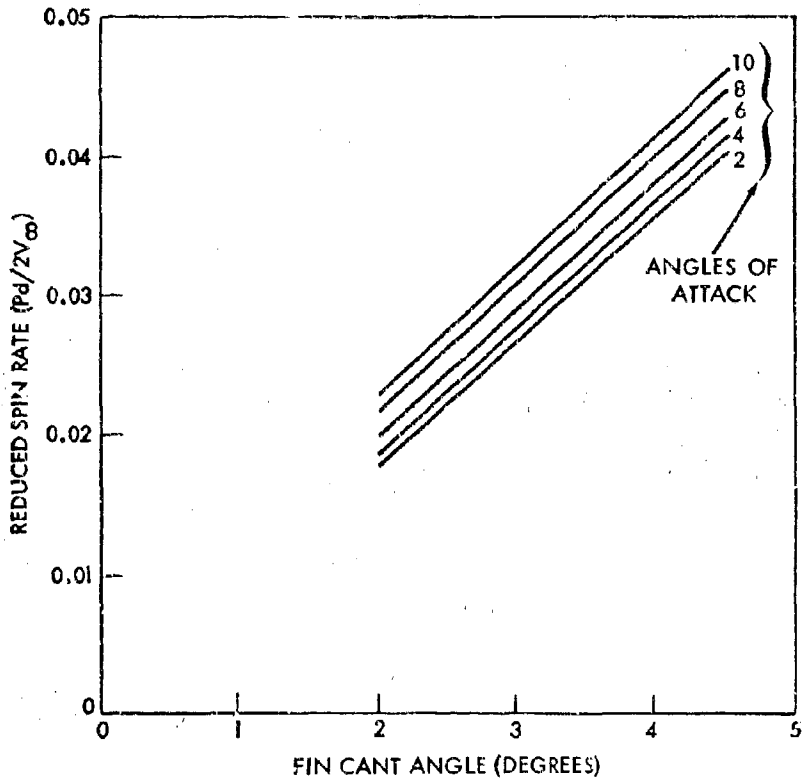

FIG. 37 REDUCED SPIN RATE VERSUS ANGLE OF FIN CANT AT MACH 2.0

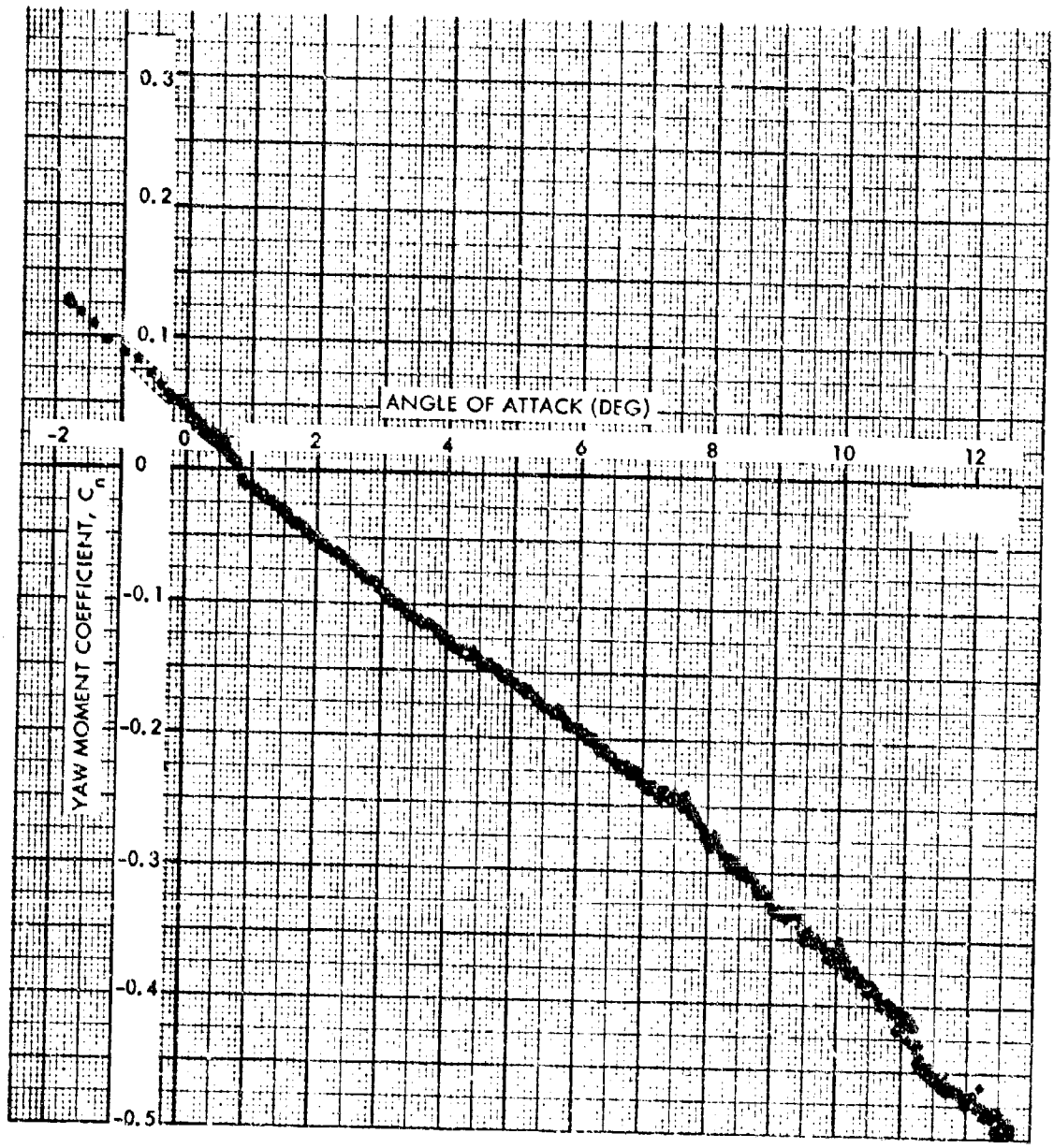

FIG. 38 YAW MOMENT COEFFICIENT VERSUS ANGLE OF ATTACK AT A MACH NUMBER OF 1.76 AND A FIN CANT ANGLE OF 2.00 DEGREES

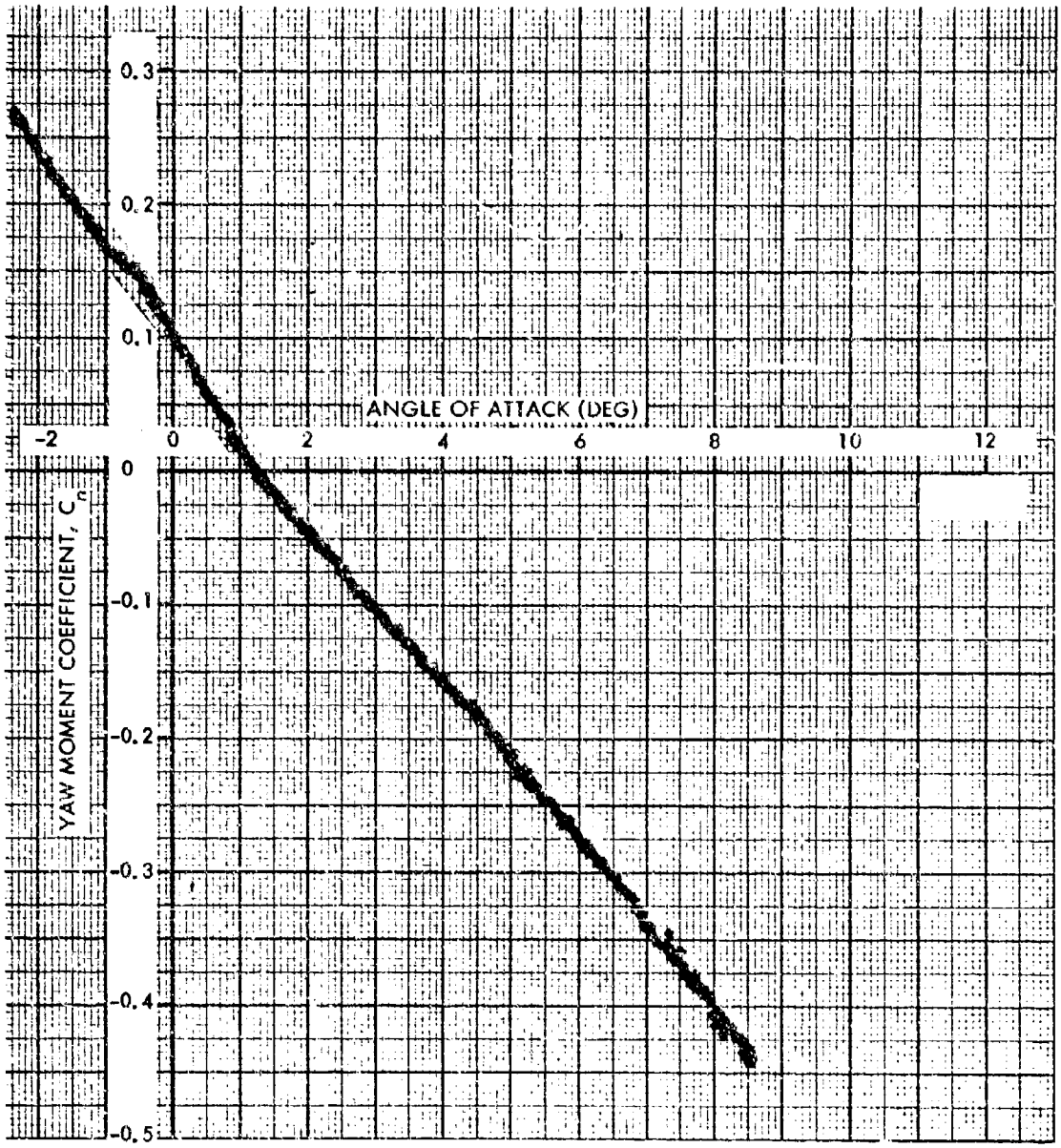

FIG. 39 YAW MOMENT COEFFICIENT VERSUS ANGLE OF ATTACK AT A MACH NUMBER OF 1.76 AND A FIN CANT ANGLE OF 3.25 DEGREES

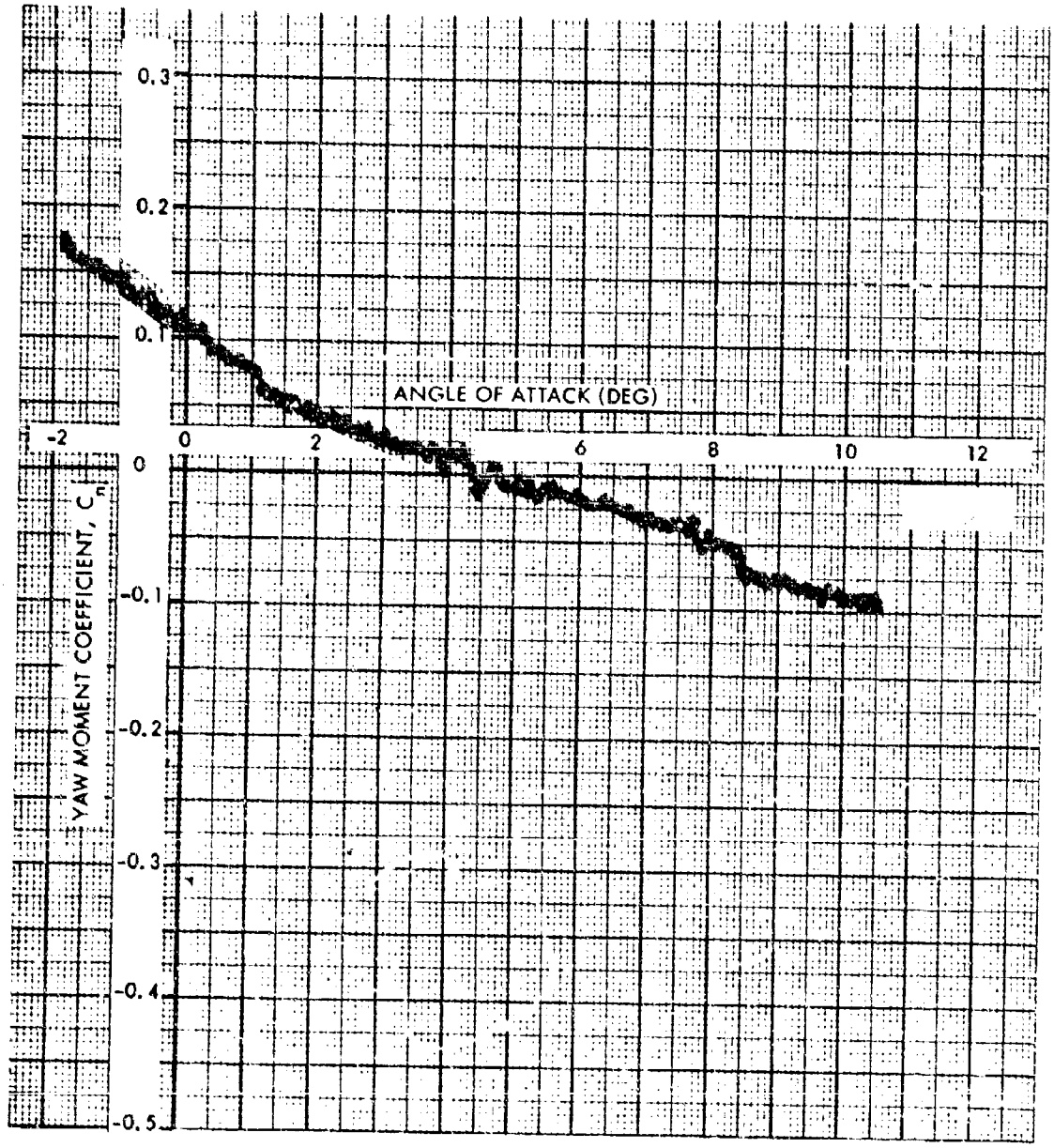

FIG. 40 YAW MOMENT COEFFICIENT VERSUS ANGLE OF ATTACK AT A MACH NUMBER OF 2.0 AND A FIN CANT ANGLE OF 2.00 DEGREES

FIG. 41 YAW MOMENT COEFFICIENT VERSUS ANGLE OF ATTACK AT A MACH NUMBER OF 2.0 AND A FIN CANT ANGLE OF 3.25 DEGREES

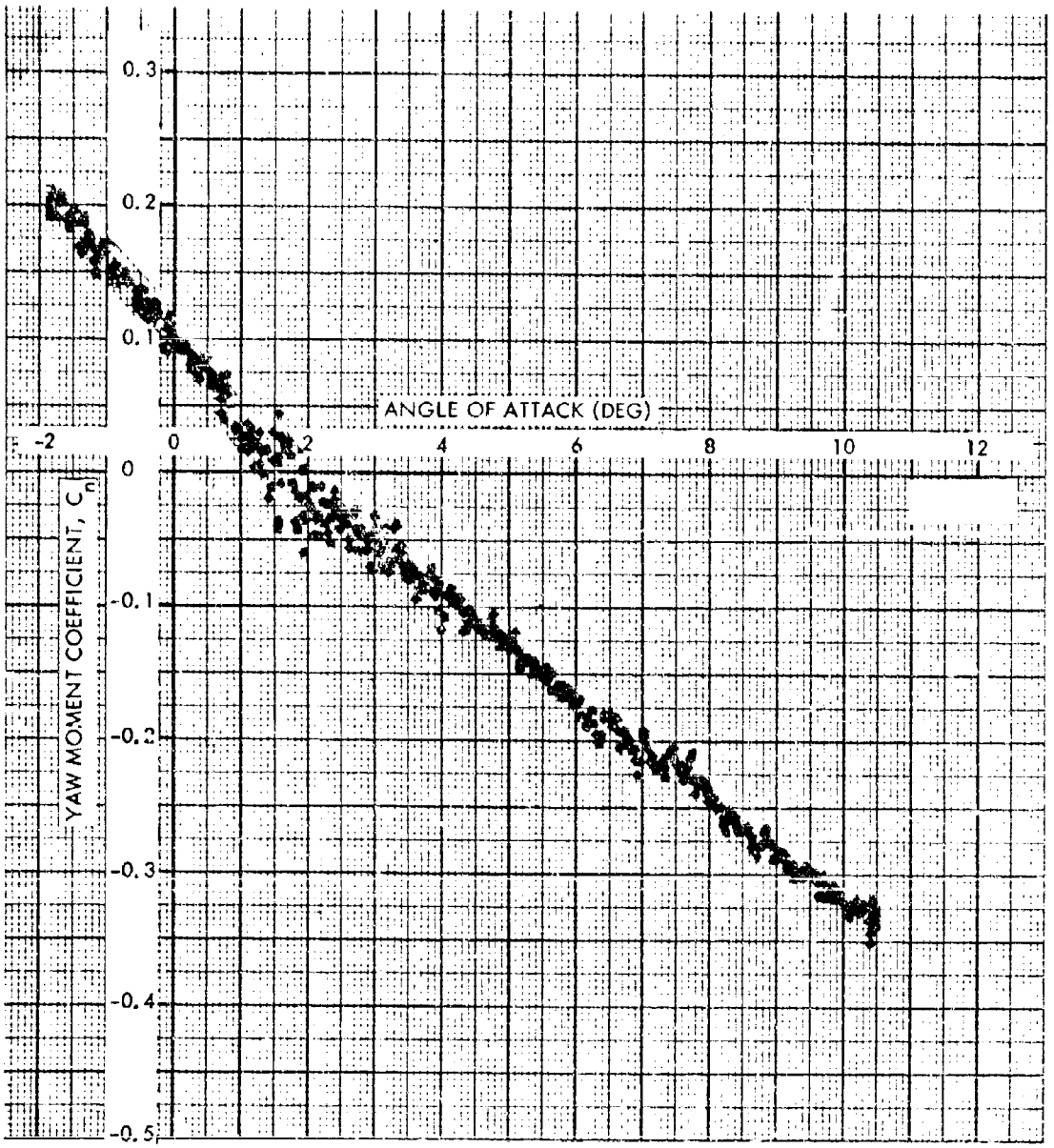

FIG. 42 YAW MOMENT COEFFICIENT VERSUS ANGLE OF ATTACK AT A MACH NUMBER OF 2.0 AND A FIN CANT ANGLE OF 4.50 DEGREES

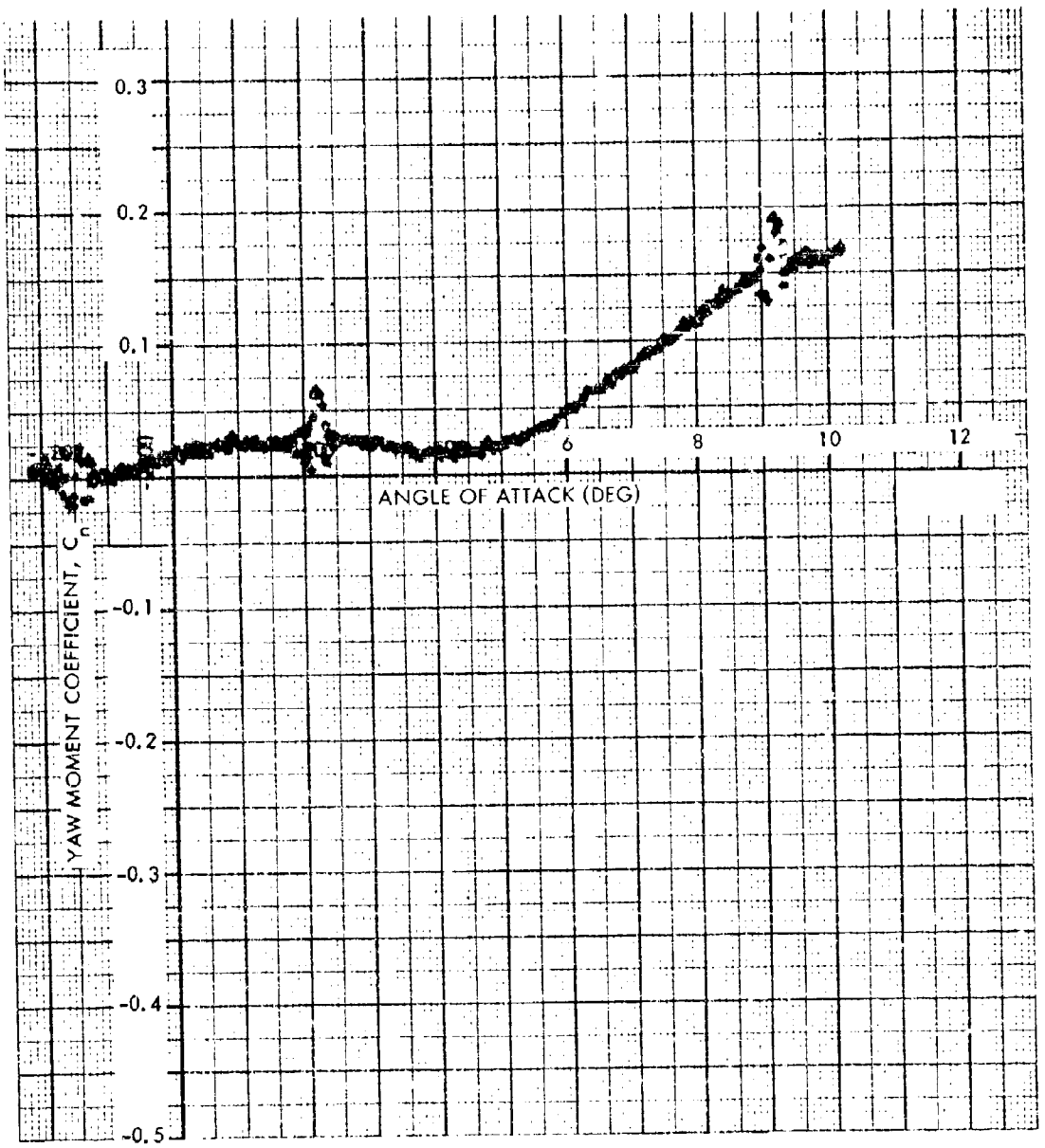

FIG. 43 YAW MOMENT COEFFICIENT VERSUS ANGLE OF ATTACK AT A MACH NUMBER OF 2.5 AND A FIN CANT ANGLE OF 2.00 DEGREES

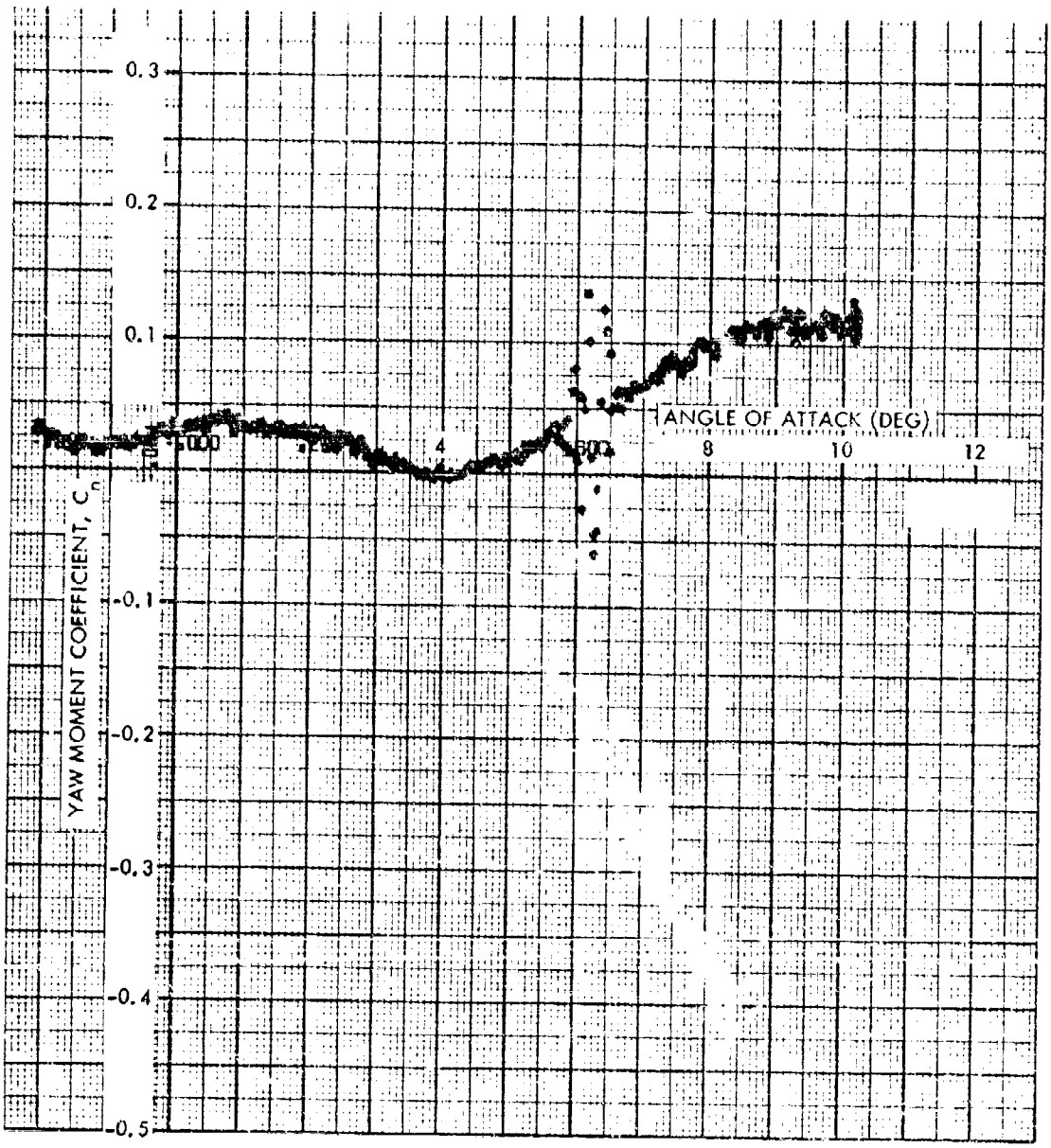

FIG. 44 YAW MOMENT COEFFICIENT VERSUS ANGLE OF ATTACK AT A MACH NUMBER OF 2.5 AND A FIN CANT ANGLE OF 3.25 DEGREES

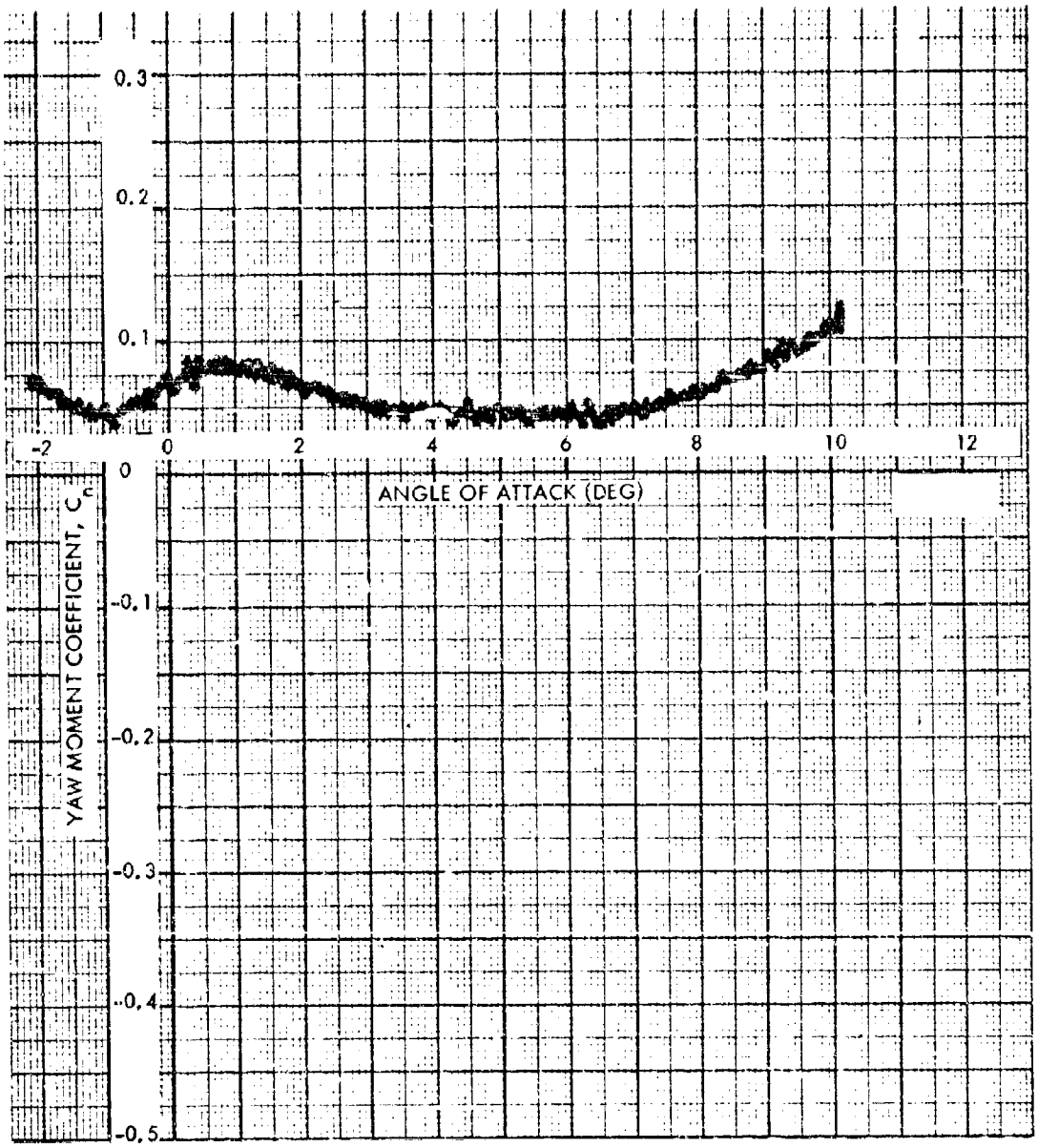

FIG. 45 YAW MOMENT COEFFICIENT VERSUS ANGLE OF ATTACK AT A MACH NUMBER OF 2.5 AND A FIN CANT ANGLE OF 4.50 DEGREES

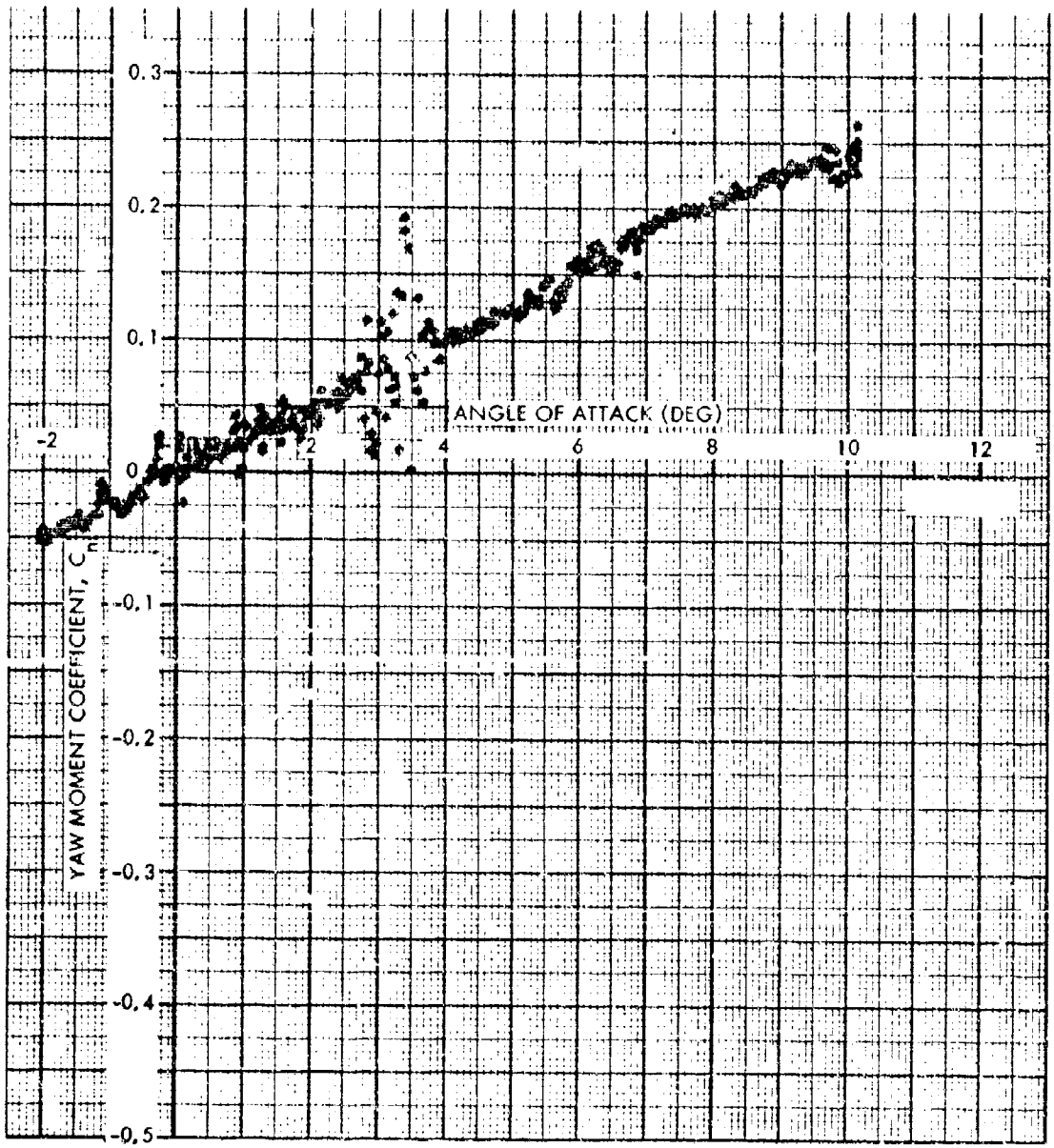

FIG. 46 YAW MOMENT COEFFICIENT VERSUS ANGLE OF ATTACK AT A MACH NUMBER OF 3.0 AND A FIN CANT ANGLE OF 2.00 DEGREES

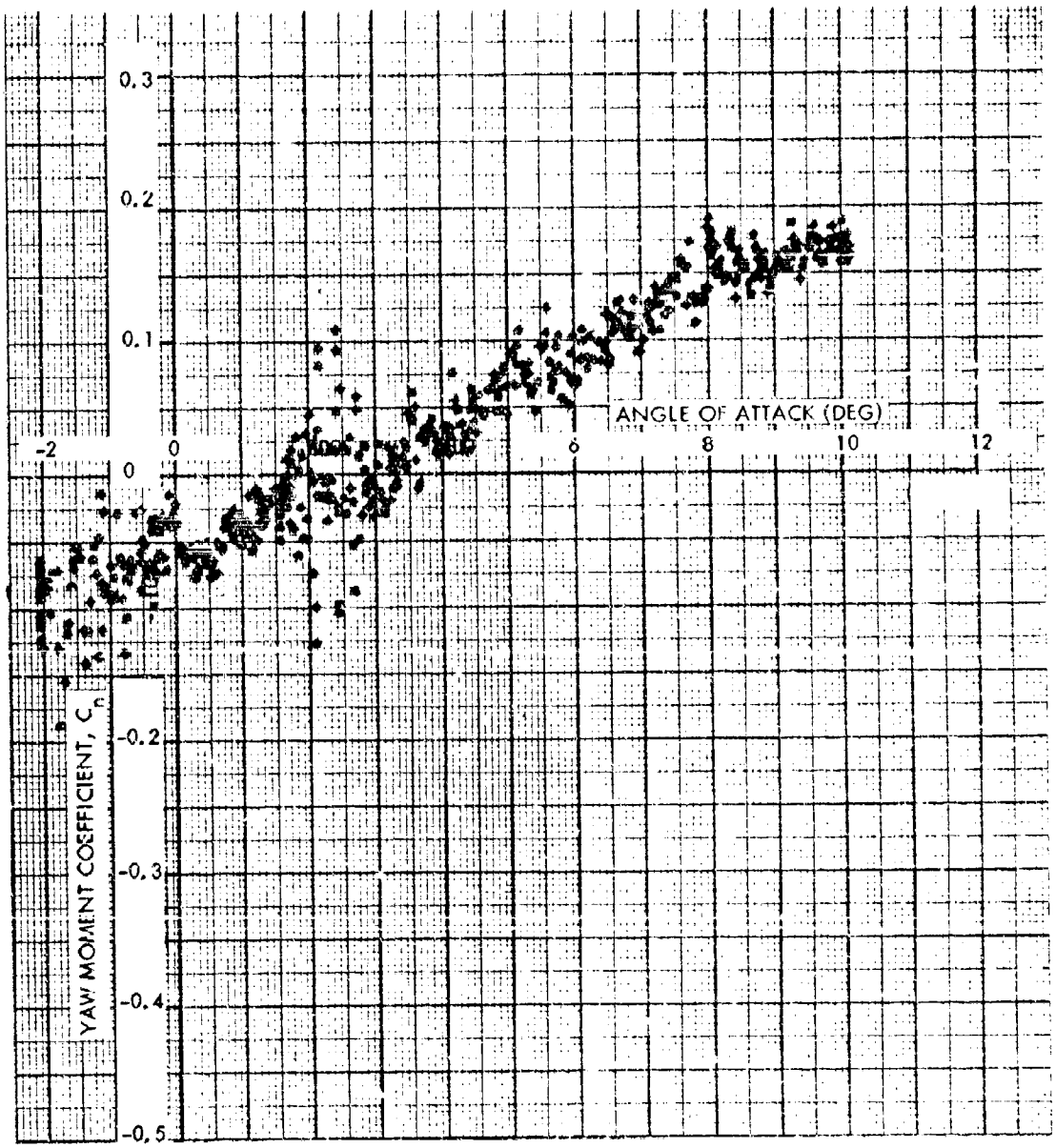

FIG. 47 YAW MOMENT COEFFICIENT VERSUS ANGLE OF ATTACK AT A MACH NUMBER OF 3.0 AND A FIN CANT ANGLE OF 3.25 DEGREES

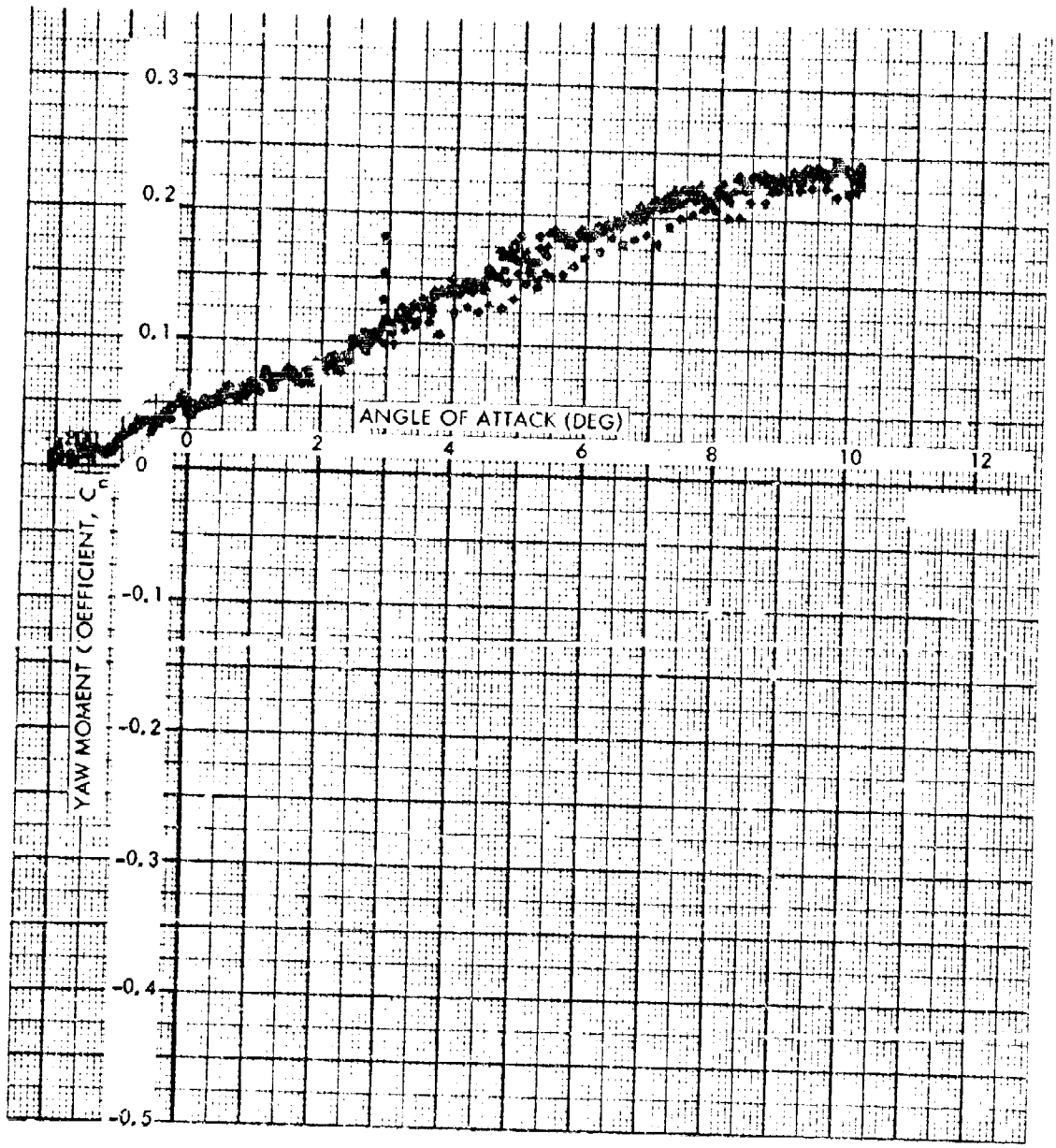

FIG. 48 YAW MOMENT COEFFICIENT VERSUS ANGLE OF ATTACK AT A MACH NUMBER OF 3.0 AND A FIN CANT ANGLE OF 4.50 DEGREES

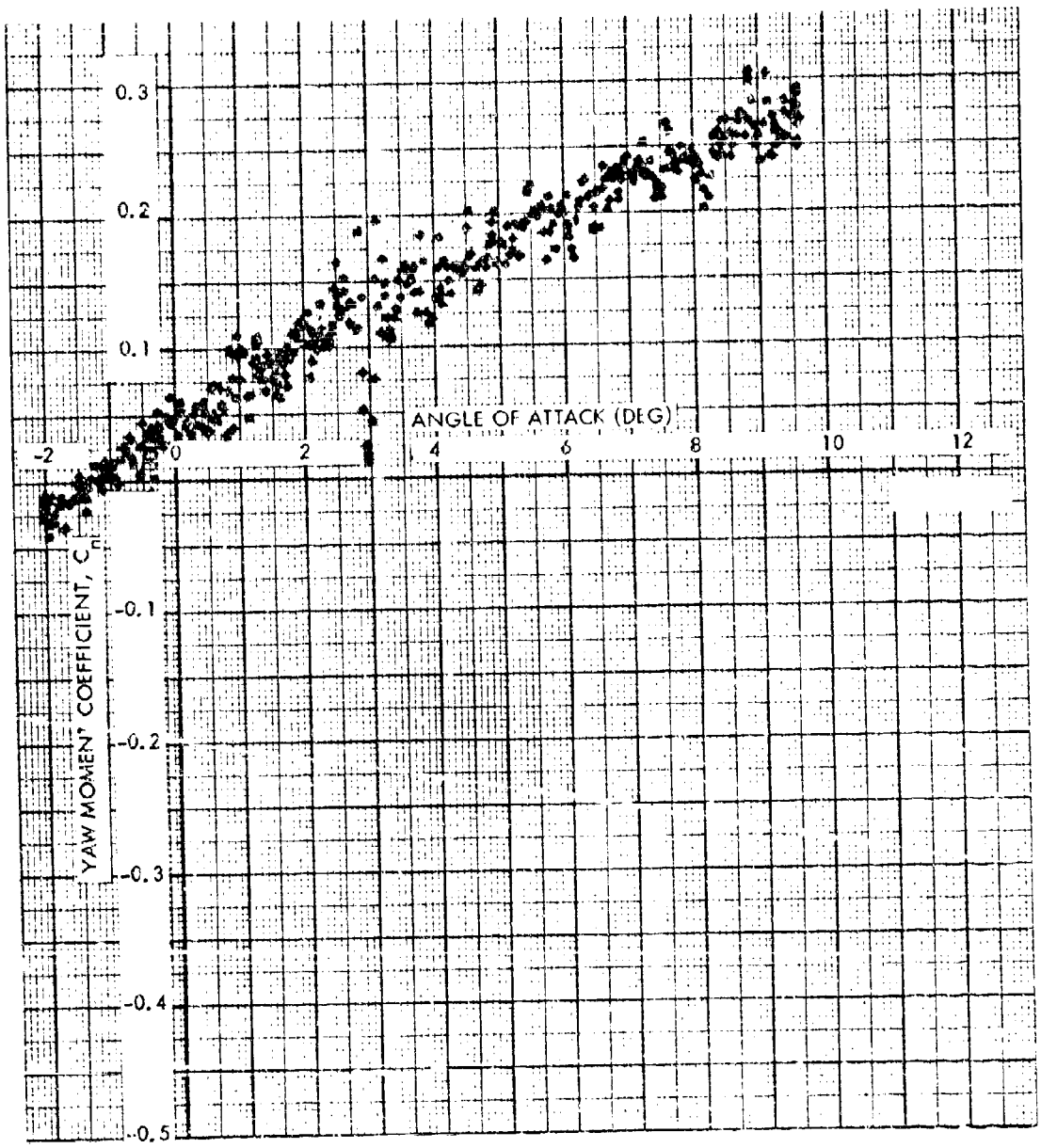

FIG. 49 YAW MOMENT COEFFICIENT VERSUS ANGLE OF ATTACK AT A MACH NUMBER OF 3.5 AND A FIN CANT ANGLE OF 2.00 DEGREES

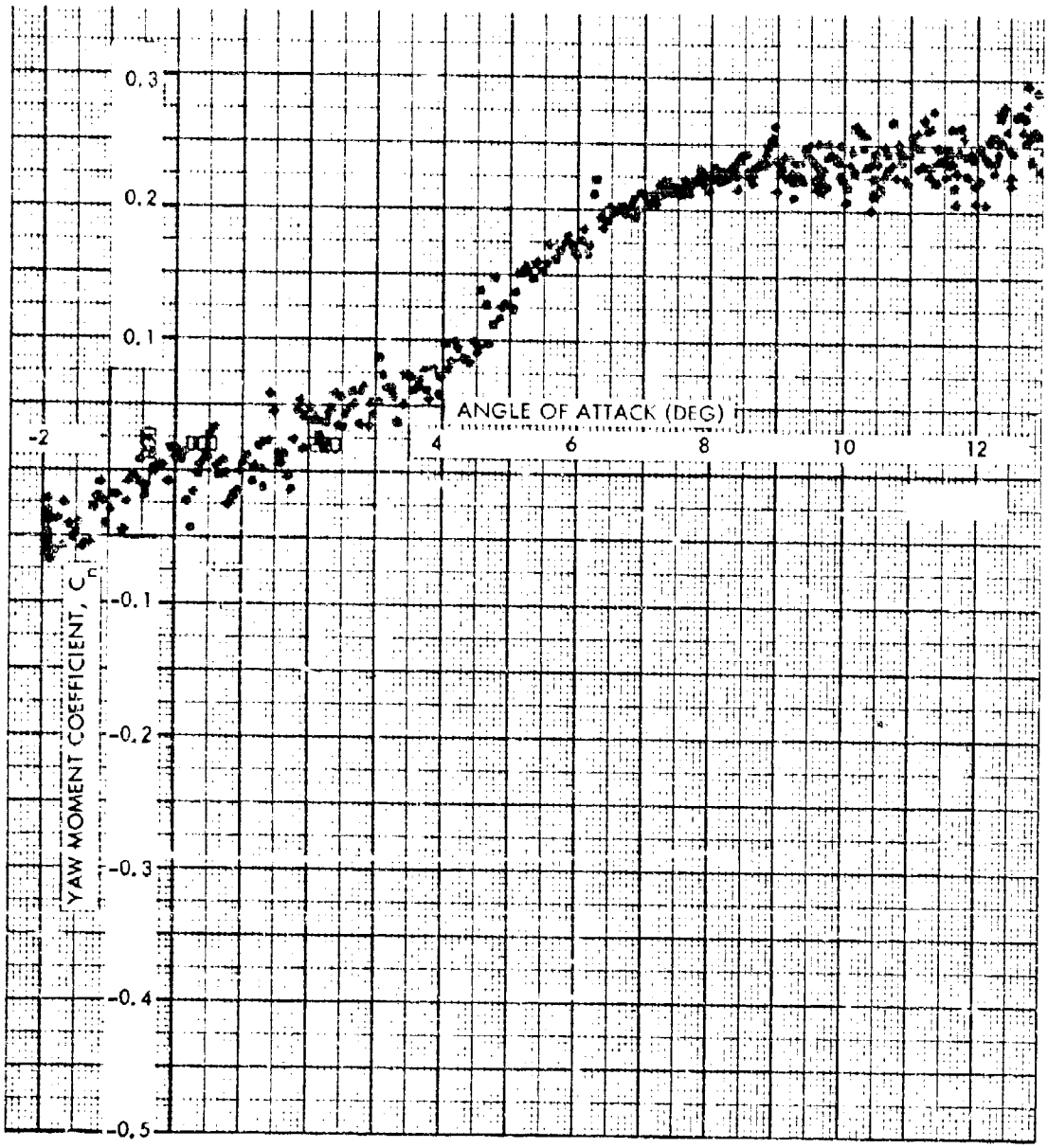

FIG. 50 YAW MOMENT COEFFICIENT VERSUS ANGLE OF ATTACK AT A MACH NUMBER OF 3 5 AND A FIN CANT ANGLE OF 3.25 DEGREES

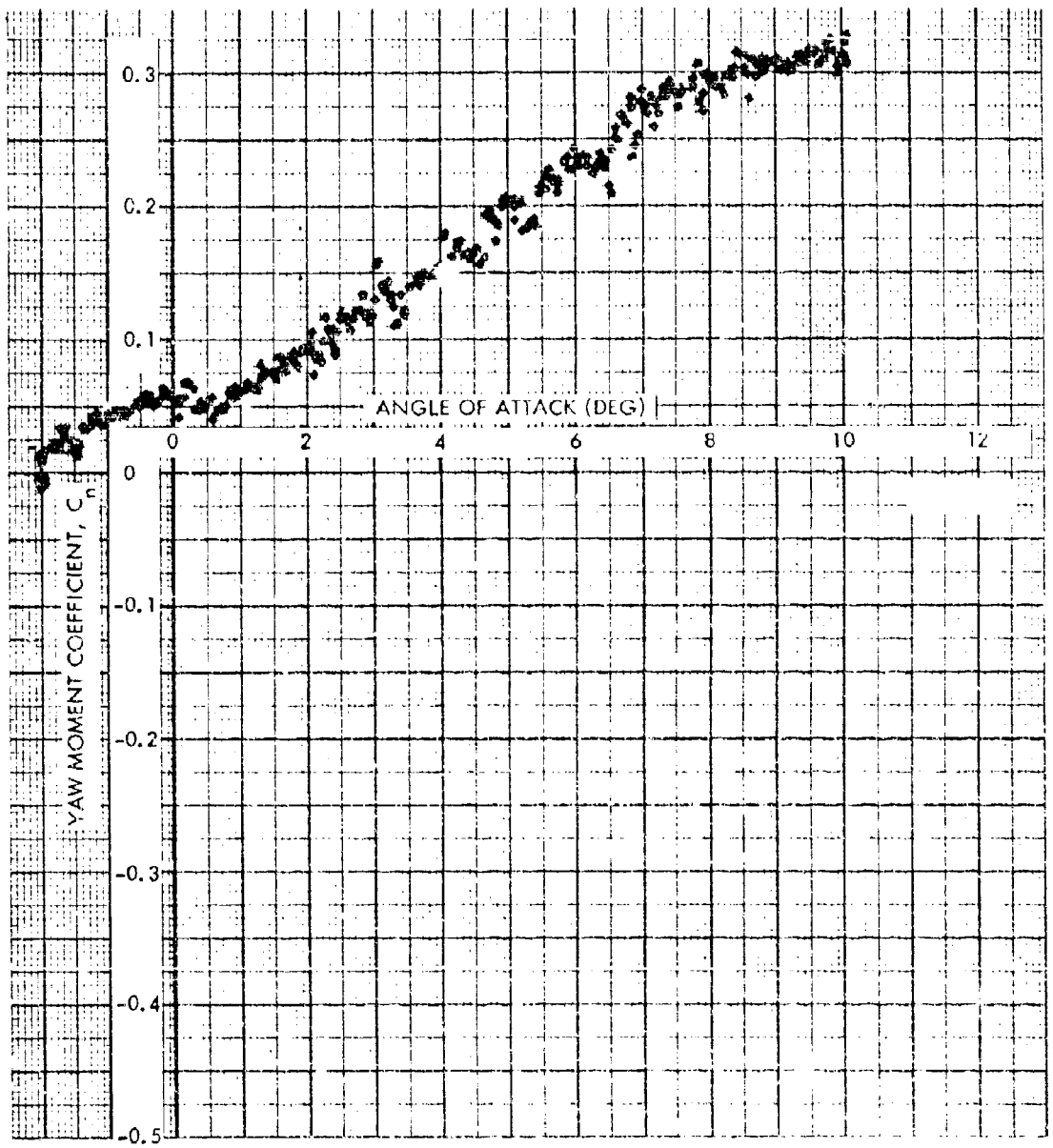

FIG. 51 YAW MOMENT COEFFICIENT VERSUS ANGLE OF ATTACK AT A MACH NUMBER OF 3.5 AND A FIN CANT ANGLE OF 4.50 DEGREES

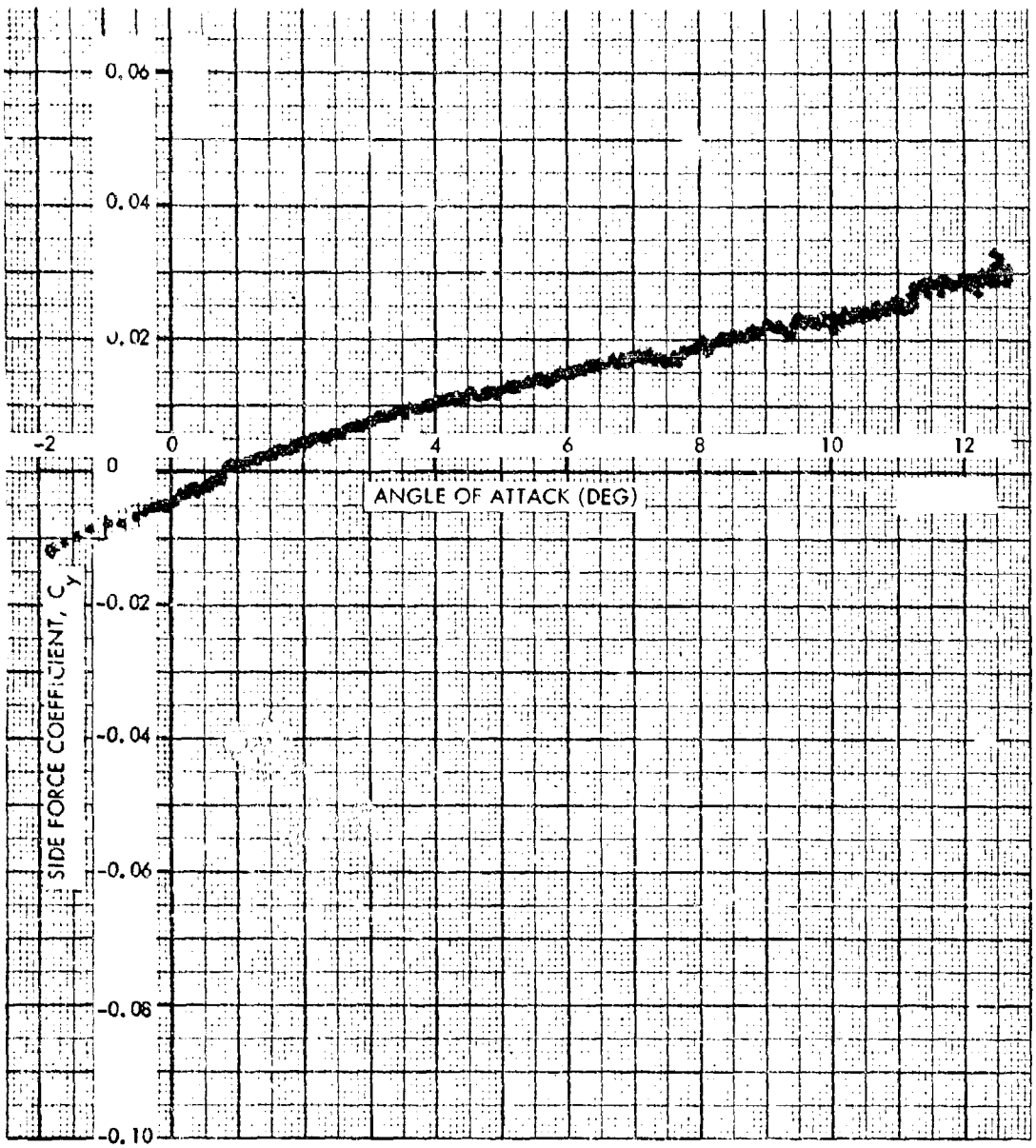

FIG. 52 SIDE FORCE COEFFICIENT VERSUS ANGLE OF ATTACK AT A MACH NUMBER OF 1.76 AND A FIN CANT ANGLE OF 2.00 DEGREES

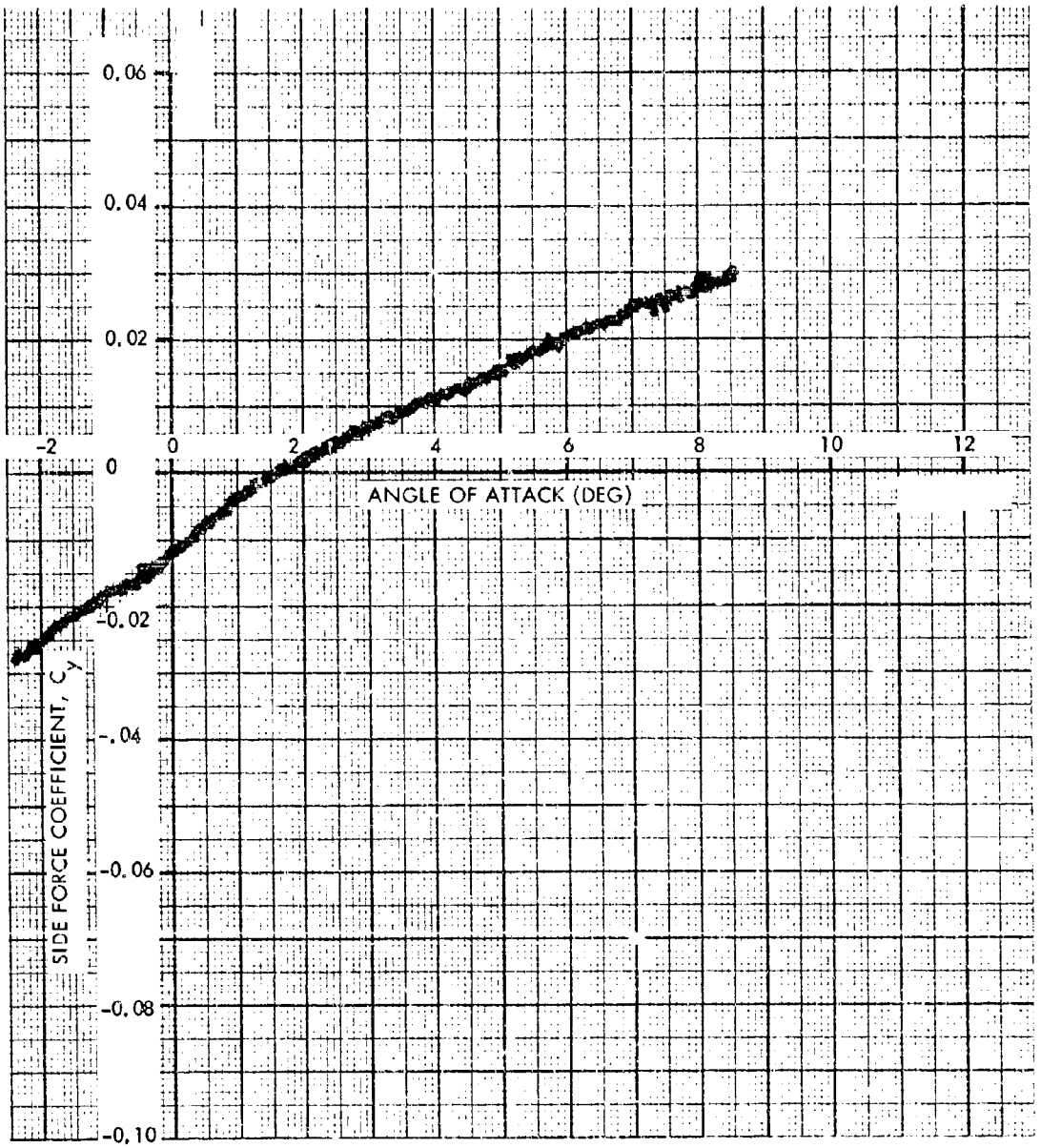

FIG. 53 SIDE FORCE COEFFICIENT VERSUS ANGLE OF ATTACK AT A MACH NUMBER OF 1.76 AND A FIN CANT ANGLE OF 3.25 DEGREES

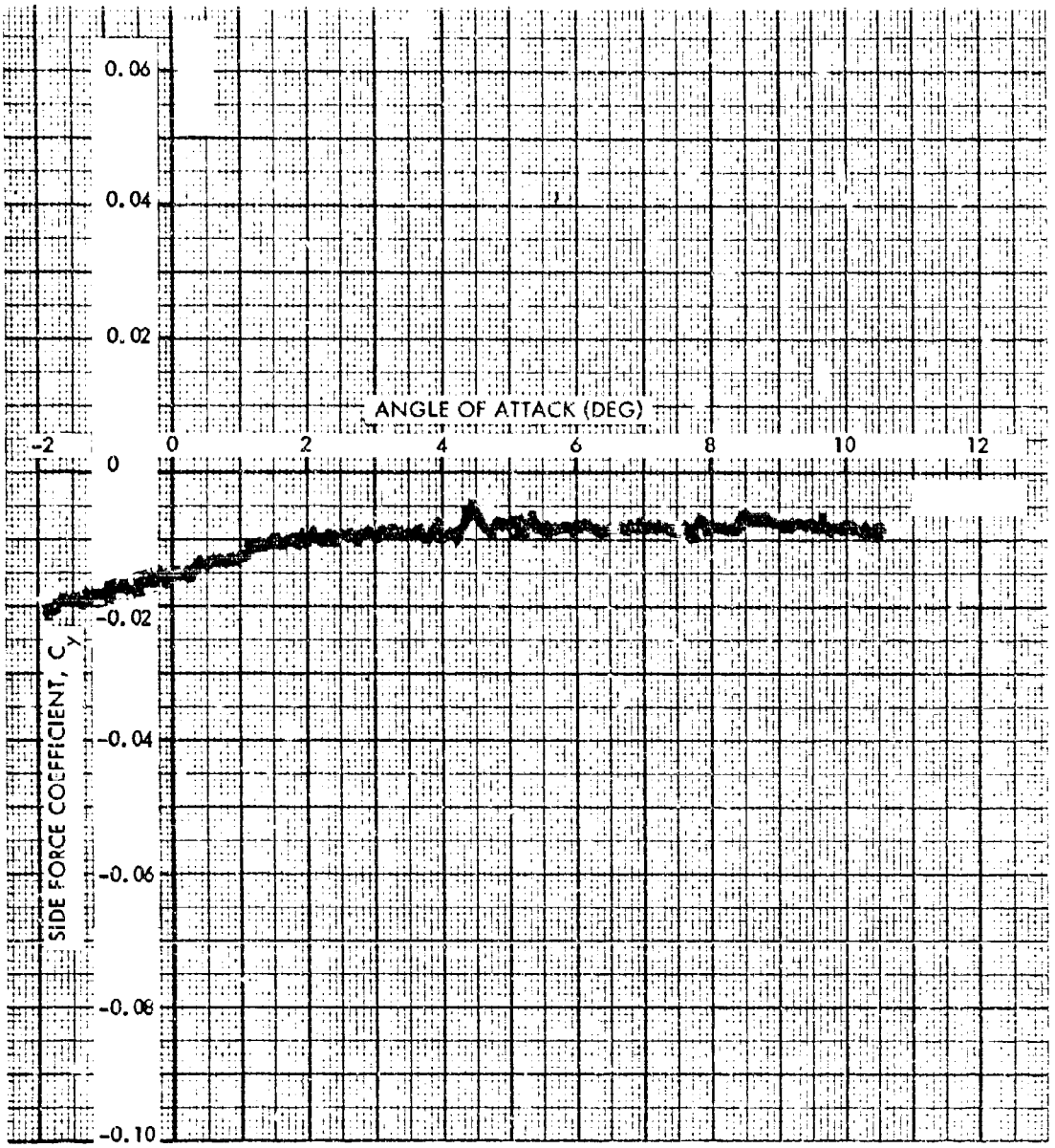

FIG. 54 SIDE FORCE COEFFICIENT VERSUS ANGLE OF ATTACK AT A MACH NUMBER OF 2.0 AND A FIN CANT ANGLE OF 2.00 DEGREES

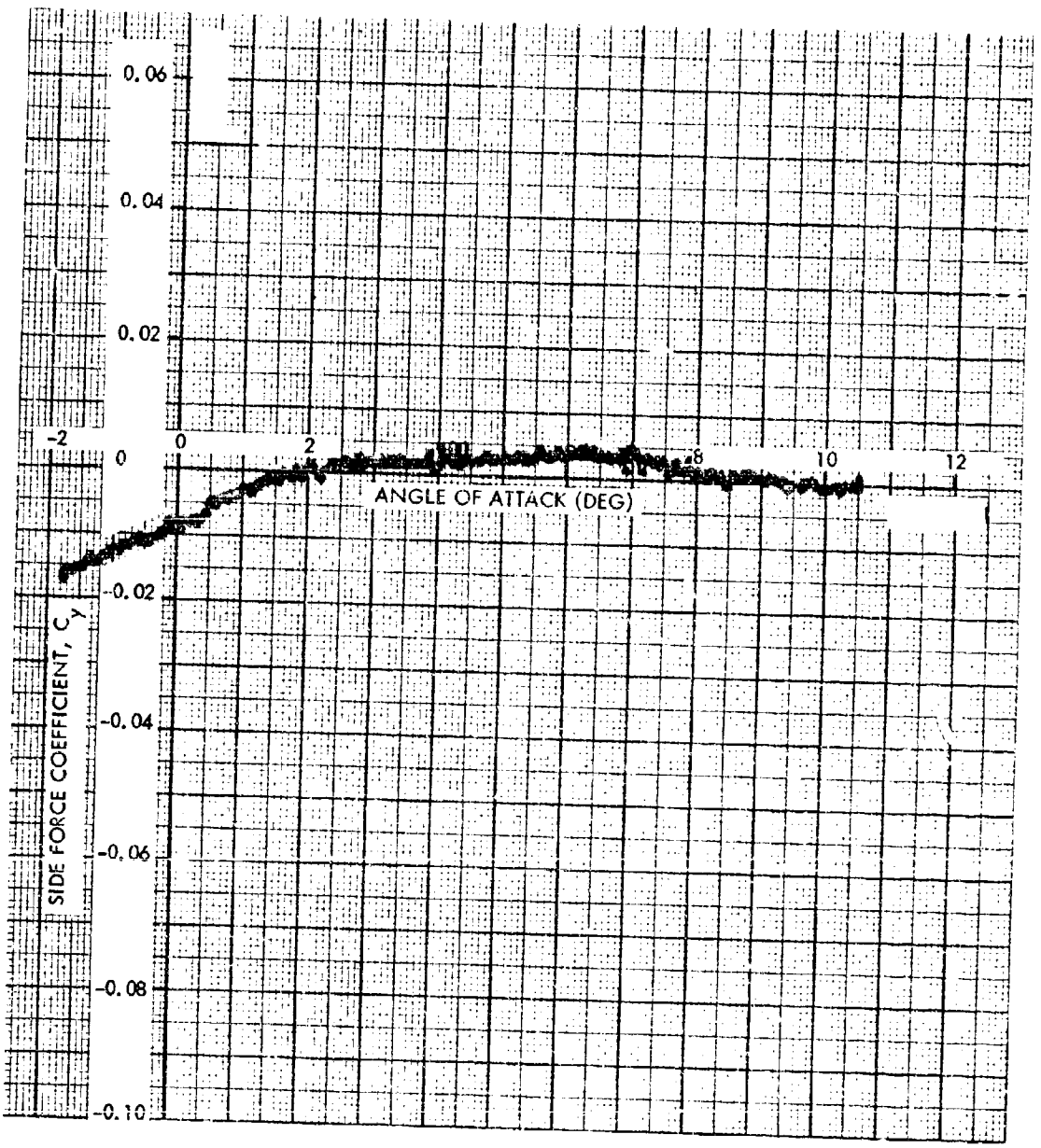

FIG. 55 SIDE FORCE COEFFICIENT VERSUS ANGLE OF ATTACK AT A MACH NUMBER OF 2.0 AND A FIN CANT ANGLE OF 3.25 DEGREES

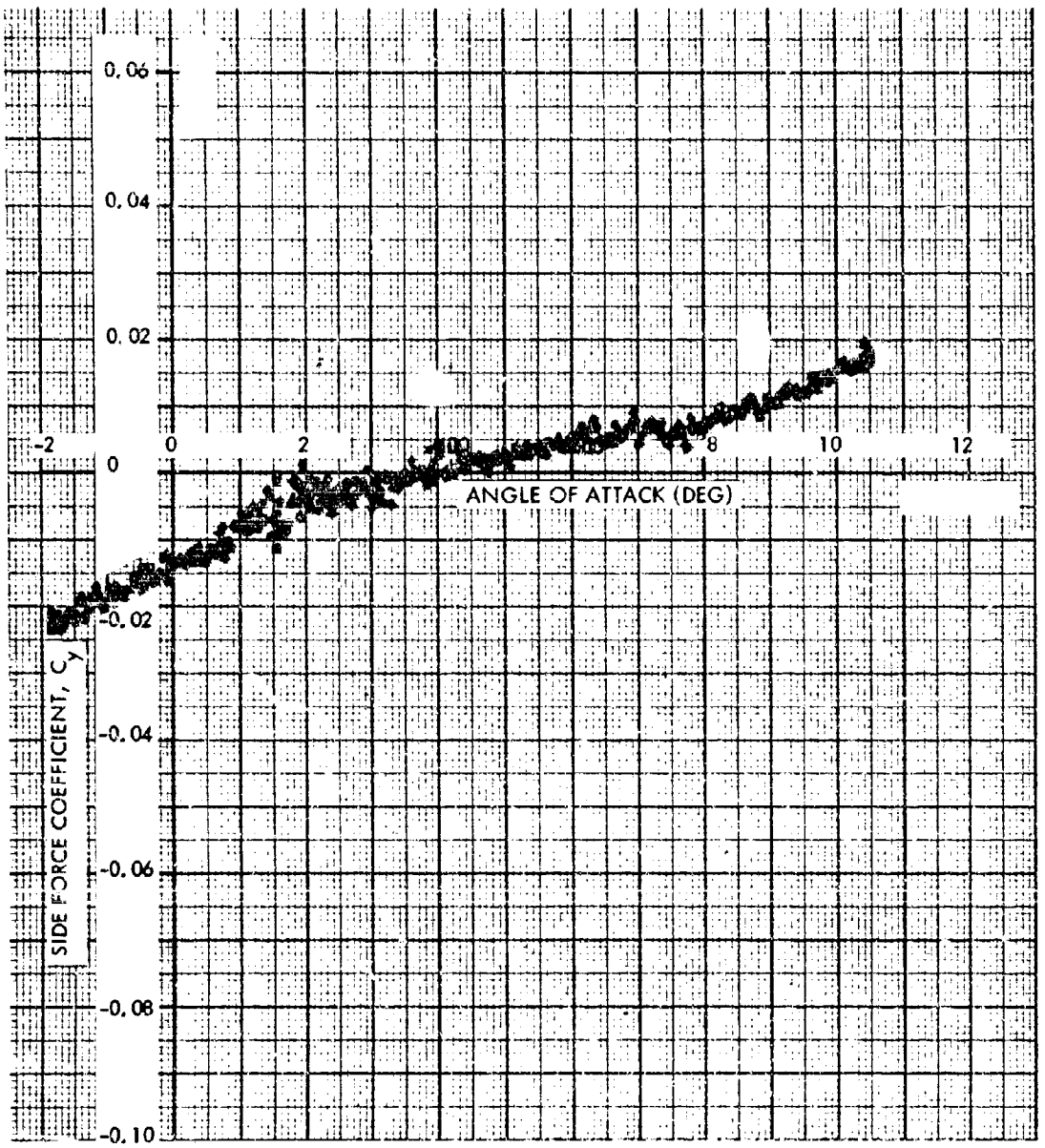

FIG. 56 SIDE FORCE COEFFICIENT VERSUS ANGLE OF ATTACK AT A MACH NUMBER OF 2.0 AND A FIN CANT ANGLE OF 4.50 DEGREES

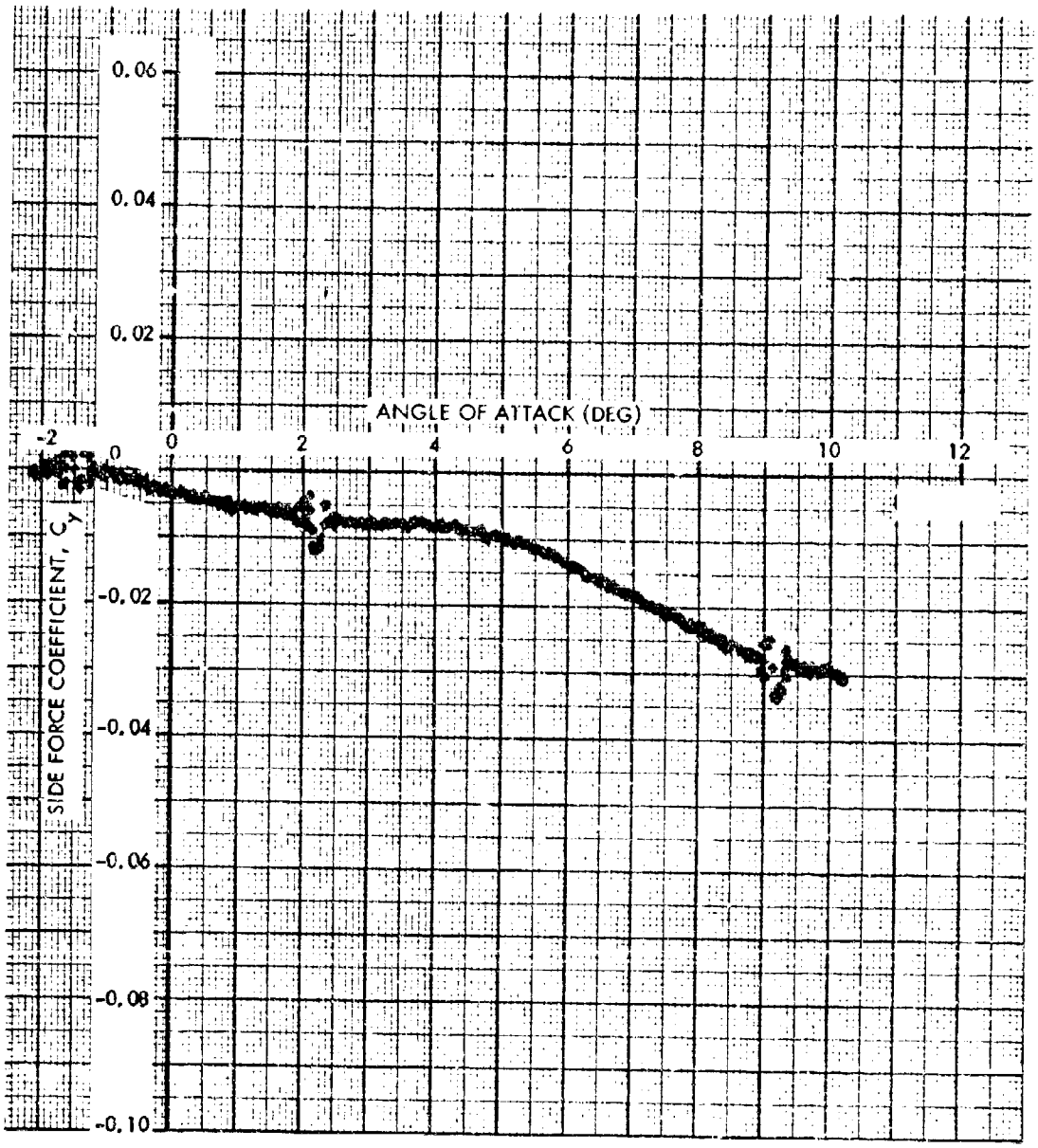

FIG. 57 SIDE FORCE COEFFICIENT VERSUS ANGLE OF ATTACK AT A MACH NUMBER OF 2.5 AND A FIN CANT ANGLE OF 2.00 DEGREES

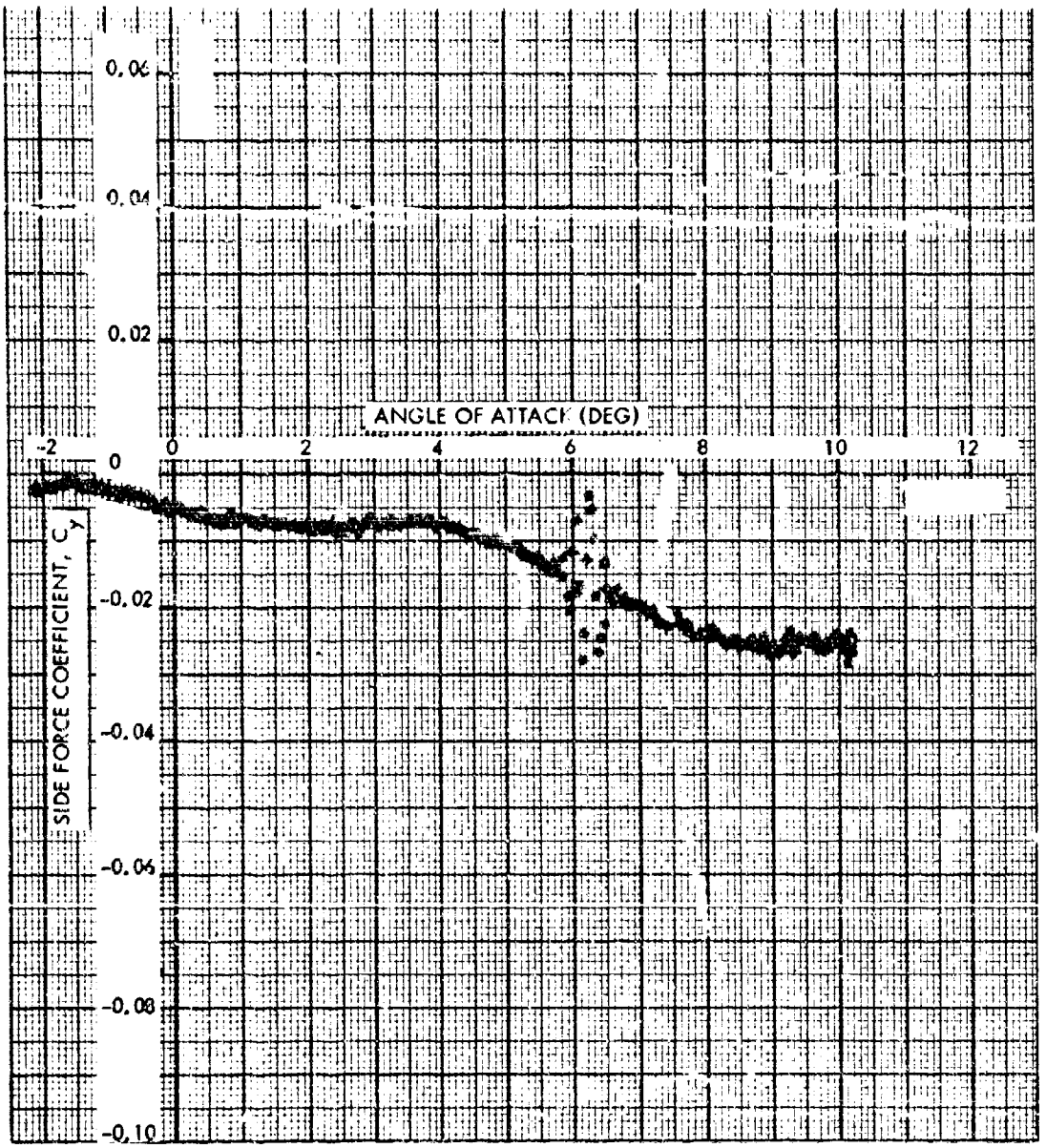

FIG. 58 SIDE FORCE COEFFICIENT VERSUS ANGLE OF ATTACK AT A MACH NUMBER OF 2.5 AND A FIN CANT ANGLE OF 3.25 DEGREES

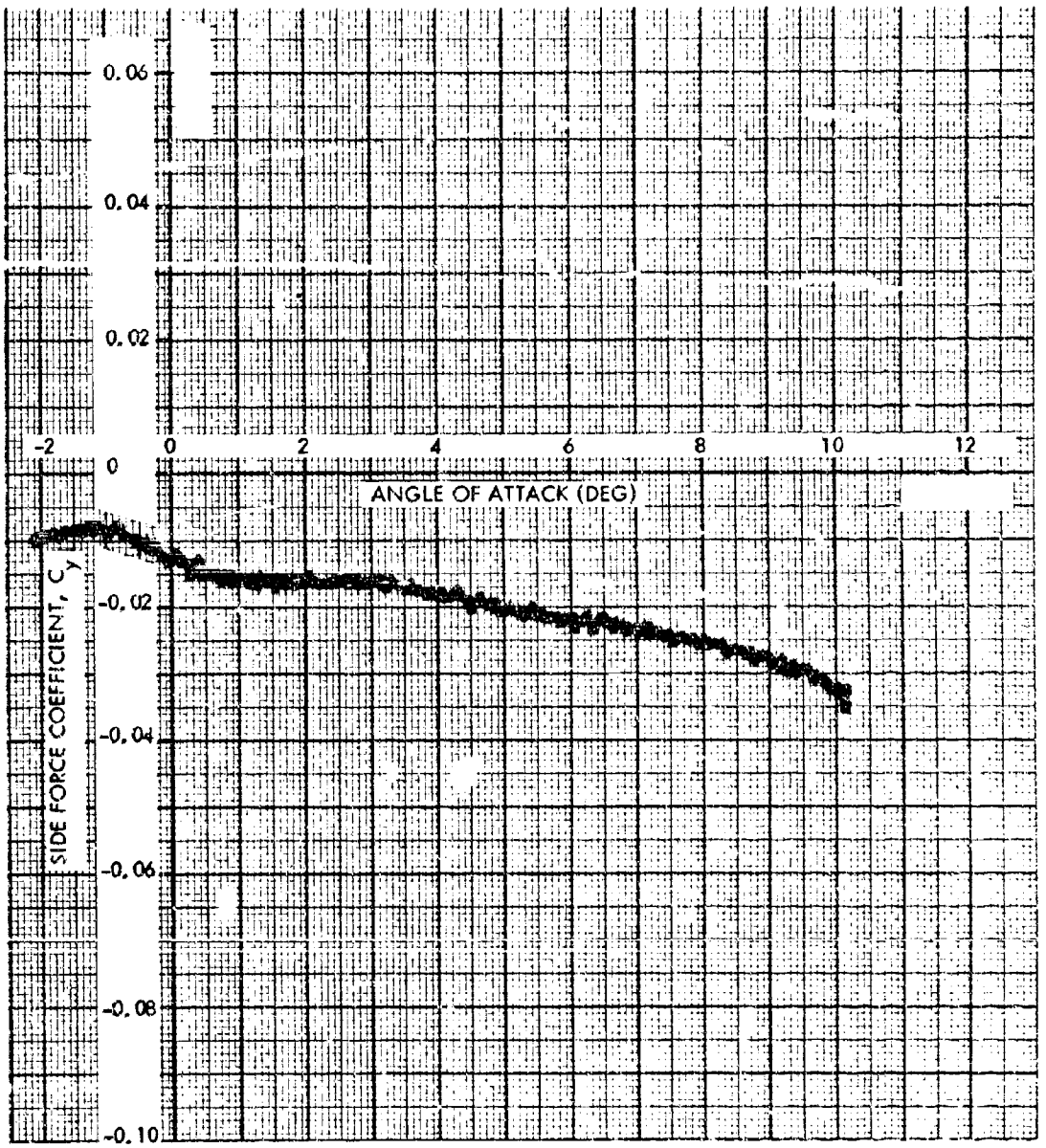

FIG. 59 SIDE FORCE COEFFICIENT VERSUS ANGLE OF ATTACK AT A MACH NUMBER OF 2.5 AND A FIN CANT ANGLE OF 4.50 DEGREES

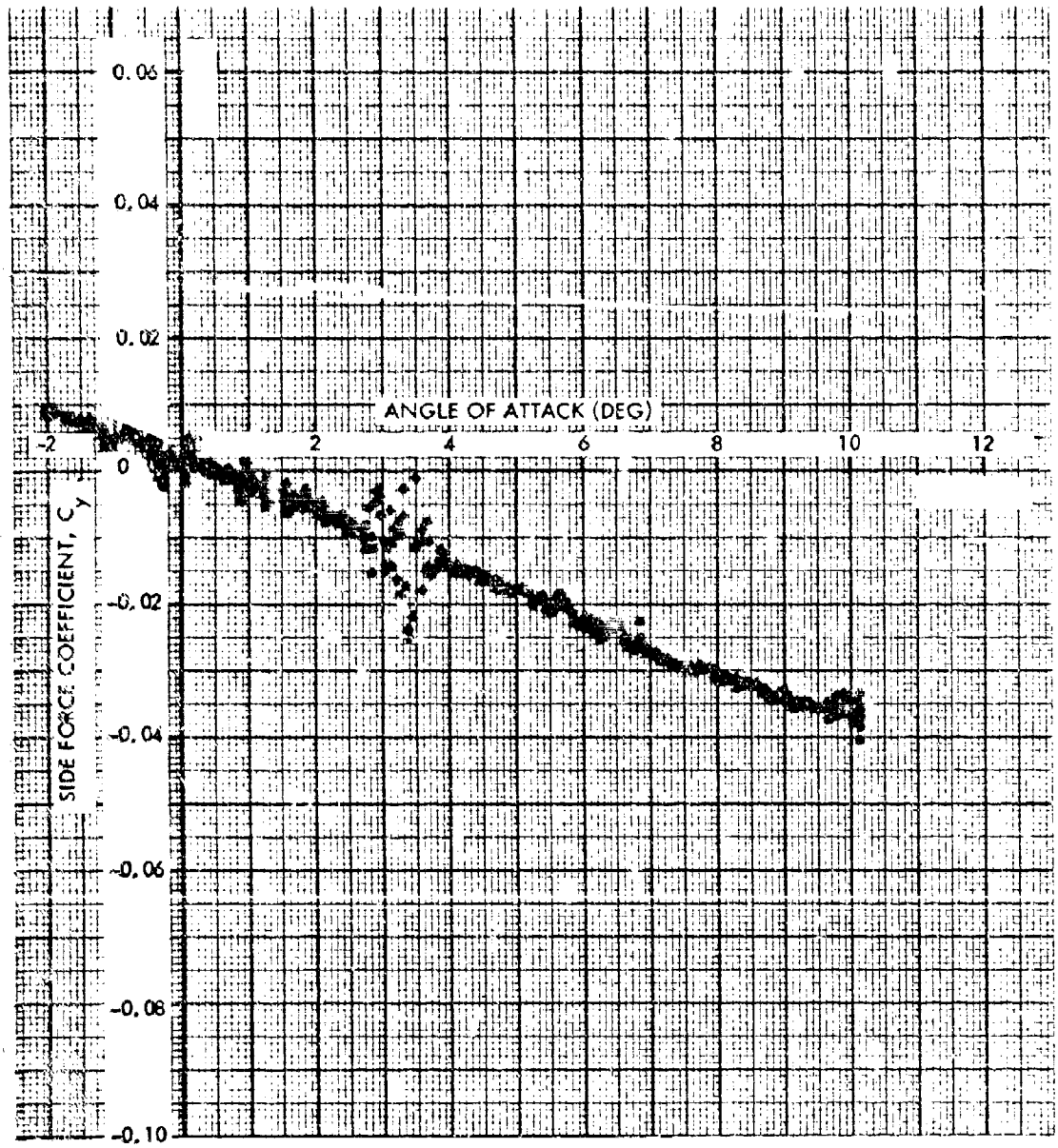

FIG. 60 SIDE FORCE COEFFICIENT VERSUS ANGLE OF ATTACK AT A MACH NUMBER OF 3.0 AND A FIN CANT ANGLE OF 2.00 DEGREES

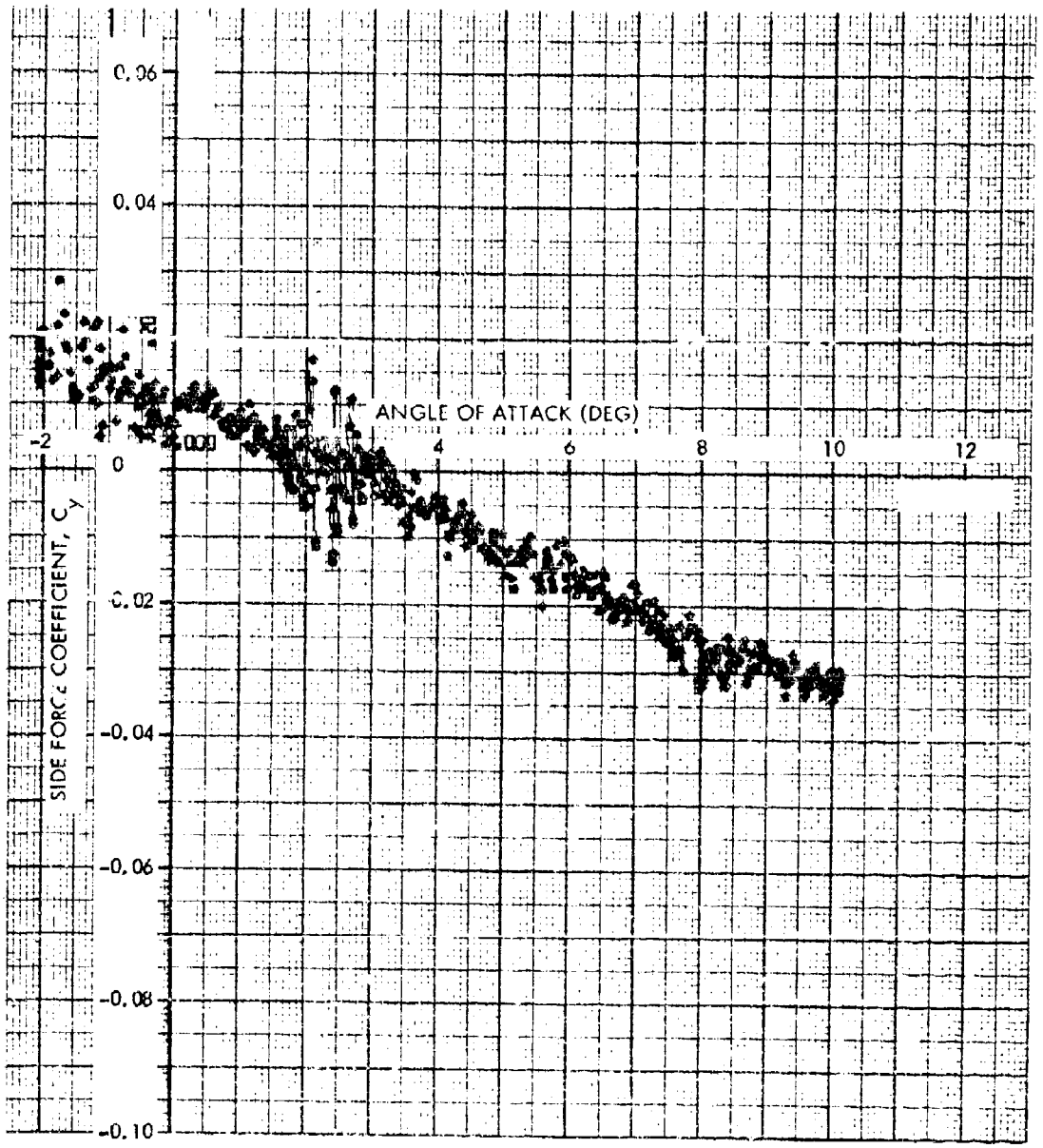

FIG. 61 SIDE FORCE COEFFICIENT VERSUS ANGLE OF ATTACK AT A MACH NUMBER OF 3.0 AND A FIN CANT ANGLE OF 3.25 DEGREES

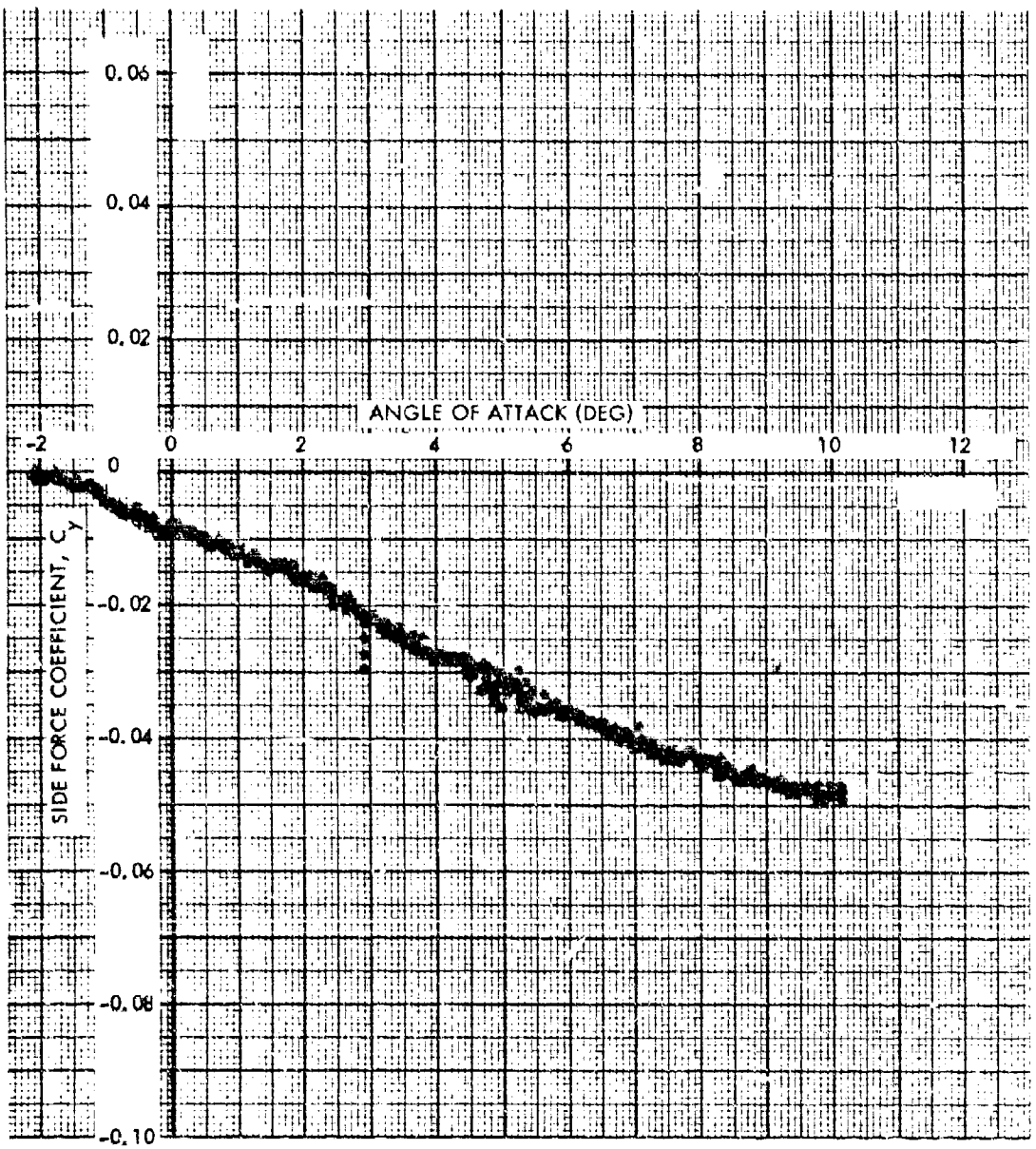

FIG. 62 SIDE FORCE COEFFICIENT VERSUS ANGLE OF ATTACK AT A MACH NUMBER OF 3.0 AND A FIN CANT ANGLE OF 4.50 DEGREES

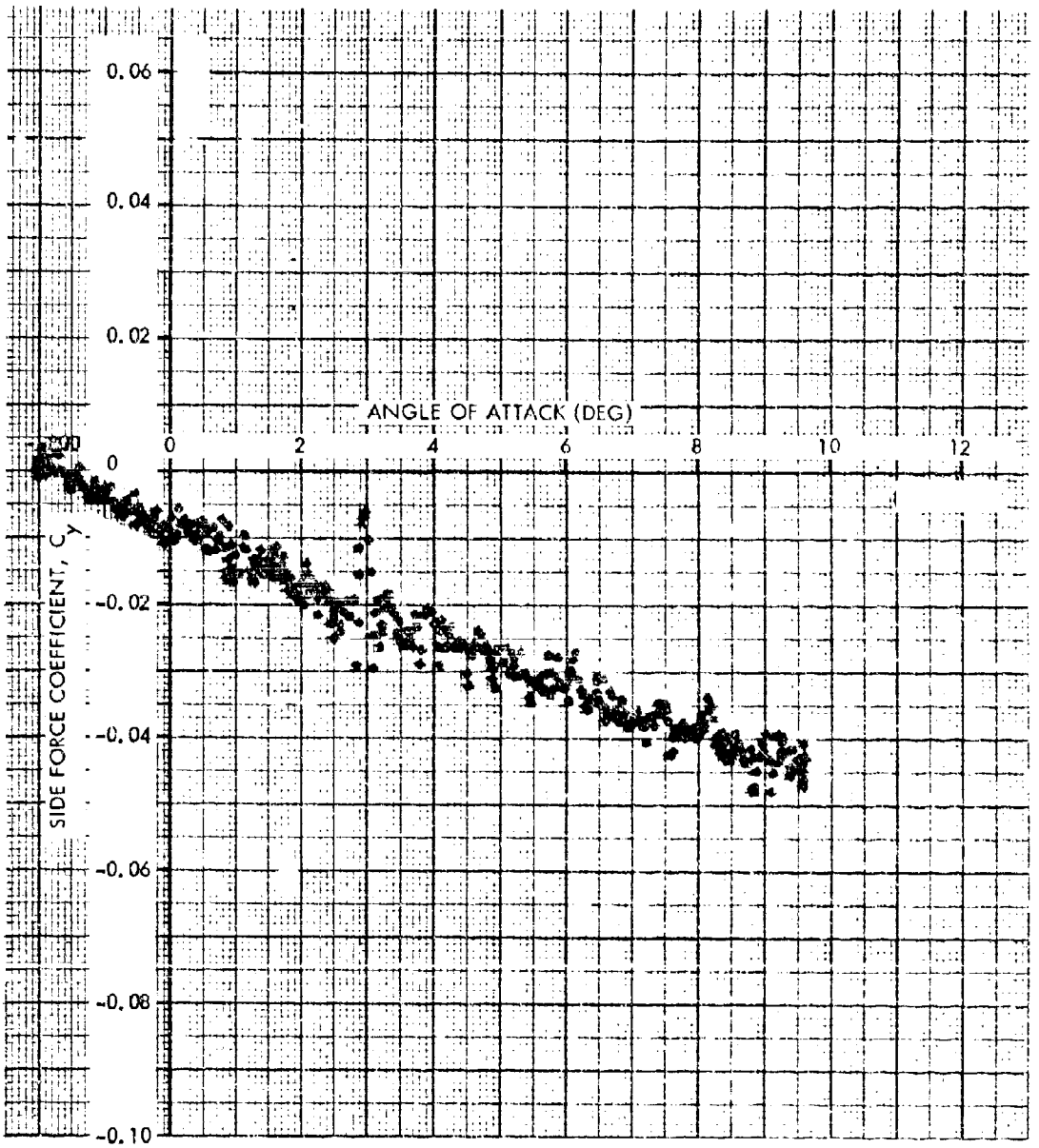

FIG. 63 SIDE FORCE COEFFICIENT VERSUS ANGLE OF ATTACK AT A MACH NUMBER OF 3.5 AND A FIN CANT ANGLE OF 2.00 DEGREES

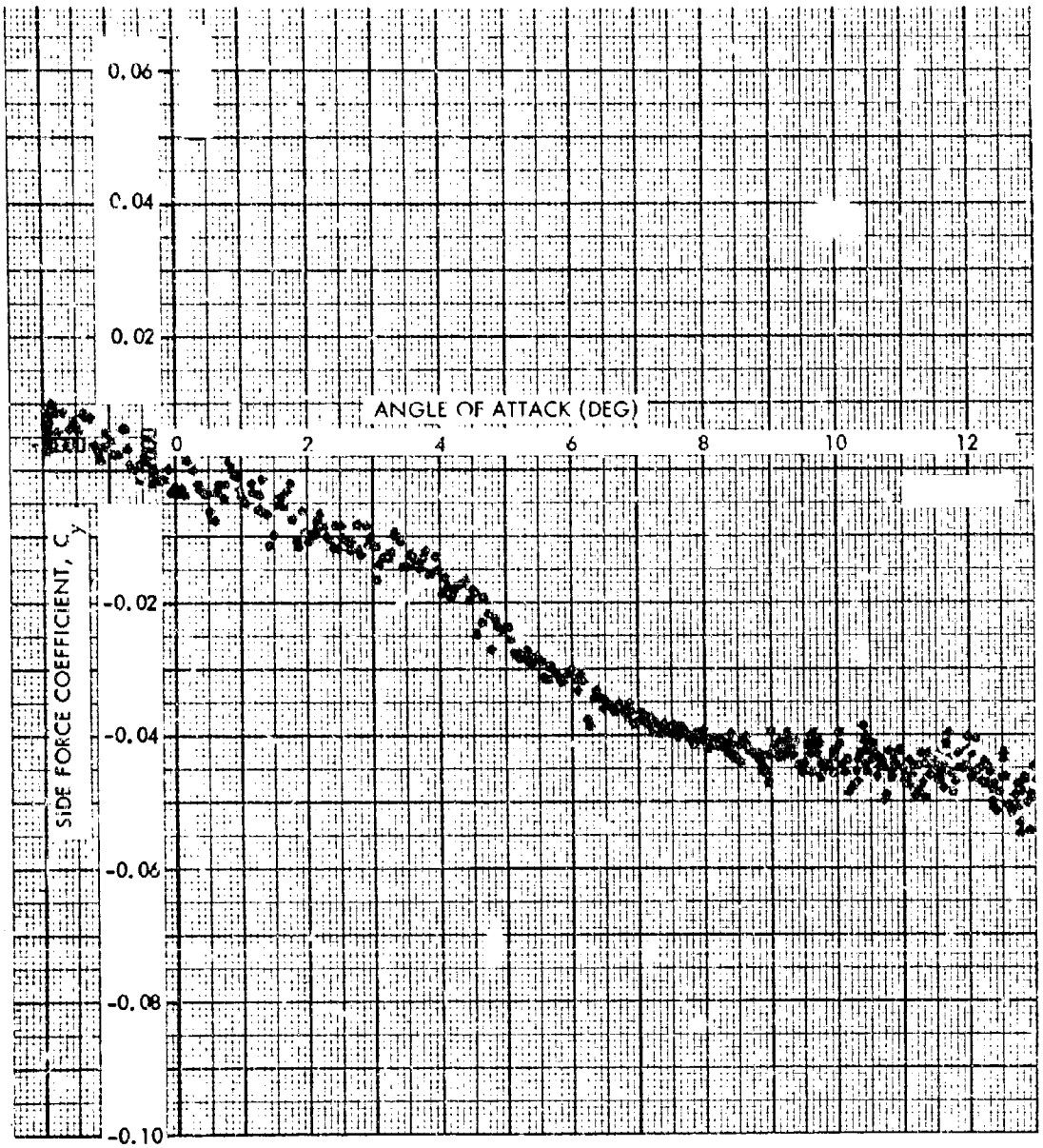

FIG. 64 SIDE FORCE COEFFICIENT VERSUS ANGLE OF ATTACK AT A MACH NUMBER OF 3.5 AND A FIN CANT ANGLE OF 3.25 DEGREES

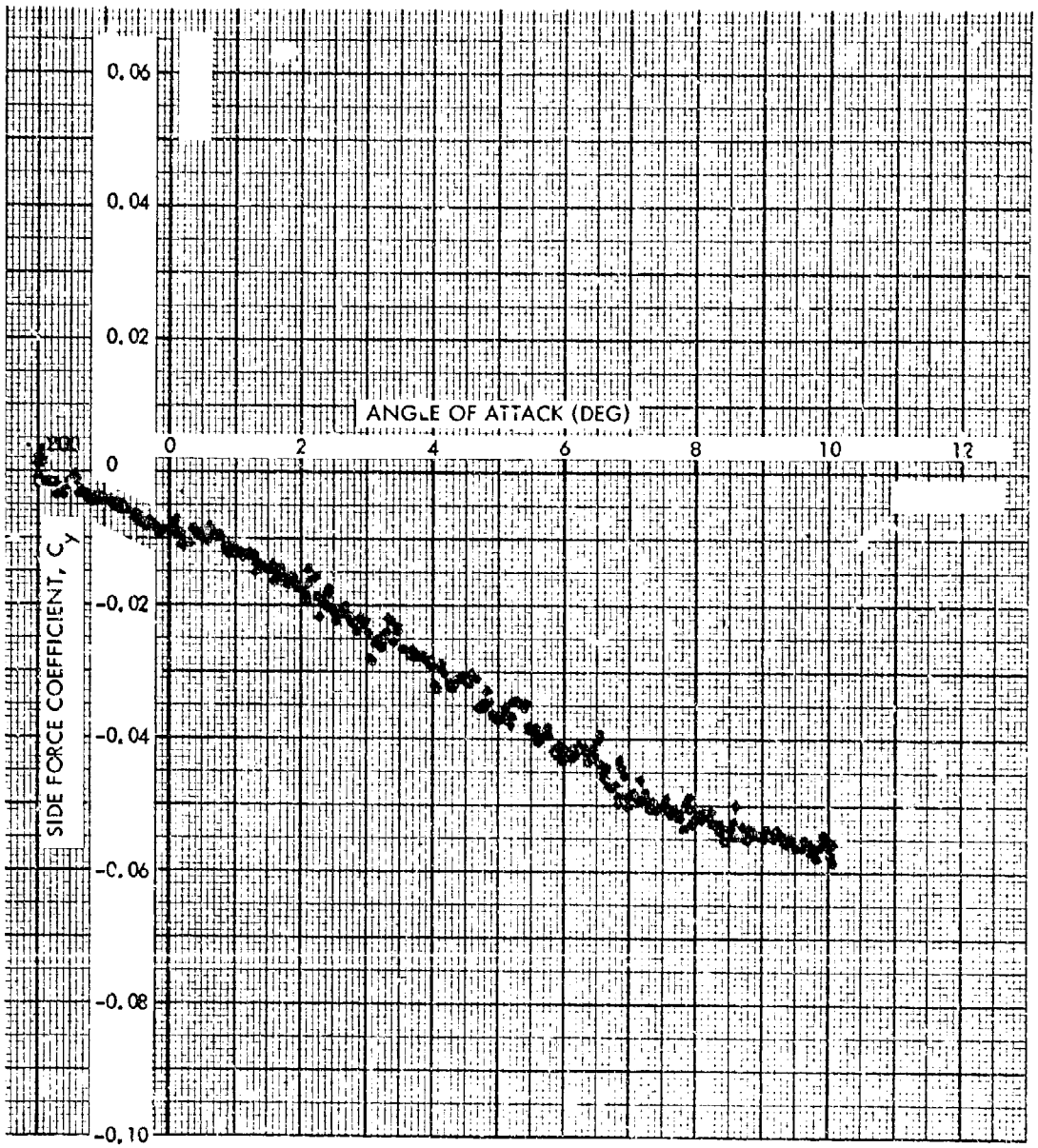

FIG. 65 SIDE FORCE COEFFICIENT VERSUS ANGLE OF ATTACK AT A MACH NUMBER OF 3.5 AND A FIN CANT ANGLE OF 4.50 DEGREES

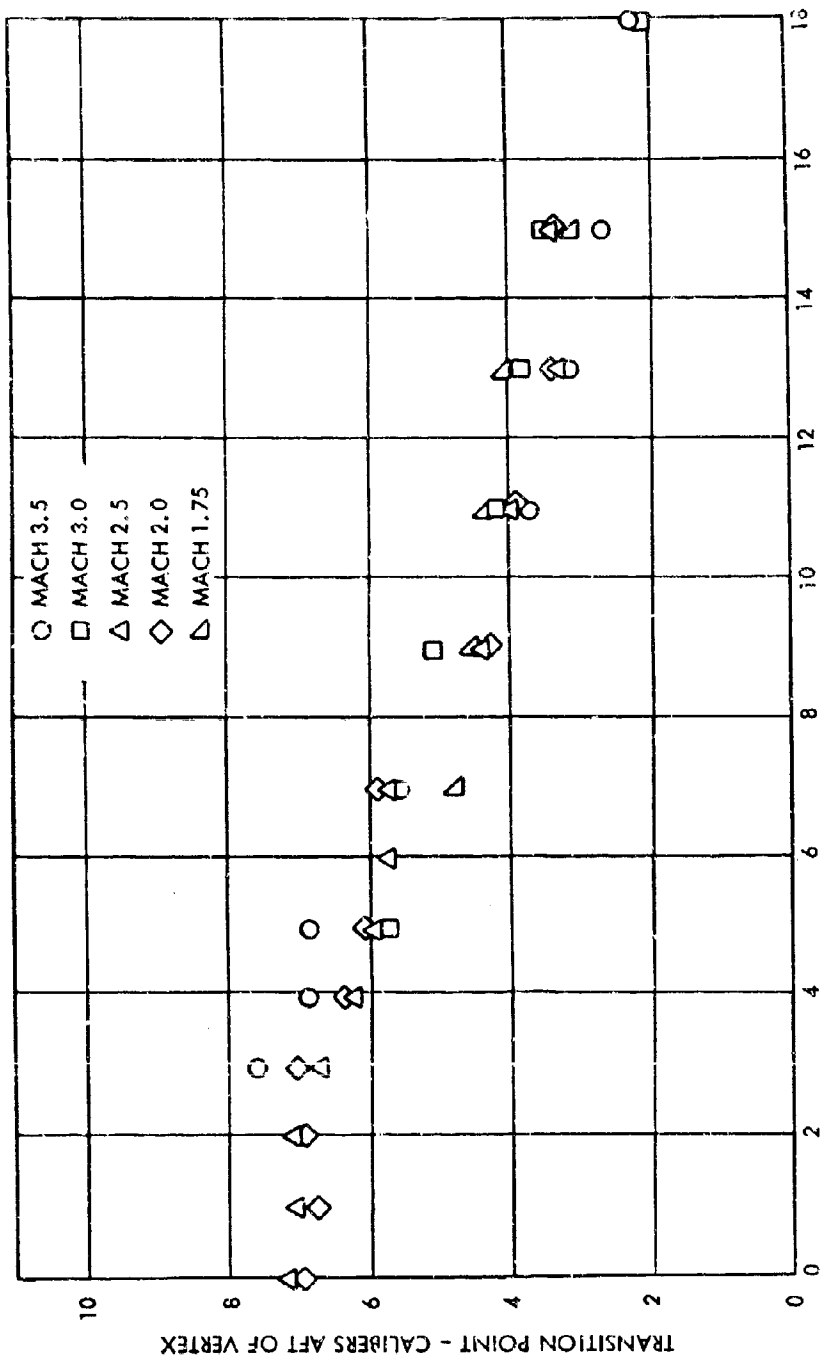

FIG. 66 TRANSITION LOCATION IN CALIBERS VERSUS ANGLE OF ATTACK FOR INDICATED MACH NUMBERS

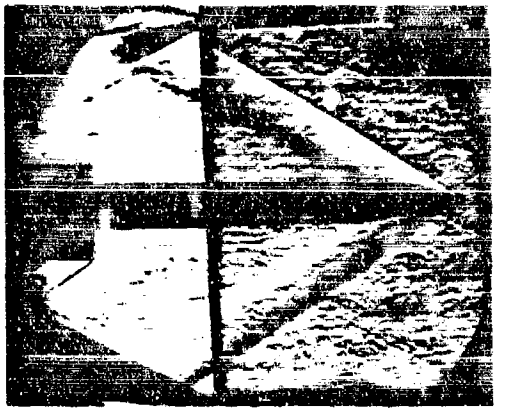

ANGLE OF ATTACK 0 DEG

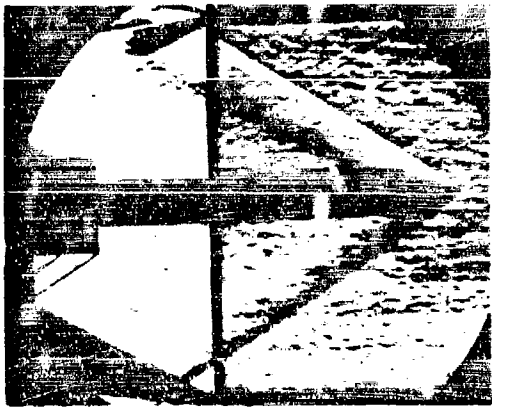

ANGLE OF ATTACK 1 DEG

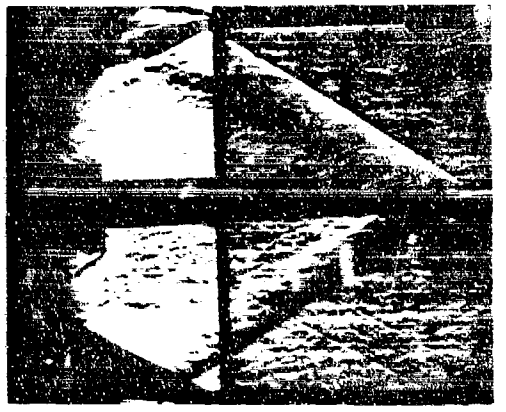

ANGLE OF ATTACK 2 DEG

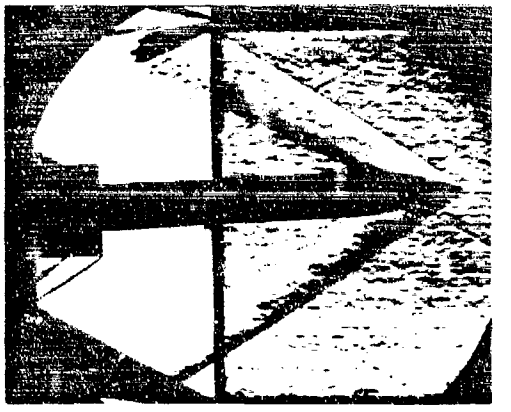

ANGLE OF ATTACK 3 DEG

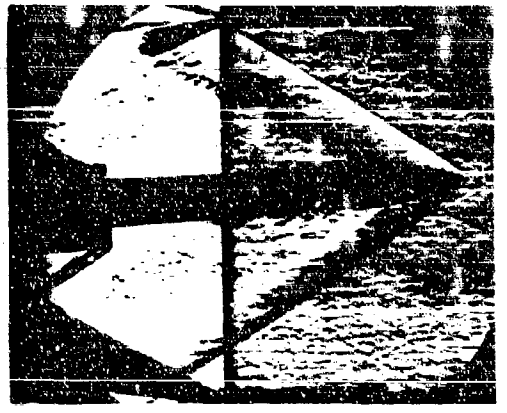

ANGLE OF ATTACK 4 DEG

ANGLE OF ATTACK 5 DEG

FIG. 67 (a) SCHLIEREN PHOTOGRAPHS OF THE WRAP AROUND FIN MAGNUS MODEL AT A MACH NUMBER OF 2.0 AND AT ANGLES OF ATTACK BETWEEN 0 AND 5 DEGREES

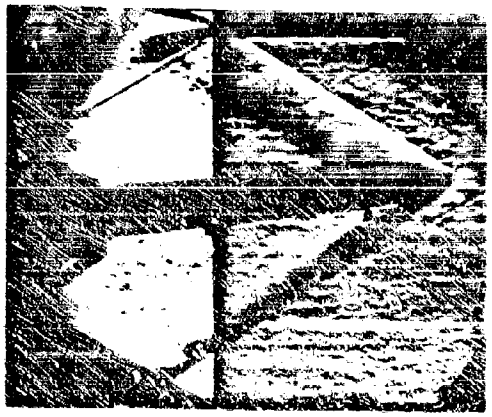

ANGLE OF ATTACK 7 DEG

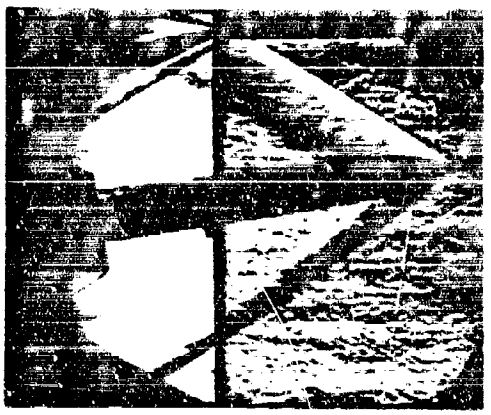

ANGLE OF ATTACK 9 DEG

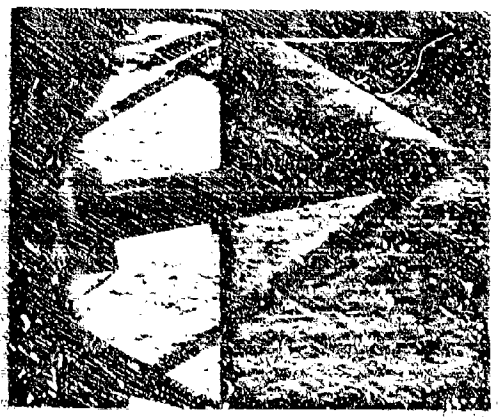

ANGLE OF ATTACK 11 DEG

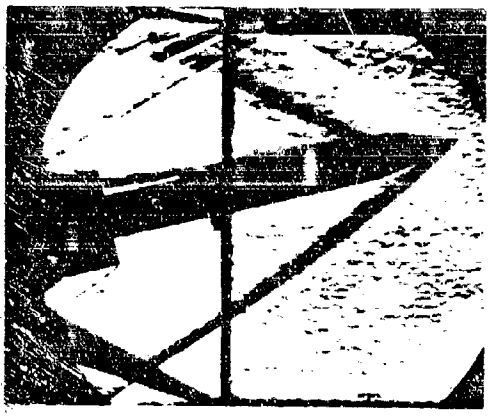

ANGLE OF ATTACK 13 DEG

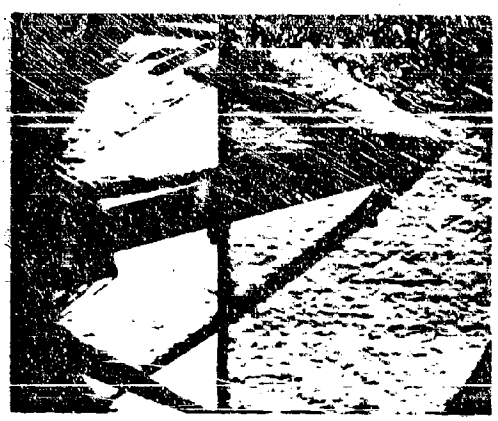

ANGLE OF ATTACK 15 DEG

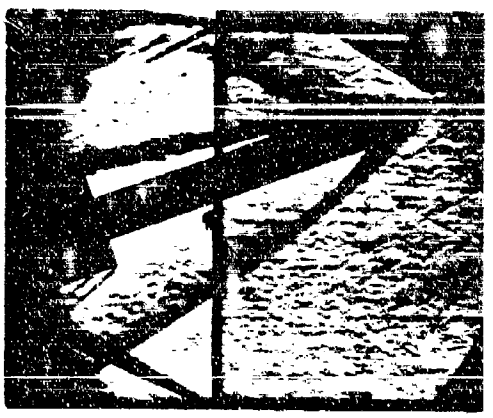

ANGLE OF ATTACK 20 DEG

FIG. 67 (b) SCHLIEREN PHOTOGRAPHS OF THE WRAP AROUND FIN MAGNUS MODEL AT A MACH NUMBER OF 2.0 AND AT ANGLES OF ATTACK BETWEEN 7 AND 20 DEGREES

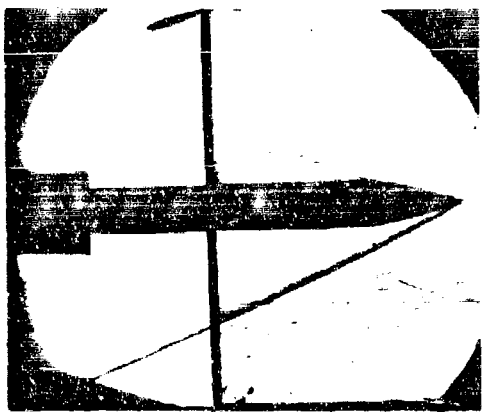

ANGLE OF ATTACK 0 DEG

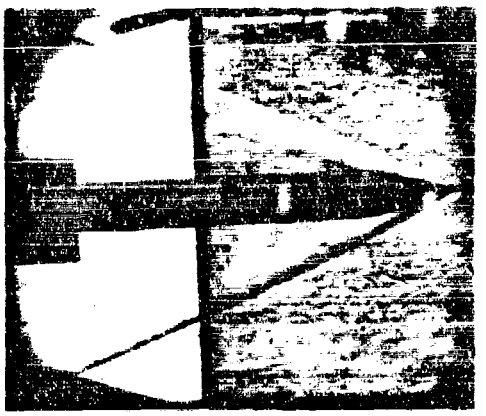

ANGLE OF ATTACK 1 DEG

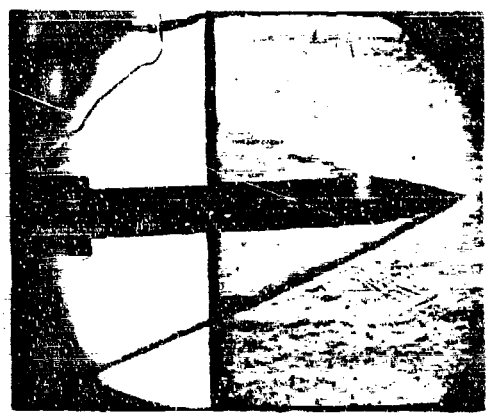

ANGLE OF ATTACK 2 DEG

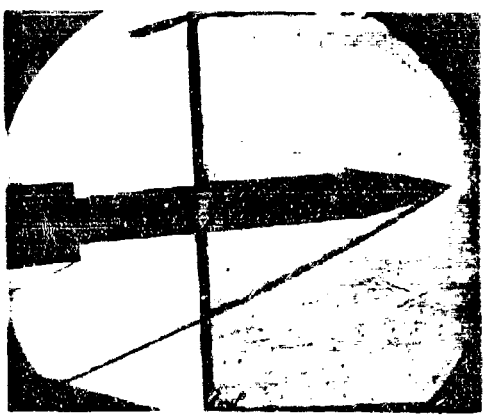

ANGLE OF ATTACK 3 DEG

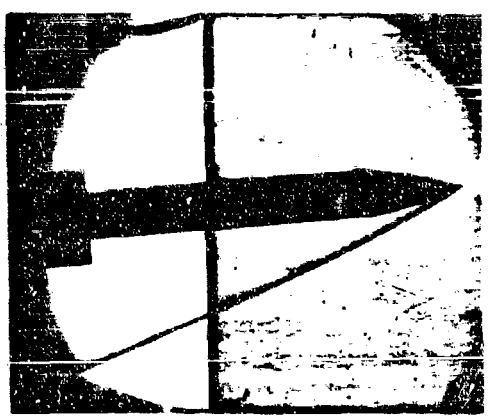

ANGLE OF ATTACK 4 DEG

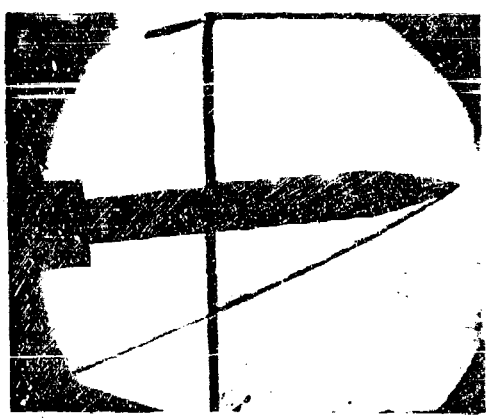

ANGLE OF ATTACK 5 DEG

FIG. 68 (a) SCHLIEREN PHOTOGRAPHS OF THE WRAP AROUND FIN MAGNUS MODEL AT A MACH NUMBER OF 3.0 AND AT ANGLES OF ATTACK BETWEEN 0 AND 7 DEGREES

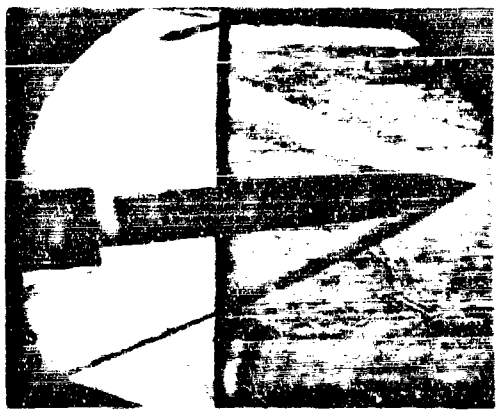

ANGLE OF ATTACK 7 DEG

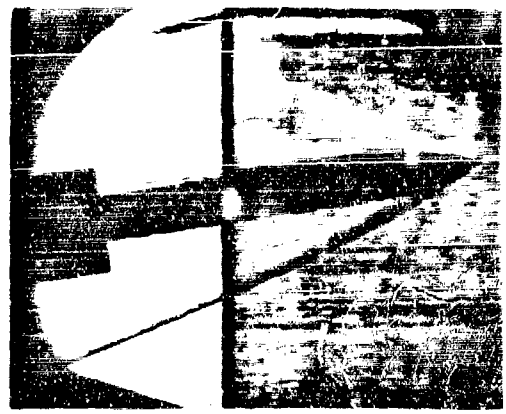

ANGLE OF ATTACK 9 DEG

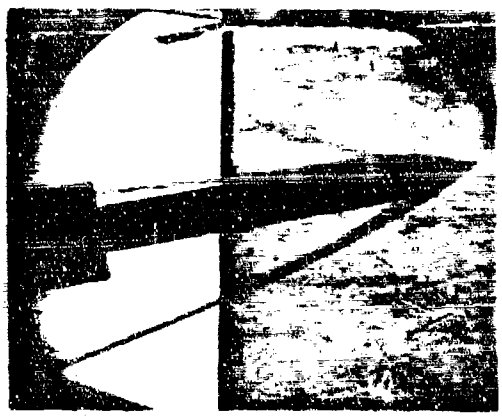

ANGLE OF ATTACK 11 DEG

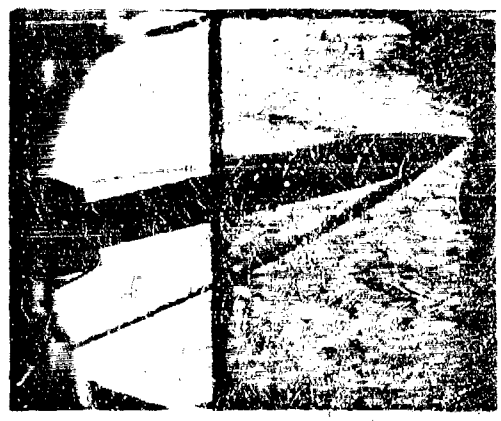

ANGLE OF ATTACK 13 DEG

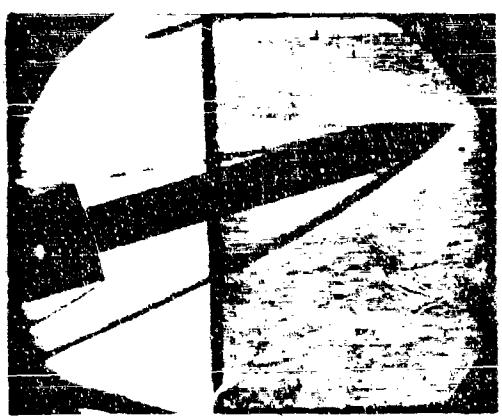

ANGLE OF ATTACK 15 DEG

ANGLE OF ATTACK 20 DEG

FIG. 68 (b) SCHLIEREN PHOTOGRAPHS OF THE WRAP AROUND FIN MAGNUS MODEL AT A MACH NUMBER OF 3.0 AND AT ANGLES OF ATTACK BETWEEN 7 AND 20 DEGREES

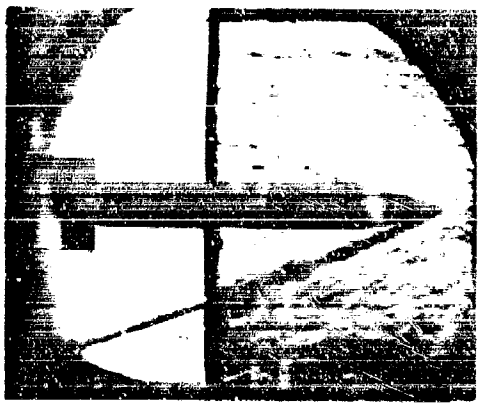

ANGLE OF ATTACK 0 DEG

ANGLE OF ATTACK 1 DEG

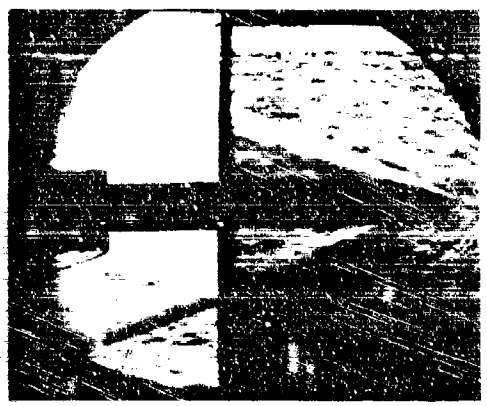

ANGLE OF ATTACK 2 DEG

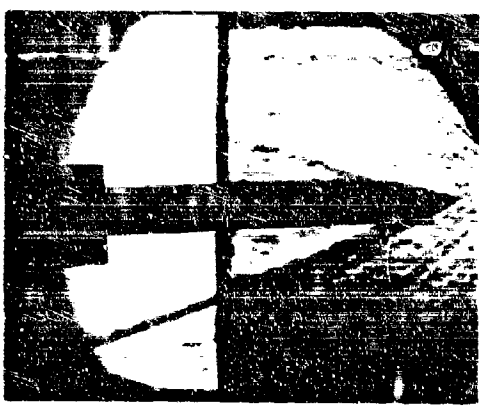

ANGLE OF ATTACK 3 DEG

ANGLE OF ATTACK 4 DEG

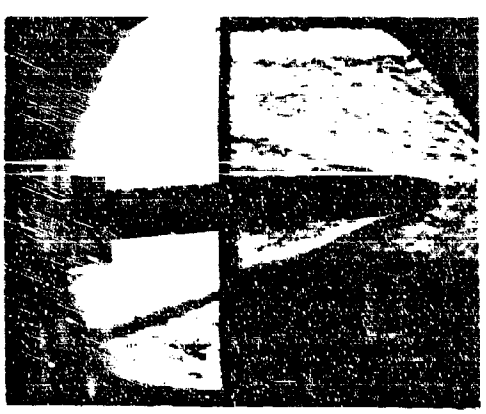

ANGLE OF ATTACK 5 DEG

FIG. 69 (a) SCHLIEREN PHOTOGRAPHS OF THE WRAP AROUND FIN MAGNUS MODEL AT A MACH NUMBER OF 3.5 AND AT ANGLES OF ATTACK BETWEEN 0 AND 5 DEGREES

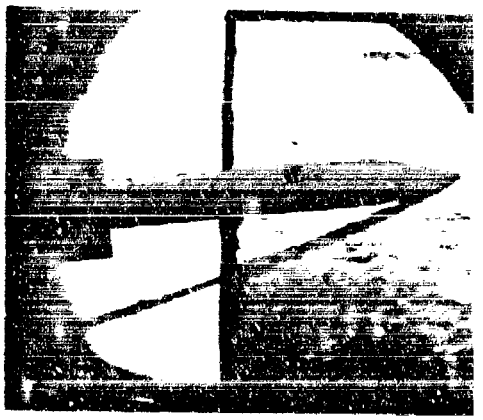

ANGLE OF ATTACK 7 DEG

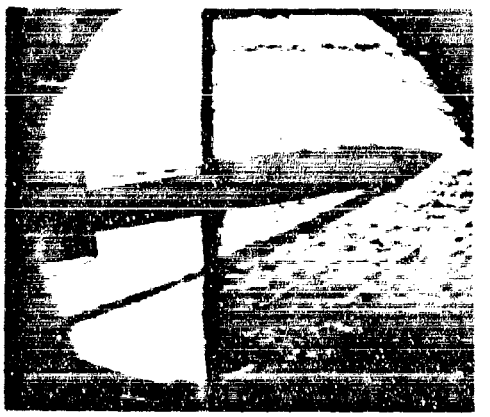

ANGLE OF ATTACK 9 DEG

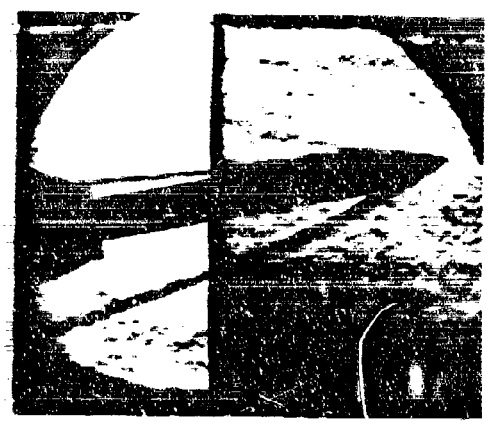

ANGLE OF ATTACK 11 DEG

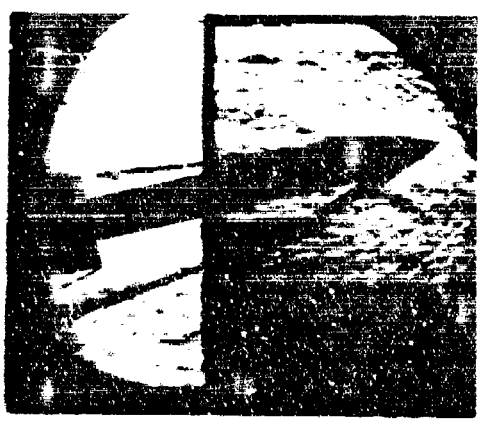

ANGLE OF ATTACK 13 DEG

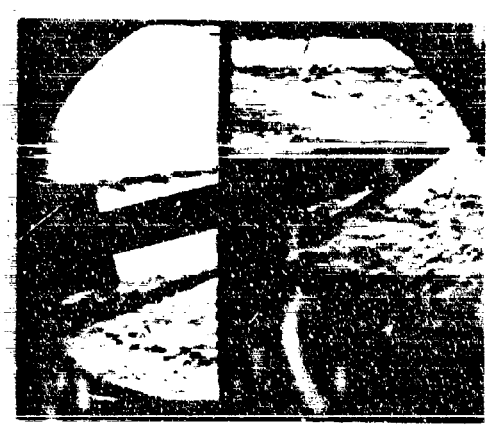

ANGLE OF ATTACK 15 DEG

ANGLE OF ATTACK 20 DEG

FIG. 69 (b) SCHLIEREN PHOTOGRAPHS OF THE WRAP AROUND FIN MAGNUS MODEL AT A MACH NUMBER OF 3.5 AND AT ANGLES OF ATTACK BETWEEN 7 AND 20 DEGREES

UNCLASSIFIED

Security Classification

DOCUMENT CONTROL DATA - R&D

(Security classification of title, body of abstract and indexing annotation must be entered when the overall report is classified)

1 ORIGINATING ACTIVITY (Corporate author)

U. S. Naval Ordnance Laboratory
White Oak, Silver Spring, Maryland

2a REPORT SECURITY CLASSIFICATION

UNCLASSIFIED

2b GROUP

3 REPORT TITLE

SUPERSONIC MAGNUS MEASUREMENTS OF THE 10-CALIBER ARMY-NAVY SPINNER PROJECTILE WITH WRAP-AROUND FINS

4 DESCRIPTIVE NOTES (Type of report and inclusive dates)

5 AUTHOR(S) (Last name, first name, initial)

Regan, Frank J
Schermerhorn, Virginia L.

6 REPORT DATE	7a TOTAL NO OF PAGES	7b NO OF REFS
1 October 1970	84	7

8a CONTRACT OR GRANT NO.	9a ORIGINATOR'S REPORT NUMBER(S)
b PROJECT NO.	NOLTR 70-211
c Task No. A32 320/292/69F 20311202 WU-3	9b OTHER REPORT NO(S) (Any other numbers that may be assigned this report)
d.	

10 AVAILABILITY/LIMITATION NOTICES

This document is subject to special export controls and each transmittal to foreign governments or foreign nationals may be made only with prior approval of NOL.

11 SUPPLEMENTARY NOTES	12 SPONSORING MILITARY ACTIVITY
	Naval Air Systems Command Washington, D. C.

13 ABSTRACT

A research configuration was formed by attaching wrap-around fins in a cruciform arrangement to a 10-caliber Army-Navy Spinner Projectile. This configuration was tested in the Naval Ordnance Laboratory's Supersonic Tunnel No. 2 to get the Magnus force and moment, as well as the normal force and pitching moment. Model spin rate was generated by means of fin cant.

DD FORM 1 JAN 64 1473

UNCLASSIFIED

Security Classification

UNCLASSIFIED

Security Classification

14 KEY WORDS	LINK A		LINK B		LINK C	
	ROLE	WT	ROLE	WT	ROLE	WT
Projectile						
Wrap-around-fin stabilizer						
Magnus measurements						
Army-Navy Spinner Projectile						

INSTRUCTIONS

1. ORIGINATING ACTIVITY: Enter the name and address of the contractor, subcontractor, grantee, Department of Defense activity or other organization *(corporate author)* issuing the report.

2a. REPORT SECURITY CLASSIFICATION: Enter the overall security classification of the report. Indicate whether "Restricted Data" is included. Marking is to be in accordance with appropriate security regulations.

2b. GROUP: Automatic downgrading is specified in DoD Directive 5200.10 and Armed Forces Industrial Manual. Enter the group number. Also, when applicable, show that optional markings have been used for Group 3 and Group 4 as authorized.

3. REPORT TITLE: Enter the complete report title in all capital letters. Titles in all cases should be unclassified. If a meaningful title cannot be selected without classification, show title classification in all capitals in parenthesis immediately following the title.

4. DESCRIPTIVE NOTES: If appropriate, enter the type of report, e.g., interim, progress, summary, annual, or final. Give the inclusive dates when a specific reporting period is covered.

5. AUTHOR(S): Enter the name(s) of author(s) as shown on or in the report. Enter last name, first name, middle initial. If military, show rank and branch of service. The name of the principal author is an absolute minimum requirement.

6. REPORT DATE: Enter the date of the report as day, month, year, or month, year. If more than one date appears on the report, use date of publication.

7a. TOTAL NUMBER OF PAGES: The total page count should follow normal pagination procedures, i.e., enter the number of pages containing information.

7b. NUMBER OF REFERENCES: Enter the total number of references cited in the report.

8a. CONTRACT OR GRANT NUMBER: If appropriate, enter the applicable number of the contract or grant under which the report was written.

8b, 8c, & 8d. PROJECT NUMBER: Enter the appropriate military department identification, such as project number, subproject number, system numbers, task number, etc.

9a. ORIGINATOR'S REPORT NUMBER(S): Enter the official report number by which the document will be identified and controlled by the originating activity. This number must be unique to this report.

9b. OTHER REPORT NUMBER(S): If the report has been assigned any other report numbers *(either by the originator or by the sponsor)*, also enter this number(s).

10. AVAILABILITY/LIMITATION NOTICES: Enter any limitations on further dissemination of the report, other than those imposed by security classification, using standard statements such as:

(1) "Qualified requesters may obtain copies of this report from DDC."

(2) "Foreign announcement and dissemination of this report by DDC is not authorized."

(3) "U. S. Government agencies may obtain copies of this report directly from DDC. Other qualified DDC users shall request through

_____."

(4) "U. S. military agencies may obtain copies of this report directly from DDC. Other qualified users shall request through

_____."

(5) "All distribution of this report is controlled. Qualified DDC users shall request through

_____."

If the report has been furnished to the Office of Technical Services, Department of Commerce, for sale to the public, indicate this fact and enter the price, if known.

11. SUPPLEMENTARY NOTES: Use for additional explanatory notes.

12. SPONSORING MILITARY ACTIVITY: Enter the name of the departmental project office or laboratory sponsoring *(paying for)* the research and development. Include address.

13. ABSTRACT: Enter an abstract giving a brief and factual summary of the document indicative of the report, even though it may also appear elsewhere in the body of the technical report. If additional space is required, a continuation sheet shall be attached.

It is highly desirable that the abstract of classified reports be unclassified. Each paragraph of the abstract shall end with an indication of the military security classification of the information in the paragraph, represented as *(TS)*, *(S)*, *(C)*, or *(U)*.

There is no limitation on the length of the abstract. However, the suggested length is from 150 to 225 words.

14. KEY WORDS: Key words are technically meaningful terms or short phrases that characterize a report and may be used as index entries for cataloging the report. Key words must be selected so that no security classification is required. Identifiers, such as equipment model designation, trade name, military project code name, geographic location, may be used as key words but will be followed by an indication of technical context. The assignment of links, roles, and weights is optional.

UNCLASSIFIED

Security Classification

DOCUMENT TRANSMITTAL
NAVSHIP FORM 3900/3 (10-67)

CLASSIFICATION
UNCLASSIFIED
UNCLASSIFIED WHEN ENCLOSURE IS REMOVED
SERIAL NUMBER (When required)/DATE

AD NUMBER (To be inserted by DDC)

ORIGINATING AGENCY
Naval Ordnance Laboratory

ENCLOSURE (Report Title)
Supersonic Magnus Measurements of the 10-Caliber Army-Navy Spinner Projectile with Wrap-Around Fins

RELATED REPORT AND NUMBER
NOLTR 70-211

REPORT DATE
1 Oct. '70

CONTRACT/PROJECT/TASK/WORK UNIT NUMBER
A32 320/292/6 0R
20211202 KU-3

SECURITY CLASSIFICATION

	UNCLAS	CONFL	SECRET	RD
REPORT	X			
TITLE OR SUBJECT	X			
ABSTRACT OR SUMMARY	X			

TO: Administrator
Defense Documentation Center for Scientific and Technical Information (DDC)
Bldg #5, Cameron Station
Alexandria, Virginia 22314

Enclosure is forwarded for distribution subject to limitations checked below. Request AD number be inserted in space above; two copies of this letter be returned to originating activity if shown below; two copies be sent to Commander, Naval Air Systems Command; and one copy be retained by DDC.

☐ 1. This document has been approved for public release and sale. Its distribution is unlimited.

☐ 3. Each transmittal of this document outside the agencies of the U. S. Government must have prior approval of

IN ADDITION TO SECURITY REQUIREMENTS WHICH APPLY TO THIS DOCUMENT AND MUST BE MET —

☐ 4. Each transmittal of this document outside the Department of Defense must have prior approval of

☒ 2. This document is subject to special export controls and each transmittal to foreign governments or foreign nationals may be made only with the prior approval of

Naval Ordnance Laboratory

☐ 5. This document may be further distributed by the holder only with specific prior approval of

Library Division, Room 1-355
U. S. Naval Ordnance Laboratory
Silver Spring, Maryland 20910
Attn: Technical Library, Code 730/3

20 copies forwarded

SIGNATURE
Sharon B. Murray

TITLE
Library Division

CODE
730

DATE
31 Dec. '70

Commander Naval Air Systems Command (AIR-604)
Navy Department
Washington, D. C. 20360

CLASSIFICATION
UNCLASSIFIED

UNCLASSIFIED WHEN ENCLOSURE IS REMOVED

S/N 0102-650-3020

GPO 878-404 C-11965